ISSN 1331-7210 (Print)
ISSN 2718-322X (Online)

Engineering Power

BULLETIN OF THE CROATIAN ACADEMY OF ENGINEERING Vol. 18(2-3) 2023

EDITOR-IN-CHIEF'S WORD

It is my great pleasure to present another issue of Engineering Power to our readers. This issue brings together innovative research in energy engineering, with a focus on the urgent need for a transition toward sustainable, renewable energy sources, as the detrimental effects of fossil fuel reliance continue to challenge both our environment and global economies.

It highlights the pivotal role that energy engineering plays in facilitating this shift, alongside the increasing impact of digitalization in shaping smarter, more efficient technological solutions. The contributions in this issue not only reflect cutting-edge advances but also emphasize the importance of integrating environmental considerations into every stage of technological development.

Together, these papers aim to bridge gaps in addressing key global challenges related to energy and the environment. I hope that you find the insights and findings presented here to be both thought-provoking and impactful as we work together toward a more sustainable future.

Editor-in-Chief
Vedran Mornar, President of the Croatian Academy of Engineering

EDITOR'S WORD

Dear readers,

I am pleased to introduce you to the Engineering Power issue, edited by Prof. Sandro Nižetić, PhD and Assoc. Prof. Goran Krajačić, PhD. Four publications cover the following topics: the novel battery charging control system, strategies to secure the green transition in China, a systematic review of thermal management of electric vehicle batteries and remote sensing methods to assess the Surface Urban Heat Island (SUHI) effect. This issue concludes with a report on the CAETS 2023 conference e2-mobility - Solutions and Opportunities, which took place in Zagreb from October 9-11, 2023. I hope you enjoy reading it!

Editor
Bruno Zelić, Vice-President of the Croatian Academy of Engineering

FOREWORD

In modern and developed society the energy aspect plays a key role, and it can be considered as a major driver of global economies. Excessive utilization of fossil fuels for power generation in the past decades has caused sensible environmental issues that are becoming more severe, more frequent and unpredictable. Therefore, there is a clear necessity for a determined shift towards cleaner energy generation technologies that should be based on renewables. Advances and developments in energy engineering are playing pivotal role to meet desired shift from fossil-based technologies to renewables. Moreover, intense digitalization in various fields of engineering has become rapid and allowed different smart solutions in engineering. Digitalization can help to accelerate desired energy transition and in general can bring beneficial opportunities for humanity. However, novel developed technological solutions should consider also environmental implications, besides the performance and economic aspect. Environmental related problems are finally ending as economic problems; thus, all novel developed engineering solutions should be carefully evaluated from an environmental point of view. The environmental aspect is a key one to confirm and to secure long-term suitability of novel technological solutions in the field of engineering. The integration and targeted implementation of smart solutions can bring beneficial opportunities for humanity. This special issue brings new knowledge that contributes to bridge above mentioned key population challenges. This special issue consists of the overall four published papers. In the work Comparison of Conventional and Fuzzy Logic-based Charging Control Systems without and with State-of-Charge Estimator, the novel battery charging control system was proposed, and that uses fuzz logic controller. The obtained simulations on lithium-titanate battery cell model proved that examined approach has potential to reduce charging time to about 17.7% when compared to the conventional constant-current constant-voltage charging control strategy. The work Energy development status and emerging technologies in China discussed strategies that will secure green transformation in China, with special emphasis on hydrogen-based technologies. The work delivered analysis of current state regarding energy supply system and provided in-depth discussion of future possible development strategies for China. The systematic review of battery thermal management systems for electric vehicles was provided in work A systematic review on battery thermal management systems for electric vehicles. Within the work effective thermal management strategies were discussed such as air-based cooling, cooling with phase change materials, heat pipe cooling, liquid cooling as well as hybrid cooling methods, to secure desired temperature rise in the battery. The work contributed to the present knowledge and deeper understanding of various cooling approaches for batteries in electric vehicles. The work Utilizing Satellite Remote Sensing and Geographic Information Systems for Assessing Urban Heat Island Effects as Urban Planning Tools for Emerging Economies considered remote sensing methods to assess the Surface Urban Heat Island (SUHI) effect. Landsat satellite spectral images were used to evaluate variations of land surface temperature and finally to estimate urban heat island intensity. The research outcomes indicated the importance of green infrastructure such as parks or green roofs for instance as they can significantly reduce urban heat island effect. The previously discussed contributions within this special issue contributed to the further development of smart technologies in energy engineering applications. The Guest Editors would like to thank the authors for their contribution as well as to the anonymous reviewers who have helped to improve the quality of published papers. Finally, we would like to thank Prof. Dr. Bruno Zelić for providing us with technical support for managing of this special issue.

Guest-Editors
Sandro Nižetić, University of Split, Faculty of Electrical Engineering, Mechanical Engineering and Naval Architecture
Goran Krajačić, University of Zagreb, Faculty of Mechanical Engineering and Naval Architecture

CONTENT

Editors' Words 1
Comparison of Conventional and Fuzzy Logic-based Charging Control Systems without and with State-of-Charge Estimator 2
Energy development status and emerging technologies in China 15
A systematic review on battery thermal management systems for electronic vehicles 27
Utilizing Satellite Remote Sensing and Geographic Information Systems for Assessing Urban Heat Island Effects as Urban Planning Tools for Emerging Economies 41
CAETS 2023 Conference: e2-mobility Solution and Opportunities 48

Karlo Kvaternik[1], Danijel Pavković[2], Josip Kasać[2], Mihael Cipek[2]

Comparison of Conventional and Fuzzy Logic-based Charging Control Systems without and with State-of-Charge Estimator

[1]AVL-AST d.o.o., Strojarska cesta 22, 10000 Zagreb, Croatia
[2]Faculty of Mechanical Engineering and Naval Architecture, University of Zagreb, Ivana Lučića 5, 10000 Zagreb, Croatia

Abstract

Lithium-titanate battery cells stand out among the various rechargeable lithium battery chemistries available today due to their exceptional thermal stability and operational safety, which make them suitable for highly demanding applications characterized by high charging/discharging rates and operating temperatures. This paper proposes a battery charging control system arranged in the so-called cascade control structure, wherein the battery voltage and state-of-charge control is performed by means of a fuzzy logic controller. An extended Kalman filter is used to provide the state-of-charge feedback utilizing the realistic nonlinear Thevenin model of the battery cell equivalent circuit. Simulations using a readily available lithium-titanate battery cell model demonstrate that fuzzy logic-based charging control reduces the time needed to recharge from deeply discharged state (from 20% state-of-charge initial value) by 17.7% compared to the conventional constant-current constant-voltage charging control strategy, with the average charging current used as the criterion for the comparison of these heterogenous control strategies.

***Keywords**: Lithium-Titanate Battery Cell; Constant-Current/Constant Voltage Charging; State-of-Charge Estimation; Extended Kalman Filter.*

1. Introduction

A comprehensive analysis conducted in [1] has revealed that approximately 20% of the global fossil fuel production is utilized by the transportation sector, leading to a significant contribution to greenhouse gas emissions. To enhance energy efficiency, reduce environmental impact, and decrease reliance on oil reserves, the electrification of the transportation sector has been advocated [2], wherein advanced battery technologies play a crucial role. It also proposed integrating the transport sector into the smart electricity grid paradigm, as later discussed in [3] for the case of road transport. The integration of the transport and energy sector into smart grids places particular demands on electric vehicle fleets, including the degree of electrification of the fleet, the cost of charging infrastructure and passenger capacity, as outlined in [4]. Monitoring the electric vehicle battery status during charging and discharging is crucial to ensure its prolonged service life, as shown in [5]. Battery energy storage technologies are also gaining traction in the railway transportation sector, with battery-hybridized locomotives and battery-electric locomotives offering advantages over conventional freight haul, as presented in [6].

Lithium secondary batteries are currently state-of-the-art electrochemical battery technology with favorable calendar life of up to 15 years and specific costs of about 145 EUR/kWh of stored electrical energy for the most advanced lithium titanate battery technology [7]. Presently the discharge power capacity of batteries is still significantly more favorable than that of alternative energy sources such as hydrogen fuel cells, especially when round-trip efficiency of energy conversion is considered [7]. The lithium-titanate oxide anode material has been proposed about a decade ago as a good replacement for commonly used carbon-based anodes in lithium-based secondary batteries due to the practical absence of anode material straining during high-rate discharging [8]. In fact, lithium titanate oxide may also be used as anode material in other, alternative battery chemistries such as those based on sodium-ion technology, which might be cheaper to manufacture due to the natural abundance of sodium as a raw material [9]. Moreover, lithium-titanate (LTO) batteries are considered as one of the safest available battery energy storage technologies, characterized by exceptional thermal stability, power density, cycle life and overall durability [10]. Hence, this battery production technology is likely to witness a significant growth in the

foreseeable future, wherein increased production volumes would likely bring down the overall production costs [11].

The key advantages of LTO battery cells are also discussed in [11], with additional benefits in terms of improved thermal material properties compared to other lithium-ion chemistries. These advantages lead to improved safety features, such as significant reduction of formation of dendrites and lithium plating of electrodes, even under harsh operating conditions, such as high current rates (about 25C for continuous discharging and charging), along with exceptional operational durability (20000 charging/discharging cycles with 1C current rate). The study presented in [11] concludes that LTO battery cells offer exceptional charging/discharging rate capabilities, albeit with reduced energy density compared to classical lithium-ion cells with graphite anodes. Due to their exceptional cycling characteristics and durability LTO cells appear to be well suited for hybrid power applications in electrified vehicle powertrains. Thus, extensive research has been carried out in the available literature regarding the innovative LTO cell technologies and charging characteristics [12], state-of-charge (SoC) estimation [13], state-of-health (SoH) estimation [14] and advanced control techniques [15], including those for stationary energy storage use in solar photovoltaic systems [16] and mobile applications such as those in heavy-duty vehicles [17].

Recent research in battery modeling and estimation has shown that the Thevenin equivalent circuit models are effective for modeling and estimation of the battery state-of-charge (SoC) for lithium-ion batteries in electric vehicles (EVs) [18, 19]. Simulation and experimental results have validated the accuracy of these models in predicting battery behavior under different operating conditions [18, 19], and ongoing research is directed towards exploring the general applicability of these relatively straightforward models for estimating the SoC of battery packs, which is crucial for the safe and efficient operation of electric vehicles (EVs) [20]. The electrolyte polarization dynamics within the Thevenin model can either be modeled as a first-order RC parallel term [19] or the more general second-order RC model [18], wherein the former is typically used as a trade-off in terms of simplicity compared to the more accurate second-odder polarization dynamics model. Using the equivalent circuit models within the improved extended Kalman filter algorithm has been proposed to enhance the accuracy of SoC estimation in lithium-ion batteries [21]. On the other hand, a hybrid estimator combining the extended Kalman filter (EKF) and sliding mode observer has been demonstrated to improve the robustness of SoC estimation in the presence of disturbances [22]. In fact, such advanced SoC estimation techniques, i.e. those relying on sigma point Kalman filter, long short-term memory neural networks, convolution neural networks, and different hybrid methods, have been reviewed for possible utilization in battery management systems (BMS), with a focus on reducing average error and improving performance in EV applications [23]. In particular, the development of advanced BMS is crucial for improving battery performance, safety, and longevity in EVs [23, 24]. BMS features include charging/discharging control, precise monitoring, heat management, battery safety, and protection, as well as accurate SoC estimation [23, 24]. Recent research has focused on the comprehensive analysis and comparison of charging control methods for lithium-ion battery packs, classifying them as non-feedback-based, feedback-based, and intelligent charging methods [25]. A good review of the advancements and difficulties in cutting-edge battery technology and cutting-edge BMS for EVs can be found in [26].

Efficient charging of rechargeable batteries is contingent upon the charger's circuit design and control strategy which performs three essential functions: (i) commencing the charging process, (ii) controlling the charging rate and battery terminal voltage for optimal charging performance, and (iii) terminating the charging upon completion, determined by a suitable end-of-charging criterion [24]. However, batteries typically exhibit notable terminal voltage nonlinear behavior during charging [27, 28]. This may be challenging from the standpoint of precise battery SoC tracking [29], which is key for preventing battery overcharging and related cell aging and SoH deterioration [30]. For that reason, battery SoC needs to be monitored throughout the charging process by an appropriate estimator, such as the EKF [29], which has been successfully employed in [31] to augment the conventional constant-current constant-voltage (CCCV) charging system, ultimately resulting in about 25% speed up of the charging process. Battery charging techniques (charging control strategies) can be categorized in many ways. According to [24], the charging strategies can be categorized as non-feedback based (or open-loop) strategies, feedback-based, and intelligent charging strategies, whereas reference [32] breaks down the charging strategy types into so-called simple (or traditional) charging strategies, optimized charging strategies based on different optimized current waveforms to achieve the charged state and the model-based charging strategies.

In traditional (conventional) battery charging applications, the so-called CCCV charging technique (see e.g. [24]) is usually preferred when recharging the battery from the discharged state [32], while the so-called float-charge maintenance or trickle charging approaches [33] are usually reserved for maintaining the battery charge once it has been fully charged. The main advantage of the CCCV approach is that the charging current and battery terminal voltage are effectively limited by means of respective battery controllers [27], and it can also find use in fast charging applications [34]. Also, it has been considered as a good benchmark for other more sophisticated charging control strategies to be compared against [24]. Moreover, its relative simplicity and virtual independence on the sophisticated internal battery model [32], currently make it the one of the most widely used charging strategies [33]. However, batteries typically exhibit notable terminal voltage nonlinear behavior during charging [28]. This may be challenging from the standpoint of precise battery SoC tracking [29], which is key for preventing battery overcharging and related cell aging and SoH deterioration [30]. For that reason, battery SoC needs to be monitored throughout the charging process by an appropriate estimator, such as the extended Kalman filter [29], which has been successfully employed in [31] to augment the conventional CCCV charging system, ultimately resulting in about 25% speed up of the charging process. A good review of charging strategies for lithium-ion batteries can be found in [35].

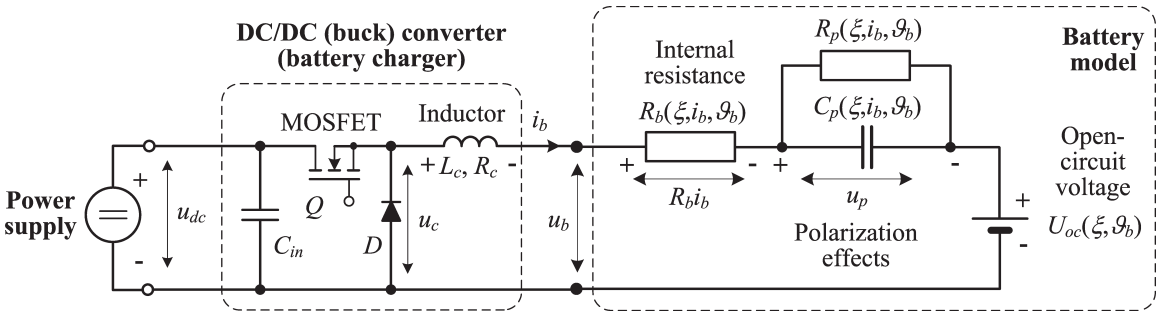

Fig. 1. Quasi-static battery equivalent electrical circuit model with charging power converter.

The implementation of sophisticated control strategies is anticipated to yield additional enhancements in both the duration of the charging process and the effectiveness of State of Charge (SoC) tracking. Among these, the optimization-based control strategies, such as the model-predictive control (MPC), may be particularly well-suited for solving multiple-criteria charging scenarios [35], such as those where battery temperature and current rate play a critical role regarding the battery SoH preservation [33]. Multistage constant current (MCC) represents a generalization of the traditional constant-current (CC) charging technique, wherein the duration of each constant-rate charging stage can either be SoC-dependent or battery terminal voltage dependent [34]. For example, the comparative study presented in [31] has pointed out that utilization of fuzzy logic control-based approach presented in [36] can yield about 13% speedup of the battery recharging, whereas MCC charging with offline optimization of the charging trajectory [37] and MPC with moving horizon estimation of the battery SoC [38], may result in relative charging process speedups of 17% and 30%, respectively. However, the latter charging algorithms can be numerically quite demanding due to requirement for charging trajectory optimization, whereas the fuzzy logic-based charging control strategy may be relatively easily implemented as a form of expert knowledge-based system utilizing the SoC estimator as a digital twin of the battery which aids the charging process (see [31]).

Several studies have investigated methods to preserve battery SoH during charging, such as the MPC approach that accounts for voltage and temperature constraints to reduce the battery stress during the charging process [39]. The study presented in [40] also focused on thermal effects, optimizing power and current profiles to balance the charging rate and temperature rise. Alternative charging profiles have shown promise as well, such as incorporating negative current pulses within the CCCV technique to improve battery SoH [41] and using a temperature-compensated model to enhance the charging speed within the CCCV charging strategy [42]. Moreover, MCC charging has been combined with the least mean squares estimation for faster charging in [43], while offline optimization, such as the genetic algorithm-based approach proposed in [44] and the dynamic programming utilized in [45] have also been explored to determine optimal charging sequences and minimize heat losses during charging.

Fast charging plays a vital role in alleviating range anxiety associated with battery electric vehicles and is a key element in promoting the widespread adoption of electric vehicles [46]. However, it also contributes to the accelerated aging of batteries [47].

Therefore, the study presented in [47] analyzed the impact of fast charging on lithium-ion batteries' aging using real-world driving cycles from European cities, considering different charger sizes and battery types, while the study conducted in [46] has evaluated different fast-charging strategies, considering their parameterization effort, battery type, and real-world applicability. In the context of fast charging, thermal management of lithium-ion batteries is essential for ensuring their safety, performance, and longevity in electric vehicles [48]. To this end, the study presented in [48] has provided a state-of-the-art review of recent advancements in lithium-ion battery thermal management strategies for high charge/discharge cycles.

Having in mind the advantageous features of LTO battery cells and the above-described aspects of battery charging control system design and performance indices, the motivation for this paper has been to design a charging strategy that can surpass the traditional CCCV charging approach while honoring the battery voltage and current constraints. The hypothesis of this paper is that using a fuzzy logic-based battery charging control strategy in conjunction with precise SoC estimation would result in notable charging process speedup without adverse effects to battery state-of-health associated with exceeding the charging current and terminal voltage. For that purpose, the fuzzy logic controller relies on battery SoC information provided by an EKF-based state estimator and readily available battery terminal voltage and current measurements, and it is subsequently compared to the conventional CCCV charging control strategy by means of simulations.

2. Battery cell model

A battery cell can be modeled by its equivalent electrical circuit model, shown on the left-hand-side in Fig. 1. The battery equivalent circuit model comprises a voltage source corresponding to the battery open-circuit voltage U_{oc}, electrolyte polarization effects modeled by an equivalent parallel RC circuit (with resistance R_p and capaci-

tance C_p parameters) and an equivalent series resistance R_b [31]. The above model results in the following voltage u_b vs. current i_b relationship in the Laplace s-domain:

$$u_b(s) - U_{oc}(s) = i_b(s)R_b + \frac{R_p i_b(s)}{\tau_p s+1}, \qquad (1)$$

where $\tau_p = R_p C_p$ is the polarization time constant.

All parameters of the above model may depend on battery temperature ϑ_b, battery current i_b and state-of-charge ξ, which is defined in the following manner:

$$\xi = \frac{1}{Q_b(I_b)} \int i_b dt, \qquad (2)$$

with battery charge capacity Q_b also depending on the average battery current load I_b, and the magnitude of these charge capacity variations depending on the battery type and chemistry [49].

The right-hand-side of Fig. 1 shows the principal schematic of the basic battery charging system featuring a buck DC/DC power converter and a battery cell represented by its equivalent electrical circuit model. The buck converter topology comprises the active (switching) element (power MOSFET transistor Q) feeding the inductor (characterized by its inductance L_c and resistance R_c) and parallel-connected freewheeling diode D. The semiconductor switch (MOSFET) modulates the DC supply voltage by means of high-frequency pulse-width modulation (PWM) thus providing the power converter output voltage u_c with adjustable magnitude and fast dynamics (negligible voltage delay).

The main advantage of the equivalent circuit model is that the battery parameters (internal resistances, polarization time constant, open-circuit voltage characteristic) that are characteristic for individual battery types can be experimentally obtained by means of suitable battery tests conducted for the anticipated operating modes (battery SoC and charging/discharging currents) and stored as parameter maps (look-up tables). In that sense, the battery charging control system and SoC estimator design can be easily adapted to the battery type in question by conducting battery model identification experiments and updating the battery parameter maps (see [31] and references therein). The above state-of-charge and current dependent parameters of the equivalent electrical circuit model (the so-called Thevenin model) of a commercial 30Ah/2.4V/6C lithium titanate battery cell [50] have been experimentally estimated using an appropriate experimental setup as described in [51].

The battery open-circuit voltage curve is recorded by using constant-current charging tests, wherein the experiment is characterized by periodic short-duration battery charging intervals followed by at least two-hour long recuperation and battery voltage settling periods. Experimental results are shown in Fig. 2a, and they have been interpolated by cubic splines to obtain a smooth (differentiable) static curve. The battery charge capacity vs. average discharging current curve has also been reconstructed based on constant-current discharging tests, and the resulting cubic spline-interpolated battery capacity vs. discharging current characteristic $Q_b(I_b)$ is shown in Fig. 2b (note that the charge capacity curve for currents below 6 A is obtained by extrapolation). The particular LTO battery cell is characterized by a relatively small decrease of its charge capacity Q_b with the discharging current I_b that amounts to less than 5% for the considered range of discharging current values (i.e. from 6A to 24 A). For both characteristics the interpolation (and extrapolation in the case of static curve in Fig. 2b) has been performed over 1001 samples of the static characteristic look-up table inputs.

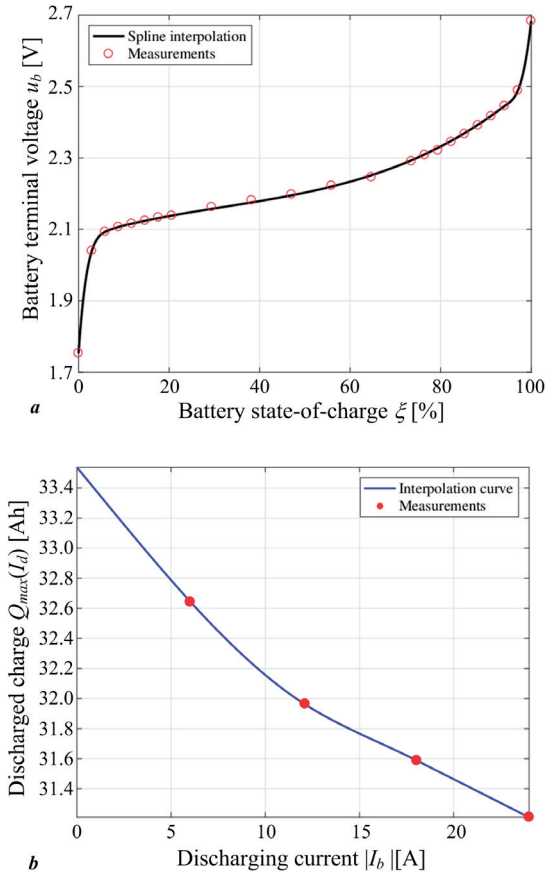

Fig. 2. Lithium-titanate battery cell charge capacity vs. average current characteristic (a) and battery charge capacity vs. current dependence (b).

Recording the battery equivalent circuit model parameter maps with respect to battery state-of-charge and battery current has been carried out by using off-line least squares identification technique [52] on the results of previously recorded battery charging and discharging tests under a pseudo-random binary sequence (PRBS) signal excitation, as explained in [52]. Figure 3 shows the two-dimensional maps of the battery equivalent circuit (Thevenin model) parameters recorded for the considered 30 Ah / 2.4 V LTO battery cell, wherein the battery series resistance R_b and polarization resistance exhibit rather low values over the middle of the state-of-charge range, but their values tend to increase when the battery cell is being fully discharged ($\xi \to 0$) or fully charged ($\xi \to 100\%$). The polarization time constant τ_p takes on values between 2 s and 12 s and is dependent on the charging/discharging current and battery state-of-charge (Fig. 3c).

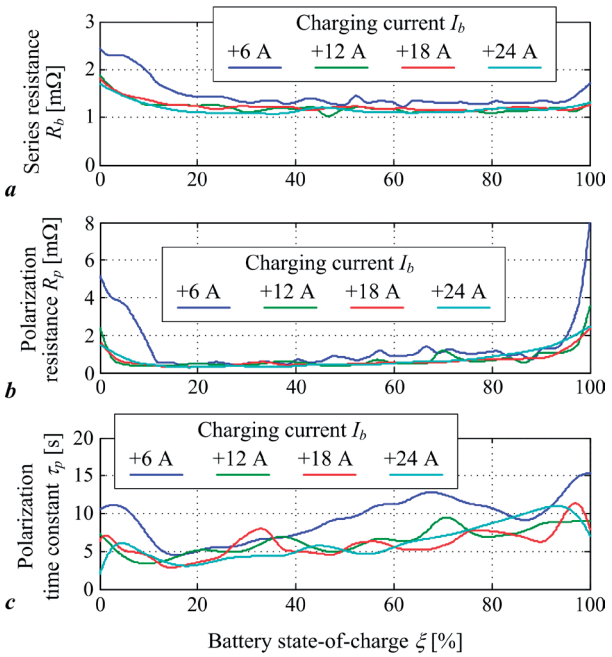

Fig. 3. Equivalent series resistance (a) polarization resistance (b) and polarization time constant (c) vs. SoC for different charging rates.

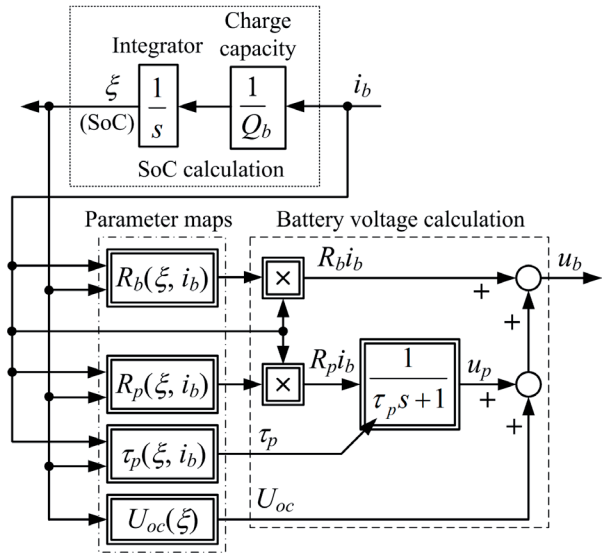

Fig. 4. Block diagram of battery equivalent circuit model.

The estimated parameters of the battery equivalent electrical circuit are used to build the battery simulation model, wherein the battery current is used as model input. Fig. 4 shows the current-input quasi-static battery model with state-of-charge ξ and polarization voltage u_p treated as model state variables. The battery terminal voltage equation $u_b = R_b i_b + U_{oc} + u_p$ is implemented by using the identified battery parameter static maps $R_b(\xi, i_b)$, $R_p(\xi, i_b)$, $\tau_p(\xi, i_b)$ and $U_{oc}(\xi)$ as shown in Fig. 4. The overall simulation model and the above parameter static maps are implemented within the MATLAB/Simulink software environment, with the above parameter maps implemented either as two-dimensional look-up tables (R_b, R_p, τ_p) or a one-dimensional look-up table (U_{oc}). To facilitate high-precision of the battery cell model during simulations, the dynamic equations within the simulation model are solved by using the variable-step ODE45 solver (a medium-order method for non-stiff equations), with relative and absolute tolerances of 10^{-3} and 10^{-6}, respectively.

It should be noted that the second-order RC model can be generally more accurate in capturing the more complex aspects of battery polarization voltage dynamics, as shown in [20] where the second-order RC network polarization voltage model has been identified based on the battery current step response characteristic. In contrast, the first-order RC model of polarization voltage dynamics used herein has been identified by using the auto-regressive model with exogenous inputs (ARX model) and least-squares identification technique [51], which primarily identified the dominant dynamics of the polarization voltage model. More precisely, the less dominant dynamic modes have been shown to exhibit very fast response dynamics (typically much less than the identification data sampling time $T = 1$s used in [51]), which has been attributed to the numerical error of the LS-based parameter estimation technique. One way of dealing with this problem would have been to utilize the battery model identification methodology presented in [20], but that would be beyond the scope of this work.

3. Charging control systems and state-of-charge estimator

This section outlines the design of the benchmark CCCV control system based on battery voltage PI controller and the fuzzy logic-based battery charging controller, along with the design of the EKF-based SoC estimator.

3.1. Charging control systems

Figure 5 shows the control system structure for constant-current/constant voltage (CCCV) battery charging based on the inner current control loop (assumed to embedded within the charging DC/DC power converter) with battery terminal voltage limiting outer feedback loop featuring a proportional-integral (PI) feedback controller. This type of charging control system may be considered a state-of-the-art benchmark case. In this so-called cascade control system arrangement, the inner current control loop receives the current reference i_{bR} as a sum of the maximum charging current I_{max} used during the constant-current stage of the charging process and the negative current command i_{blim} from the superimposed voltage limiting controller, which is activated when the battery terminal voltage measurement u_{bs} exceeds the battery voltage limit value u_{blim} (dead-zone block in Fig. 5). The main advantage of the CCCV approach is that the charging current and battery terminal voltage are effectively limited by means of respective battery controllers, thus reducing battery thermal stresses and preventing battery over-voltages [27]. In

particular, the battery current limit can be preset to the recommended battery charging current value obtained from battery manufacturers' data, whereas the battery voltage limit is typically set to the open-circuit voltage (OCV) value corresponding to 100% battery state-of-charge [27]. In that way, the CCCV charging control system can be easily adapted to different battery types, each characterized by different recommended charging current values and end-of-charge battery voltages. The detailed procedure for voltage PI controller tuning is presented in [31]. The comprehensive analysis presented therein has shown such control strategy results in battery terminal voltage asymptotically reaching the desired open-circuit voltage value $U_{oc}(\xi_R)$ related to the desired state-of-charge target ξ_R as the battery charging current i_b approaches zero in the final, constant-current phase of the charging process.

Fuzzy logic is commonly found in expert systems, wherein the expert knowledge can be represented in the form of linguistic IF-THEN relationships or linguistic rules [53]. Block diagram in Figure 6 shows the fuzzy logic-based battery charging control system comprising a fuzzy controller with two feedback variables: battery SoC difference $\Delta\xi$ (control error) and battery terminal voltage. Membership functions $\mu_i(\Delta\xi(k))$ and $\mu_j(u_b(k))$ and the output function values uch in the output set of the proposed fuzzy logic-based controller are shown in Fig. 7. In this application, smoothed trapezoidal membership functions shapes are used in the inference part of the controller, as shown in Figs. 7a and 7b. There are four membership functions associated with SoC difference (Fig. 7a): high SoC difference (red dashed curve), medium SoC difference (black dash-dotted curve), low SoC difference (blue dash-dotted curve), and near-zero SoC difference (green solid curve). The latter membership function and its associated linguistic rule basically determine the end-of-charging behavior of the fuzzy logic controller, wherein the controller output should be lowered towards its minimum value which corresponds to the fully charged battery terminal voltage and zero-current conditions. On the other hand, there are three battery voltage-related membership functions (Fig. 7b) associated with low battery voltage (red dashed curve), medium battery voltage (black solid curve) and high battery voltage (blue dash-dotted curve), which, alongside the other SoC difference membership functions determine the charging behavior (fuzzy controller output, i.e. voltage command uc) when the battery is being charged. The output (inference) part of the fuzzy control law is of the Mamdani type (see [53]), and its input-output map uc is shown in Fig. 7c. It uses triangular output weighting functions (corresponding to fast charge, normal mode and end-of-charge) to assign appropriate power converter voltage command in relation to fuzzy controller input rules. Greater weight is assigned to SoC difference values in the mid-to-high range, and the voltage command u_c is also adapted with respect to battery terminal voltage to address possible violations of battery current limitations.

3.2. State-of-charge estimator

The battery equivalent circuit model identification results are used as a basis for battery state variable estimation, which, according to equations (1) and (2), translates to on-line estimation of battery polarization voltage and state-of-charge. Due to the non-linear nature of the battery model (i.e. it is characterized by non-linear parameter maps, as illustrated in Figs. 2 and 3), a suitable non-linear state estimator, such as the EKF [54] needs to be employed for this task.

The process model given by equations (1) and (2) is re-written in the matrix-vector state-space form and transformed into its discrete-time counterpart that can be used within the EKF-based state estimator [54]:

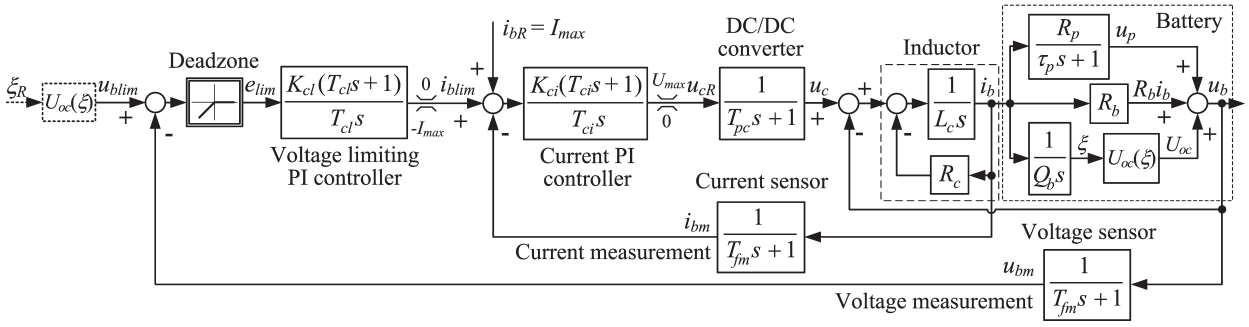

Fig. 5. Cascade control system arrangement for battery charging with battery terminal voltage limiting controller [31].

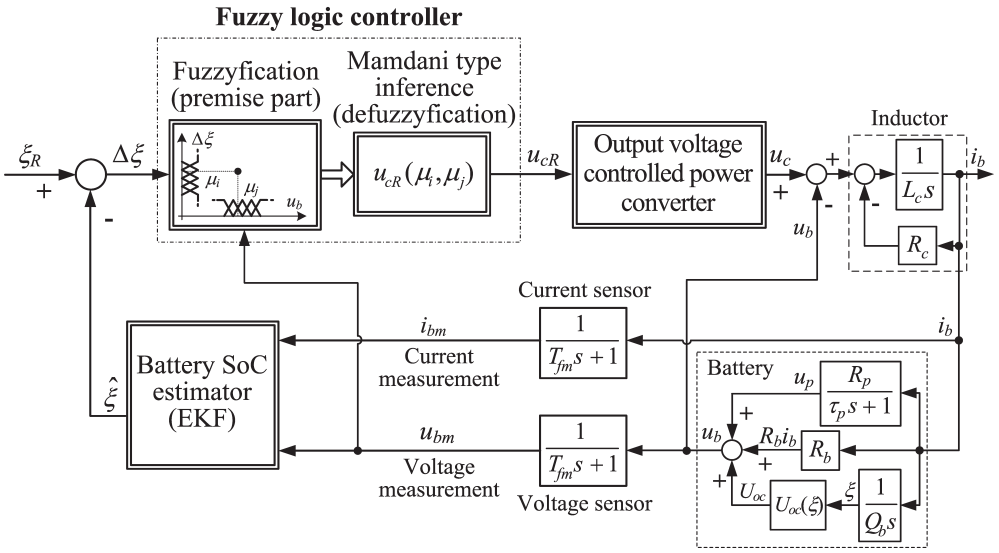

Fig. 6. Block diagram representation of fuzzy logic-based controller for battery charging utilizing SoC estimator and battery terminal voltage feedback.

$$\boldsymbol{x}(k) = \boldsymbol{f}(\boldsymbol{x}(k-1), i_{bm}(k-1)) + \boldsymbol{\Omega}\boldsymbol{v}(k), \tag{3}$$

$$u_{bm}(k) = \boldsymbol{h}(x(k), i_{bm}(k)) + e(k), \tag{4}$$

where u_{bm} and i_{bm} are battery voltage and current measurements, respectively (see Figs. 5 and 6), while the state variable vector $\mathbf{x}(k)$, the state perturbation covariance matrix $\mathbf{Q}$ and stochastic perturbation scaling matrix $\boldsymbol{\Omega}$ are defined as follows:

$$\boldsymbol{x}(k) = \begin{bmatrix} u_p(k) \\ \xi(k) \end{bmatrix}, \quad \boldsymbol{\Omega} = \begin{bmatrix} T & 0 \\ 0 & T \end{bmatrix}, \quad \boldsymbol{Q} = \begin{bmatrix} q_u & 0 \\ 0 & q_\xi \end{bmatrix}. \tag{5}$$

The block diagram representation of the EKF-based estimator is shown in Fig 8, with the nonlinear state-space model used within it to calculate the so-called a-priori state estimate $\hat{\boldsymbol{x}}(k|k-1)$, which is subsequently corrected via battery voltage measurement resulting in the final (a-posteriori) state estimate $\hat{\boldsymbol{x}}(k|k)$. For that purpose, the estimation algorithm needs to calculate the estimator correction gains based on the so-called Ricatti equation [54]. This process requires the calculation of the following Jacobian matrices, which are related to partial derivatives of all battery model parameters with respect to battery state-of-charge and polarization voltage (battery system states):

$$\boldsymbol{F}(k) = \frac{\partial \boldsymbol{f}(\hat{\boldsymbol{x}}, i_b)}{\partial \hat{\boldsymbol{x}}}\bigg|_{\substack{\hat{\boldsymbol{x}}(k-1|k-1), \\ i_b(k-1)}}, \tag{6}$$

$$\boldsymbol{H}(k) = \frac{\partial \boldsymbol{h}(\hat{\boldsymbol{x}}, i_b)}{\partial \hat{\boldsymbol{x}}}\bigg|_{\substack{\hat{\boldsymbol{x}}(k|k-1), \\ i_b(k)}}, \tag{7}$$

which are required to estimate the error covariance matrix $\mathbf{P}$ within the estimator by using the assumed variances of state perturbations $\boldsymbol{v}$ (characterized by the perturbation covariance matrix $\mathbf{Q}$ whose elements are chosen as a trade-off between estimator noise sensitivity and tracking ability) and the noise e variance r in the battery terminal voltage (measurement) u_b [55].

4. Simulation results

Figure 9 shows the results of the EKF-based SoC estimator subjected to the constant-current battery charging simulation scenario with battery current equal to 24 A. The results show rather good agreement between the state-of-charge obtained from the simulation model and the estimator in the estimator steady state (Fig. 9a), which points to favorable estimator tracking ability. Fig. 9b shows that the estimator is characterized by fast convergence towards the actual battery state-of-charge from the mismatched state, i.e. it can be tuned for rather fast and well-damped response. The state-of-charge estimator steady-state tracking error absolute value does not exceed 0.05%.

The proposed fuzzy logic-based battery charging control system has been verified against the voltage PI controller-based conventional charging control strategy [31] by means of simulations using the model of the LTO battery cell and the DC/DC (buck) power converter implemented within MATLAB/Simulink software environment, with power converter inductor modeled with inductance L_c = 0.7 mH, and series resistance R_c = 50 mΩ [31]. Since the fuzzy logic-based control strategy has different structure (i.e. it does not include the inner current control loop and associated charging current limit at the controller output) compared to the conventional voltage PI controller, it does not yield the constant-current/constant-voltage (CCCV) charging profile characterized by a rather long

constant-current (CC) charging interval followed by a relatively short constant-voltage (CV) charging interval as the voltage PI controller does [31]. Therefore, to compare these controllers in a straightforward way, the fuzzy logic-based control strategy is simulated first. The charging simulation scenario then utilizes the conventional (PI controller-based) control strategy whose charging current limit (which determines the constant current charging phase) is set to the average value of the charging current obtained by the fuzzy logic-based charging system. In this way, the charging current commanded by the PI controller during the CC charging interval would result in a similar amount of charge being stored within the battery as in the case of fuzzy logic-based charging controller with variable charging current profile. In both cases, the end of charging is indicated when the charging current drops below the minimum current value I_{min}, set in simulations to I_{min} = 10 mA.

Figure 10 shows the comparative results of the proposed fuzzy logic-based and conventional control strategy. The fuzzy logic-based control strategy initiates battery charging with relatively large currents by means of commanding the corresponding voltage reference to the voltage-controlled DC/DC power converter (see red traces in Figs. 10b and 10d), which is progressively increased until it reaches the recommended charging current value of 30 A which corresponds to the so-called 1C charging rate [50]. Large current rates are maintained in the middle of the SoC region corresponding to low values of battery series and polarization resistances (cf. traces in Figs. 10a and 10b). As the SoC increases towards the fully charged battery state, the charging current is progressively decreased by means of DC/DC power converter. Namely, throughout the charging process, the battery voltage steadily increases (Fig. 10c), and the fuzzy logic algorithm adjusts the DC/DC converter voltage command to decrease the current when the estimated SoC provided by the EKF-based estimator approaches the fully charged state, as well as to keep the battery terminal voltage within the prescribed limits [50]. The fuzzy logic-based control strategy has resulted in the total charging time of 5701 s, and the average changing current of about 20 A. The latter value has been used as the charging current limit (I_{max} = 20 A in the block diagram in Fig. 7) within the

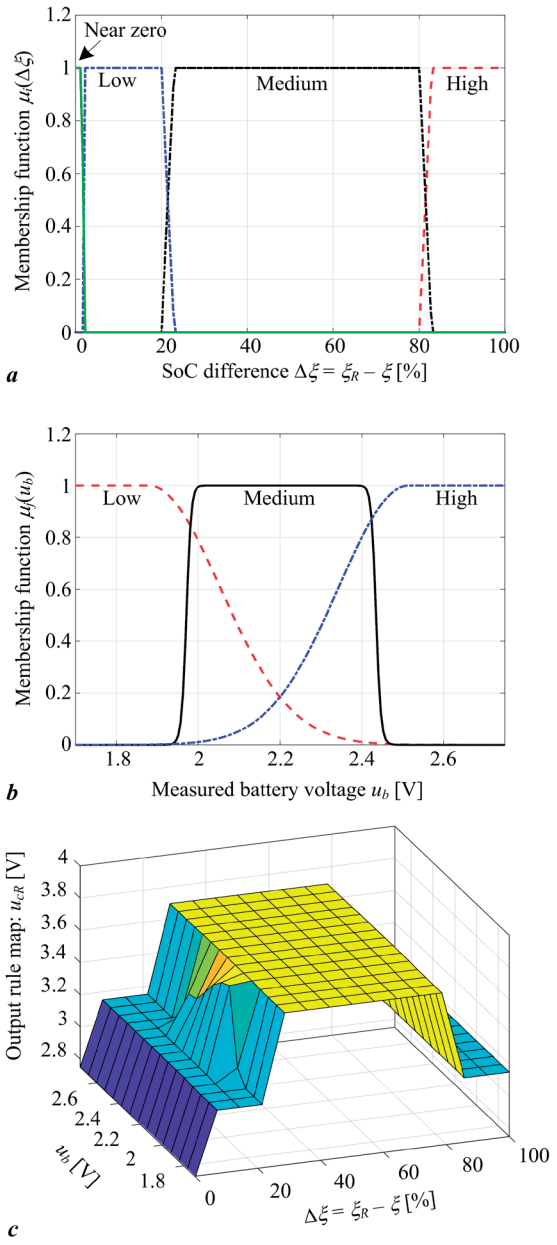

Fig. 7. Membership functions of fuzzy controller with respect to SoC control error signal (b) and battery terminal voltage signal (b), and output rule values (c).

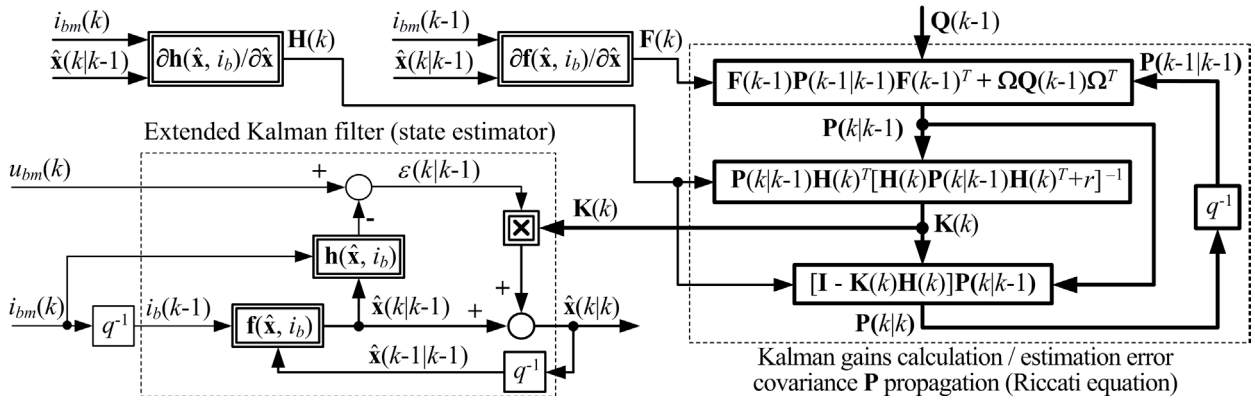

Fig. 8. Principal block diagram representation of extended Kalman filter for battery state-of-charge estimation.

conventional PI controller-based CCCV control strategy. The results in Fig. 10 show that the conventional CCCV control strategy is predominated by the constant-current regime throughout the charging process, with the constant voltage charging regime being only briefly active near the end of charging. This results in battery SoC increasing with constant slope, in contrast to the fuzzy logic-based strategy, wherein the SoC slope is variable, and adjusted with respect to the SoC operating point (Fig. 10a). The estimated SoC from the EKF estimator used as the fuzzy logic controller feedback is again very well matched with the actual battery SoC (see results in Fig. 9) which points to fast convergence and good tracking ability of the EKF-based estimator (cf. red solid trace and blue dashed trace in Fig. 10a). The conventional CCCV strategy results in the charging time of 6297 s. Consequently, the fuzzy logic-based control strategy has in fact achieved a 17.7% speedup compared to the conventional PI controller-based CCCV control strategy, while achieving nearly identical end-of-charging SoC value under these test conditions (Table 1).

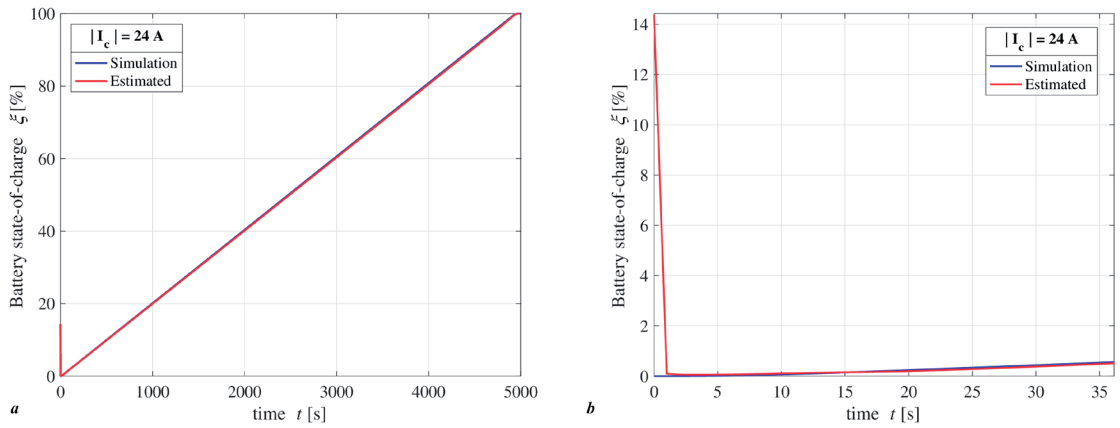

Fig. 9. Comparative EKF vs. battery simulation model responses during constant-current charging: overall results (a), and initial (transient) part of response from mismatched state (b).

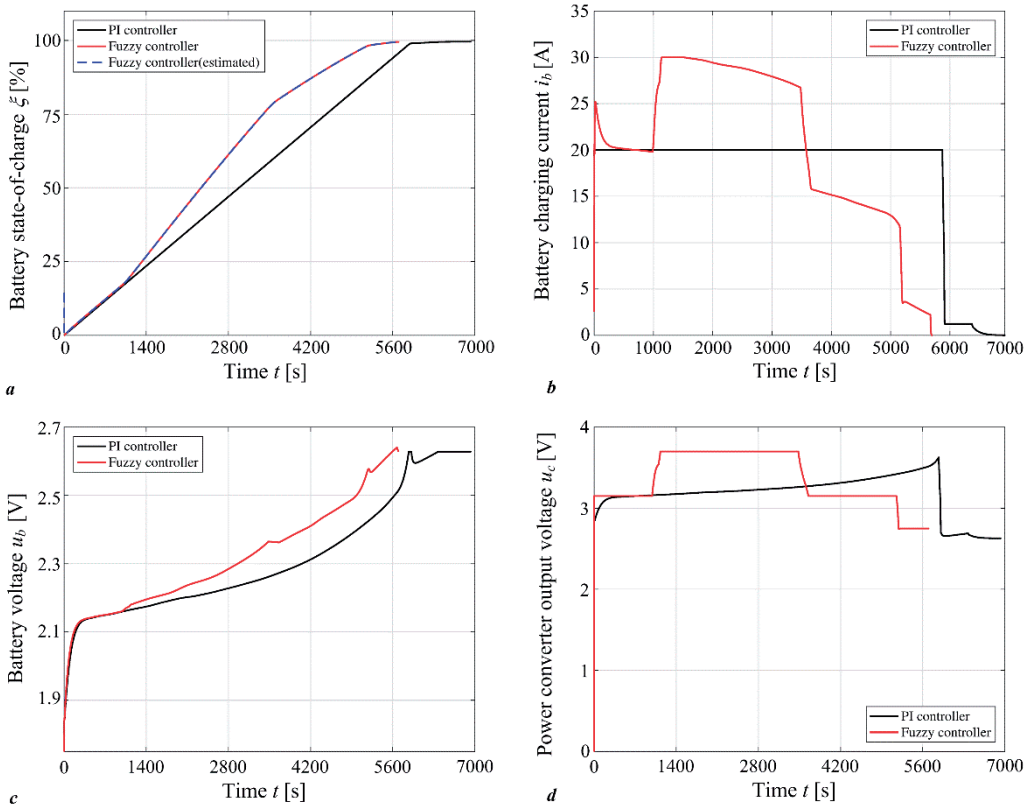

Fig. 10. Comparative simulation results of fuzzy controller-based and voltage PI controller-based battery charging systems: state-of-charge responses (a), charging current responses (b), battery terminal voltage trace (c) and DC/DC power converter output voltage traces (d).

As indicated in Fig. 10b, the CCCV charging strategy will try to maintain the constant charging rate practically until the battery terminal voltage reaches the target value, whereas the fuzzy controller (after the initial "boost" of the charging current) tends to gradually decrease the charging current before the end of charging occurs. The current profile effectively determines the battery heat losses due to series and polarization resistance ($P_t = i_b^2 R_s + u_p^2/R_p$), whose values tend to increase at higher SoC values (see Fig. 3). Figure 11 shows the profiles of battery model series and polarization resistance parameters R_b and R_p (Fig. 11a and 11b), heat dissipation losses P_t (Fig. 11c) and total generated heat $W_t = \int P_t dt$ (Fig. 11d). Simulation results show that the fuzzy controller resulting in higher battery charging currents indeed causes higher heat losses during the initial "boost" of battery current, but subsequently decreases the heat dissipation in the second part of the charging process, whereas the PI controller-based CCCV charging strategy tends to increase the heat losses towards the end of charging (Fig. 11c). Consequently, both charging strategies result in similar total generated heat at the end of charging, with the fuzzy controller-based charging generating only 7.1% larger amount of total waste heat compared with PI controller-based charging strategy (Fig. 11d). This points to similar performance of these control strategies with respect to battery heat losses, whereas the fuzzy controller-based charging strategy has been shown to be more effective with respect to battery charging time (see discussion related to Fig. 10). Thus, it may be inferred that utilization of fuzzy controller-based charging strategy may indeed be well suited for faster battery recharging, while also being characterized by similar end-of-charging battery temperature, which is directly related to the total waste heat generated during charging. In conclusion, the fuzzy logic-based charging strategy, even though being characterized by 17.7% shorter recharge time and higher charging rates, would have the same effect on heat losses-related battery aging effects and battery state-of-health, and would likely result in similar battery lifetime when compared to the conventional CCCV strategy which is typically used in practical applications.

The sampling time of the PI controller, fuzzy logic charging controller and the EKF-based state-of-charge estimator in the above simulation scenario have been set to $T = 1$ s (sampling frequency is 1 Hz), which is justified because the charging process and the dominant dynamics of the process model are rather slow. Since the sampling time is rather large, the target microcontroller operating at standard clock speeds should be able to perform the numerical calculations associated with the EKF estimator and the fuzzy logic-based controller algorithms, provided that it also possesses embedded floating point arithmetic functionality. One such example would be the ARM Cortex-M4 and Arm Cortex-M7 architectures [56], which also feature analog interfaces needed for battery measurement signals acquisition. An example of a development board that could be used for prototyping and testing such solutions within the open-source software environment would be the Arduino GIGA R1 [57].

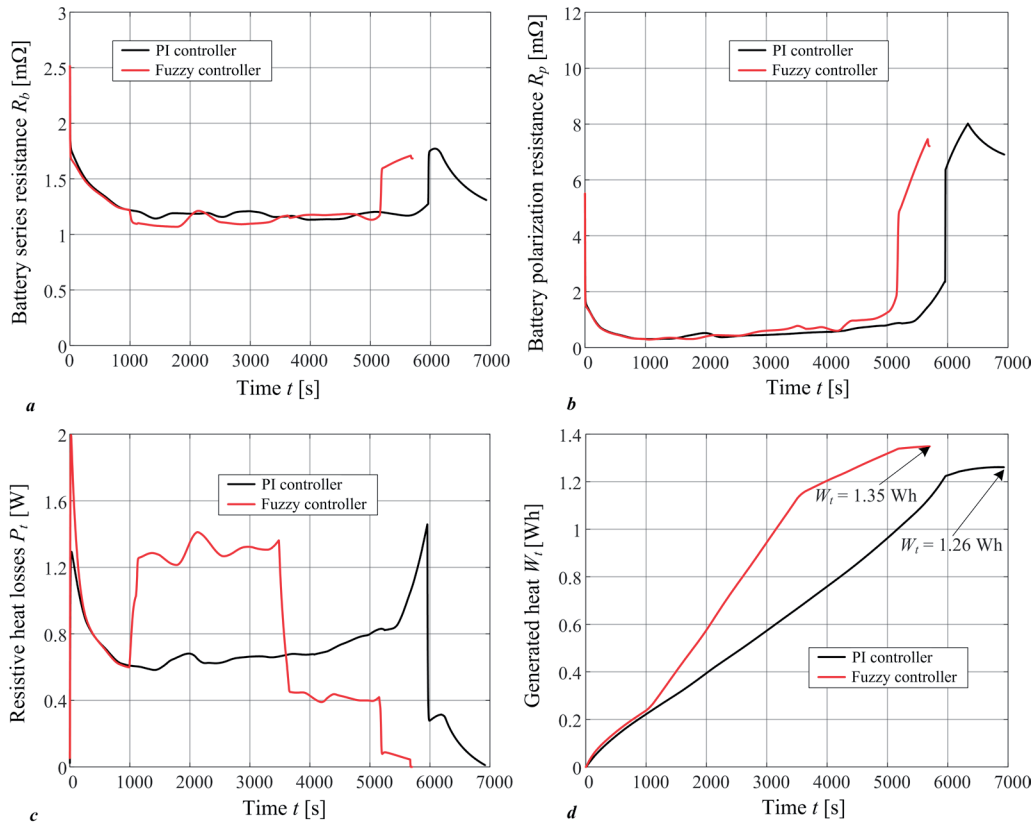

Fig. 11. Comparative simulation traces of battery series resistance (a), battery polarization resistance (b), resistive heat losses (c) and overall generated heat (d) during charging by means of conventional PI control and fuzzy logic control.

Table 1. Comparative results of conventional vs. fuzzy logic-based charging control strategy.

	Fuzzy controller	PI voltage controller
Charging time [s]	5701	6927
Final battery voltage [V]	2.6280	2.6283
Final battery SoC [%]	0.9950	0.9956

5. Conclusion

The paper has presented the results of simulation verification and benchmarking of the fuzzy logic-based charging control system with respect to the battery voltage PI controller-based conventional constant-current/constant voltage (CCCV) control strategy for a state-of-the-art lithium titanate (LTO) 30 Ah/2.4 V battery cell. For simulation verification of both control strategies, a dedicated equivalent electrical circuit simulation model of the LTO battery cell has been built based on the previously obtained experimental data. The results have indicated that the fuzzy logic-based charging controller can recharge the battery in a much shorter time compared to the conventional CCCV charging, while achieving approximately the same average charging current value.

The charging control system benchmark, i.e. the conventional battery terminal voltage PI controller-based system has been arranged in the co-called cascade control structure, with the superimposed PI controller commanding the current target to the DC/DC power converter with straightforward limitation of the battery charging current. In the case of fuzzy logic-based charging control, the fuzzy logic controller commands an appropriate voltage reference to the DC/DC power converter. The DC/DC converter voltage reference is determined based on the finite set of linguistic rules in the input (premise) part of the fuzzy control law, which determine the membership levels of battery state-of-charge tracking error and terminal voltage to corresponding input sets. Based on those membership levels, the output (inference) part of the fuzzy control law calculates the so-called "crisp" output value which corresponds to the DC/DC power converter voltage reference. In order to implement the fuzzy control law, a suitable battery state-of-charge estimator has been designed using the battery cell equivalent electrical circuit model and the extended Kalman filter (EKF) design methodology.

The proposed charging control strategies have been verified and compared within the MATLAB/Simulink software environment. The EKF-based estimator has been capable of accurately tracking the battery state-of-charge (SoC), while also being characterized by fast convergence. The fuzzy logic-based charging control system utilizing the additional estimated battery SoC feedback in combination with the battery terminal voltage feedback has shown distinct advantages over the conventional PI controller-based CCCV control strategy based on battery terminal voltage feedback. In particular, the fuzzy logic-based charging control system has achieved a 17.7% speedup of the charging process while honoring the battery terminal voltage and current limitations, which is primarily due to the additional degree of freedom with respect to battery charging current in the low-to-middle battery *SoC* operating regime, which the conventional CCCV charging strategy cannot take advantage of.

Future work is going to be directed towards further refinement of the fuzzy logic-based charging control system and its adaptation for the more general case of current-controlled DC/DC power converter, and state-of-health (SoH) aware adaptation aimed at minimizing battery stresses during charging. Further developments of suitable battery SoC/SoH estimators are also foreseen along with the experimental verification of the proposed fuzzy logic-based charging control system.

6. Acknowledgment

This research has been supported by the European Commission through the Horizon 2020 project "Maximizing the impact of innovative energy approaches in the EU islands" (INSULAE).

7. References

[1] McCollum, D., Krey, V., Kolp, P., Nagai, Y., & Riahi, K. (2014). Transport electrification: A key element for energy system transformation and climate stabilization. *Climate Change*, *(38)*, 651-664.

[2] Buzzonii, L., & Pede, G. (2012). New prospects for public transport electrification. In *Proceedings of International Conference on Electrical Systems for Aircraft, Railway and Ship Propulsion (ESARS 2012)*.

[3] Deur, J., Škugor, B., & Cipek, M. (2015). Integration of Electric Vehicles into Energy and Transport Systems. *Automatika - Journal for Control, Measurement, Electronics, Computing and Communications*, *(56)*, 395-410.

[4] Chinese, D., Pinamonti, P., & Mauro, C. (2021). A spatially explicit optimization model for the selection of sustainable transport technologies at regional bus companies. *Optimization and Engineering*, *(22)*, 1921-1954.

[5] Cipek, M., Pavković, D., Kljaić, Z., & Mlinarić, T.J. (2019). Assessment of Battery-Hybrid Diesel-electric Locomotive Fuel Savings and Emission Reduction Potentials based on a Realistic Mountainous Rail Route. *Energy*, *(173)*, 1154-1171.

[6] Cipek, M., Pavković, D., Krznar, M., Kljaić, Z., & Mlinarić, T.J. (2021). Comparative Analysis of Conventional Diesel-Electric and Hypothetical Battery-Electric Heavy Haul Locomotive Operation in terms of Fuel Savings and Emissions Reduction Potentials. *Energy*, *(232)*, 121097.

[7] Victoria, M., Zhu, K., Brown, T., Andresen, G.B., & Greiner, M. (2019). The role of storage technologies throughout the decarbonisation of the sector-coupled European energy system. *Energy Conversion and Management*, *(201)*, 111977.

[8] Sandhya, C.P., John, B., & Gouri, C. (2014). Lithium titanate as anode material for lithium-ion cells: a review. *Ionics*, *(20)*, 601–620.

[9] Liang, Z., Hui-Lin, P., Yong-Sheng, H., Hong, L., & Li-Quan, C. (2012). Spinel lithium titanate (Li4Ti5O12) as novel anode material for room-temperature sodium-ion battery. *Chinese Physics B*, *(21)*, 028201.

[10] Zhang, X., Peng, H., Wang, H., & Ouyang, M. (2018). Hybrid Lithium Iron Phosphate Battery and Lithium Titanate Battery Systems for Electric Buses. *IEEE Transactions on Vehicular Technology*, *(67)*, 956–965.

[11] Nemeth, T., Schröer, P., Kuipers, M., & Sauer, D.U. (2020). Lithium titanate oxide battery cells for high-power automotive applications – Electro-thermal properties, aging behavior and cost considerations. *Journal of Energy Storage*, *(31)*, 101656.

[12] Odziomek, M., Chaput, F., Rutkowska, A., Świerczek, K., Olszewska, D., Sitarz, M., Lerouge, F., & Parola, S. (2017). Hierarchically structured lithium titanate for ultrafast charging in long-life high-capacity batteries. *Nature Communications*, *(8)*, 15636.

[13] Song, C., Luo, J., Chen, X., & Peng, Z. (2023). SoC Estimation of Lithium Titanate Battery Based on Variable Temperature Equivalent Model. In S. Patnaik, R. Kountchev, Y. Tai, & R. Kountcheva (Eds.), *3D Imaging—Multidimensional Signal Processing and Deep Learning* (pp. 123-143). Smart Innovation, Systems and Technologies, Vol 349.

[14] Jenu, S., Hentunen, A., Haavisto, J., Pihlatie, M. (2022). State of health estimation of cycle aged large format lithium-ion cells based on partial charging. *Journal of Energy Storage, 46*, 103855.

[15] Patnaik, L., Praneeth, A. V. J. S., & Williamson, S. S. (2019). A Closed-Loop Constant-Temperature Constant-Voltage Charging Technique to Reduce Charge Time of Lithium-Ion Batteries. *IEEE Transactions on Industrial Electronics*, *66*(5), 1059-1067.

[16] Fu, Z., Fan, Y., Cai, X., Zheng, Z., Xue, J., & Zhang, K. (2018). Lithium Titanate Battery Management System Based on MPPT and Four-Stage Charging Control for Photovoltaic Energy Storage. *Applied Sciences*, *8*(12), 2520.

[17] Dang, G., Zhang, M., Min, F., Zhang, Y., Zhang, B., Zhang, Q., Wang, J., Zhou, Y., Liu, W., Xie, J., & Mao, S. S. (2023). Lithium titanate battery system enables hybrid electric heavy-duty vehicles. *Journal of Energy Storage*, *74*, 109313.

[18] Xie, J., Wei, X., Bo, X., Zhang, P., Chen, P., Hao, W, & Yuan, M. (2023). State of charge estimation of lithium-ion battery based on extended Kalman filter algorithm. *Frontiers in Energy Research*, *11*, 1180881.

[19] Awelewa, A., Omiloli, K., Samuel, I., Olajube, A., & Popoola, O. (2023). Robust hybrid estimator for the state of charge of a lithium-ion battery. *Frontiers in Energy Research*, *10*, 1069364.

[20] Madani, S. S., Schaltz, E., Knudsen Kær, S. (2019) An Electrical Equivalent Circuit Model of a Lithium Titanate Oxide Battery. *Batteries, 5,* 31.

[21] Sarda, J., Patel, H., Popat, Y., Hui, K. L., & Sain, M. (2023). Review of Management System and State-of-Charge Estimation Methods for Electric Vehicles. *World Electric Vehicle Journal*, *14*, 325.

[22] Girijaprasanna, T., Dhanamjayulu, C. (2022). A Review on Different State of Battery Charge Estimation Techniques and Management Systems for EV Applications. *Electronics, 11*, 1795.

[23] Omiloli, K., Awelewa, A., Samuel, I., Obiazi, O., & Katende, J. (2023). State of charge estimation based on a modified extended Kalman filter. *International Journal of Electrical and Computer Engineering (IJECE)*, *13*(5), 5054-5065.

[24] Ghaeminezhad, N., & Monfared, M. (2022). Charging control strategies for lithium-ion battery packs: Review and recent developments. *IET Power Electronics*, *15*, 349–367.

[25] Salazar, D., & Garcia, M. (2022). Estimation and Comparison of SoC in Batteries Used in Electromobility Using the Thevenin Model and Coulomb Ampere Counting. *Energies*, *15*, 7204.

[26] Singirikonda, S., & Obulesu, Y. P. (2020). Battery modelling and state of charge estimation methods for Energy Management in Electric Vehicle – A review. *IOP Conference Series: Materials Science and Engineering*, *937*(1), 012046.

[27] Pavković, D., Lobrović, M., Hrgetić, M., Komljenović, A., & Smetko, V. (2014). Battery Current and Voltage Control System Design with Charging Application. In *Proceedings of 2014 IEEE Multi-Conference on Systems and Control* (pp. 1133–1138).

[28] Szumanowski, A., & Chang, Y. (2008). Battery Management System Based on Battery Nonlinear Dynamics Modeling. *IEEE Transactions on Vehicular Technology*, *57*(3), 1425 – 1432.

[29] Kvaternik, K., Pavković, D., Kozhushko, Y., & Cipek, M. (2022). Extended Kalman Filter Design for State-of-Charge Estimation of a Lithium-Titanate Battery Cell. In *Proceedings of the 2022 International Conference on Smart Systems and Technologies (SST)* (pp. 249–254).

[30] Namor, E., Torregrossa, D., Sossan, F., Cherkaoui, R., & Paolone, M. (2016). Assessment of battery ageing and implementation of an ageing aware control strategy for a load leveling application of a lithium titanate battery energy storage system. In *Proceedings of 2016 IEEE 17th Workshop on Control and Modeling for Power Electronics (COMPEL)* (pp. 1-6).

[31] Pavković, D., Premec, A., Krznar, M., & Cipek, M. (2022). Current and voltage control system designs with EKF-based state-of-charge estimator for the purpose of LiFePO4 battery cell charging. *Optimization and Engineering*, *23*, 2235-2263.

[32] Lin, Q., Wang, J., Xiong, R., Shen, W., & He, H. (2019). Towards a smarter battery management system: A critical review on optimal charging methods of lithium-ion batteries. *Energy*, *183*, 220-234.

[33] Banguero, E., Correcher, A., Pérez-Navarro, Á., Morant, F., & Aristizabal, A. (2018). A Review on Battery Charging and Discharging Control Strategies: Application to Renewable Energy Systems. *Energies*, *11*(4), 1021.

[34] Tomaszewska, A., Chu, Z., Feng, X., O'Kane, S., Liu, X., Chen, J., Ji, C., Endler, E., Li, R., Liu, L., Li, Y., Zheng, S., Vetterlein, S., Gao, M., Du, J., Parkes, M., Ouyang, M., Marinescu, M., Offer, G., & Wu, B. (2019). Lithium-ion battery fast charging: A review. *eTransportation*, *1*, 100011.

[35] Gao, Y., Zhang, X., Cheng, Q., Guo, B., & Yang, J. (2019). Classification and Review of the Charging Strategies for Commercial Lithium-Ion Batteries. *IEEE Access*, *7*, 43511-43524.

[36] Hsieh, G.-C., Chen, L.-R., & Huang, K.-S. (2001). Fuzzy-Controlled Li-Ion Battery Charge System with Active State-of-Charge Controller. *IEEE Transactions on Industrial Electronics*, *48*(3), 585-593.

[37] Vo, T.T., Chen, X., Shen, W., & Kapoor, A. (2015). New charging strategy for lithium-ion batteries based on the integration of Taguchi method and state of charge estimation. *Journal of Power Sources*, *273*, 413-422.

[38] Zou, C., Hu, X., Wei, Z., Wik, T., & Egardt, B. (2018). Electrochemical Estimation and Control for Lithium-Ion Battery Health-Aware Fast Charging. *IEEE Transactions on Industrial Electronics*, *65*(8), 6635-6645.

[39] Zou, C., Hu, X., Wei, Z., & Tang, X. (2017) Electrothermal dynamics-conscious lithium-ion battery cell-level charging management via state-monitored predictive control, *Energy, 141*, 250-259.

[40] Jiang, J., Liu, Q., Zhang, C., & Zhang, W. (2014). Evaluation of Acceptable Charging Current of Power Li-Ion Batteries Based on Polarization Characteristics. *IEEE Transactions on Industrial Electronics*, *61*(12), 6844-6851.

[41] Abdel-Monem, M., Trad, K., Omar, N., Hegazy, O., Van den Bossche, P., & Van Mierlo, J. (2017). Influence analysis of static and dynamic fast-charging current profiles on ageing performance of commercial lithium-ion batteries. *Energy*, *120*, 171-191.

[42] Lee, K.-T., Dai, M.-J., & Chuang, C.-C. (2018). Temperature-Compensated Model for Lithium-Ion Polymer Batteries with Extended Kalman Filter State-of-Charge Estimation for an Implantable Charger. *IEEE Transactions on Industrial Electronics*, *65*(1), 589-596.

[43] Rai, R., Gaglani, M., Das, S., & Panigrahi, T. (2020). Multi-Level Constant Current Based Fast Li-Ion Battery Charging Scheme with LMS Based Online State of Charge Estimation. In *Proceedings of 2020 IEEE Kansas Power and Energy Conference (KPEC 2020)*. Manhattan, KS, USA.

[44] Jiang, L., Huang, Y., Li, Y., Yu, J., Qiao, X., Huang, C., Cao, Y. (2021) Optimization of Variable-Current Charging Strategy Based on SOC Segmentation for Li-ion Battery, *IEEE Transactions on Intelligent Transportation Systems, 22*(1), 622-629.

[45] Chen, Z., Xia, B., Mi, C. C., & Xiong, R. (2015). Loss-Minimization-Based Charging Strategy for Lithium-Ion Battery. *IEEE Transactions on Industry Applications*, *51*(5), 4121-4129.

[46] Wassiliadis, N., Schneider, J., Frank, A., Wildfeuer, L., Lin, X., Jossen, A., & Lienkamp, M. (2021). Review of fast charging strategies for lithium-ion battery systems and their applicability for battery electric vehicles. *Journal of Energy Storage*, *44*, 103306.

[47] Al-Saadi, M., Olmos, J., Saez-de-Ibarra, A., Van Mierlo, J., & Berecibar, M. (2022). Fast Charging Impact on the Lithium-Ion Batteries' Lifetime and Cost-Effective Battery Sizing in Heavy-Duty Electric Vehicles Applications. *Energies*, *15*(4), 1278.

[48] Thakur, A. K., Sathyamurthy, R., Velraj, R., Saidur, R., Pandey, A. K., Ma, Z., Singh, P., Hazra, S., K., Sharshir, S. W., Prabakaran, R., Chul Kim, S., Panchal, S., & Ali, H. M. (2023). A state-of-the art review on advancing battery thermal management systems for fast-charging. *Applied Thermal Engineering*, *226*, 120303.

[49] Ceraolo, M. (2000). New Dynamical Models of Lead-Acid Batteries. *IEEE Transactions on Power Systems*, *15*(4), 1184-1190.

[50] https://shop.gwl.eu/LTO-technology/Cylindrical-Lithium-Titanate-Oxid-Battery-Cell-LTO-2-3V-30AH.html (Accessed 9.2.2024.)

[51] Kvaternik, K., Pavković, D., Kozhushko, Y., Cipek, M., & Krznar, M. (2023). Lithium-Titanate Battery Cell Experimental Identification and State-of-Charge Estimator Design. In *Proceedings of the 18th Conference on Sustainable Development of Energy, Water, and Environment Systems* (Paper No. 0036). Dubrovnik, Croatia.

[52] Ljung, L. (1987). *System identification – theory for the user*. Prentice Hall

[53] Ross, T.J. (2004). *Fuzzy Logic with Engineering Applications*. Chichester, UK: John Wiley & Sons.

[54] Grewal, M.S., & Andrews, A.P. (2001). *Kalman filtering – theory and practice*. John Wiley and Sons Ltd.

[55] Pavković, D., Krznar, M., Komljenović, A., Hrgetić, M., & Zorc, D. (2017). Dual EKF-based State and Parameter Estimator for a $LiFePO_4$ Battery Cell. *Journal of Power Electronics*, *17*(2), 398-410.

[56] STMicroelectronics: 32-bit Arm® Cortex®-M7 480MHz MCUs. Data Sheet No. DS12110 Rev 10, 2023. https://www.st.com/content/st_com/en/arm-32-bit-microcontrollers/arm-cortex-m7.html (Accessed 19.7.2024.)

[57] Arduino® GIGA R1 WiFi. Reference Manual SKU ABX00063. https://store.arduino.cc/products/giga-r1-wifi (Accessed 22.07.2024.)

Jie Zhang[1], Kun Jiang[1], Hui Jin[1]*

Energy development status and emerging technologies in China

[1]State Key Laboratory of Multiphase Flow in Power Engineering, Xi'an Jiaotong University, Xi'an, Shaanxi, 710049, PR China

Abstract

Although countries around the world have increased the utilization of renewable and clean energy, the consumption of fossil fuels is still increasing, leading to an increasing emission of greenhouse gases, especially CO_2, into the atmosphere. The fundamental problem with this phenomenon is that most renewable energy sources are characterized by instability, low energy density, and difficulty in storage. The existing energy conversion technologies convert these primary energy sources into power energy, which is not a carrier and is not easy to transport and store. However, turning renewable energy resource into energy carriers, such as hydrogen, can solve the fundamental problem. This paper takes China as an example to deeply explore the current situation and shortcomings of the energy supply system, as well as the important tasks of energy development. The green, efficient, and low-cost production of sufficient hydrogen/power is the prerequisite and core, and low-cost long-term storage and transportation of sufficient hydrogen/power is the key. After years of research, State Key Laboratory of Multiphase Flow in Power Engineering has developed emerging technologies for preparing energy carriers based on renewable and fossil fuels. The development of these efficient and low-cost large-scale hydrogen/power generation technologies, as well as low-cost long-term hydrogen/energy storage and transportation technologies, can provide reliable core support for large-scale reduction of CO_2 emissions and sufficient and inexpensive green hydrogen/power supply, and strategic technical support for building a new green energy supply system and ensuring national energy security.

***Keywords**: H_2 production, Power generation, CO_2 reduction, Net zero, Poly-generation.*

1. Introduction

Energy is a necessity of human civilization and plays an irreplaceable role in various aspects of social development [1-3]. From the data released in the "World Energy Statistical Yearbook" from 2005 to 2020, it is evident that global consumption of oil and natural gas is on the rise. However, traditional consumption methods of fossil fuels such as oil, coal, and natural gas have always been the direct cause of serious climate and environmental problems. Greenhouse gas emissions, particularly CO_2, from the combustion and conversion of fossil fuels significantly hinder efforts to achieve the net-zero CO_2 emissions goal for global energy systems [4-7]. The significant amount of CO_2 and other greenhouse gases added to the atmosphere through the burning of fossil fuels is the main cause of extreme global climate change (El Niño, La Niña phenomena), which is irreversible on a time scale of several centuries to several thousands of years [8].

There is data indicating that global warming has been associated with the concentration of greenhouse gases in the atmosphere for a long time. In the past half century, the global average temperature has risen sharply, by about 1 °. The continuous increase in the concentration of free CO_2 in the atmosphere is currently a direct factor affecting global climate extremes, and until the mid-20th century, the annual net emissions of CO_2 have been growing slowly. However, the global emissions of CO_2 increased to 6 billion tons in 1950, and exceeded 22 billion tons by 1990. With the continuous growth of carbon emissions, the annual CO_2 emissions in recent years have exceeded 34 billion tons. Although the growth of carbon emissions has slowed down with the increase in the proportion of renewable energy utilization in recent years, it has not yet reached its peak. In addition, greenhouse gas emissions and air pollutants are usually generated from the same emission source. In 2021, PM2.5 levels in 96% or more of regional capital cities severely exceeded the upper limit values announced by the World Health Organization for air pollutants. The rapidly expanding cities are causing serious deterioration accidents in urban and surrounding air quality, and if no intervention is taken, the concentration of pollutants will continue to rise. Therefore, targeted policies must be introduced to stabilize and reduce air pollution levels. Air pollution within the biosphere will directly endanger human health, leading to approximately 4.2 million premature deaths worldwide each year. According to the research data of environmental epidemiology, the deterioration of air quality will increase the incidence rate of cardiovascular and respiratory related diseases, and further increase the mortality in serious cases. In this regard, the world urgently needs to achieve the net-zero goal as soon as possible to prevent the sustained increase in greenhouse gas and air pollutant concentrations from disrupting climate stability and endangering human health [9-10].

At present, in various fields, the energy conversion process based on fossil fuel mainly consists of two sub processes. Fossil fuel first converts chemical energy into thermal energy through violent oxidation reactions, and then converts internal energy into other forms of energy such as mechanical energy or internal energy which is directly used. However, the first process will generate a large amount of greenhouse gases mainly composed of CO_2 and harmful gases, composed of NO_x and SO_x. Numerous studies and technologies have been developed to reduce the emissions of these gases, such as carbon capture and storage technology, catalytic reduction and adsorption technology of NO_x and SO_x, IGCC (Integrated Gasification Combined Cycle) technology, etc. [11-15].

Nonetheless, the above-mentioned technologies have not yet been industrialized and applied on a large scale. The thermal power conversion in the second process is mainly used for power generation, and this process is mainly limited by the combustion efficiency of the fuel and the thermal efficiency. The thermal power generation device currently capable of achieving the highest overall plant thermal efficiency, with supercritical and ultra-supercritical devices capable of achieving approximately 46-47% and 50% plant thermal efficiency, respectively [16]. As to renewable energy, the energy conversion process is relatively simple. The most widely used renewable energy currently are wind energy, hydraulic energy, and solar energy. The utilization of wind energy and hydraulic is mainly aimed at converting mechanical energy into electrical energy, while solar energy is mainly directly converted into electrical energy through the photoelectric effect or directly converted into thermal energy through concentrated solar energy devices. Although wind power generation technology has advantages such as renewability and sustainability, environmental protection, and low operating costs, it can only generate electricity when wind drives wind turbines within a specific speed range. This fatal intermittent drawback means that wind energy cannot provide continuous and reliable power supply, and usually requires energy storage systems or backup power sources to solve this problem [17]. For hydraulic energy, it does not consume fossil fuels, does not emit harmful gases, and provides a continuous supply of clean energy. Hydroelectric power generation has almost no downtime because the water flow is only interrupted during regular maintenance and upgrades, which makes it more stable. However, the impact of hydroelectric power on the environment is its most significant drawback. The construction of dams requires the construction of additional roads and power lines, resulting in environmental damage. Dams often form reservoirs, flooding large areas and replacing natural habitats. Dams can create stagnant water areas, kill plant communities, and emit pollutants and greenhouse gases [18-19]. In comparison to wind power and hydropower, solar photovoltaic power generation is a relatively straight forward process, with no mechanical rotating parts. It does not consume fuel, nor does it emit any substances, including greenhouse gases. Furthermore, solar energy resources are widely distributed and inexhaustible, and the process is entirely noise-free and pollution-free. However, it has low energy density, large footprint, low conversion efficiency, poor stability, and also has fatal intermittent drawbacks [20-21].

For fossil fuels, the CO_2 emissions from the production of electricity, H_2, and materials mainly come from coal, oil, natural gas, and other sources [22-24]. With the transformation of the global energy supply structure system, the contribution of different fuel sources to CO_2 emissions has changed. Furthermore, as to renewable energy, a single utilization model is the main reason restricting its development towards larger scale. It is urgent to build a new type of green and low-carbon energy supply system in this regard [25-27]. The development of composite and multifunctional green H_2/electricity production technologies to achieve complementary advantages and disadvantages is a major trend in the future. The main structure of this article is as follows. The second part introduces the principles of energy conversion and utilization under traditional methods, summarizes the current status of China's energy supply structure system, and analyzes its existing problems. The third part provides a detailed introduction to the research and current status of green, efficient, and low-carbon H_2 production/power generation technologies in China. The fourth part proposes some policy recommendations for China's national strategy of achieving the "Dual Carbon" goal as soon as possible.

2. Development status of traditional energy conversion and utilization technology, industry, and supply system

Currently, traditional energy can be divided into process energy and carrier energy based on their storage capacity. The current energy supply system in our country mainly rely on renewable energy and fossil fuels converting into power energy through certain conditions to meet consumption terminals. Considering the process endowment of power energy, it has the defect of being difficult to store, which leads to the phenomenon of overproduction and large-scale abandonment of power energy in China. In this regard, the first part of this section introduces the principles and current development status of China's main power generation/ H_2 production technologies, while the second part analyzes the problems existing in related technologies, industries, and their supply systems.

2.1 The principles and current development status of the main power generation/ H_2 production technologies in China

2.1.1 Coal-fired power generation

Due to the richness of coal and the low cost of mining, China's energy relies on coal. Coal is the safest and most stable energy source in China. On a global scale, China ranks first in coal consumption. Coal accounts for approximately 65% of its energy structure, and in addition, China's coal production areas are almost ubiquitous in every region of China [28-29]. The global available coal reserves are sufficient to meet the coal production demand for 153 years. From a regional perspective, the Asia Pacific region has the highest proven reserves (46.5%). As of 2016, China's coal reserves were approximately 11.45 billion tons, accounting for 21.4% of the world's total reserves, reaching the highest level in the world, followed by India and the United States. China's coal production increased rapidly from 1981 to 2013, and then gradually declined from 2013 to 2016. Despite a decrease in production, China's total coal production in 2016 was 341 million tons, still accounting for about half of the world's total production [30]. China's household electricity and heating are mainly composed of coal, and small coal-fired boilers and stoves can meet the energy needs of rural households, accounting for about 22% of the total energy consumption. And the total energy demand of urban house-holds accounts for about 50% [31-32]. It can be seen that coal-fired power generation accounts for a significant proportion in China's energy supply system.

The process of coal-fired power generation in China mainly consists of the following parts: block coal is first sent to the coal mill for pulverization into coal powder, and the ground coal powder is sent to the separator through the hot air blown by the air preheater. The separator sends qualified coal powder to the powder bin, and finally the coal powder is fed into the burner by the powder feeder and sent to the boiler for combustion. Next, the heat released during the combustion of coal powder is used to convert liquid water into superheated steam. This process converts the chemical energy of the fuel into thermal energy. The high-temperature and high-pressure superheated steam drives the turbine to rotate, which is then converted into mechanical energy. The turbine then drives the generator to rotate, ultimately converting mechanical energy into electrical energy. The pollutant containing flue gas generated after coal powder combustion is transformed into clean flue gas through desulfurization and denitrification devices and finally discharged into the atmosphere. The schematic diagram is shown in the Figure 1.

In the context of the current national strategy of "dual carbon", China is striving to find ways to raise the threshold for new coal-fired units. For example, the average coal consumption for the power supply of newly built coal-fired units should be less than 300 gce/kWh; Newly built units of 600 MW and above should be suitable for ultra-supercritical steam conditions; 300 MW and above cogeneration and circulating fluidized bed (CFB) units should adopt supercritical steam conditions; In addition, new coal-fired units should be equipped with advanced and efficient desulfurization, denitrification, and dust removal facilities. At present, China is steadily promoting the transformation of existing thermal power generation facilities towards ultra-low emissions in the eastern, central, and western regions. China is striving to build an efficient, sustainable, and relatively low emission intensity coal-fired power industry [33].

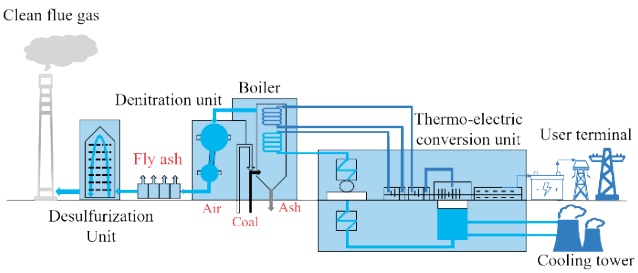

Fig. 1 Schematic diagram of coal-fired power generation

2.1.2 Renewable energy based power generation

Currently, China mainly relies on renewable energy generation technologies such as wind power, hydropower, and photovoltaic power generation. Based on publicly available data, In the first half of 2023, China's renewable energy generation, mainly consisting of photovoltaic, wind, and hydroelectric power, reached 1.34 trillion kilowatt hours, accounting for 36.2% of the country's total power generation; Among them, wind and photovoltaic power generation reached 729.1 billion kilowatt hours, accounting for 54.4%, and hydropower power generation reached 516.6 billion kilowatt hours, accounting for 38.6%. As of the first half of 2023, the installed capacity of renewable energy in China has exceeded 1.3 billion kilowatts, reaching 1.322 billion kilowatts, a year-on-year increase of 18.2%, historically surpassing coal-fired power, accounting for approximately 48.8% of the total installed capacity in China. Among them, the installed capacity of hydropower is 418 million kilowatts, wind power is 389 million kilowatts, photovoltaic power is 470 million kilowatts, and biomass power is 43 million kilowatts [34-36]. Unlike the principle of coal-fired power generation technology, the principle of energy conversion in the process of renewable energy generation is relatively simple. Taking wind power generation as an example, wind power is used to drive the rotation of wind turbine blades, and then the speed of rotation is increased by a booster engine to promote generator power generation. According to windmill technology, a gentle wind speed of approximately three meters per second (the degree of gentle wind) can start generating electricity, as shown in the Figure 2.

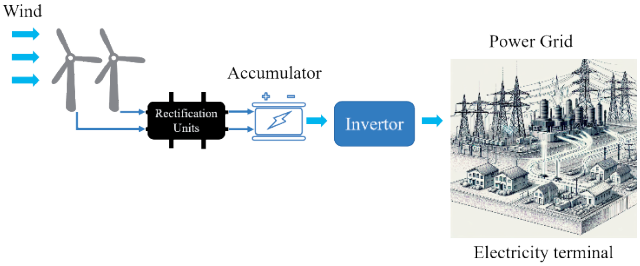

Fig. 2 Schematic diagram of wind power generation

Wind power generation is forming a trend around the world because it does not require the use of fuel, nor does it generate radiation or air pollution. Due to the unstable air volume, the output of wind turbines is alternating current ranging from 13 to 25V, so the electricity generated by wind turbines cannot be directly used. This requires rectification by the charger, followed by charging the storage battery, to convert the electrical energy generated by the wind turbine into chemical energy. Then, using an inverter power supply containing a protective circuit, the chemical energy in the battery can be converted into AC 220V mains power to ensure stable use [37-38].

The basic principle of Hydropower is to use the water level drop and cooperate with a hydroelectric generator to generate electricity, that is, to use the gravitational potential energy of water to convert it into the kinetic energy of a hydraulic turbine. The kinetic energy of a hydraulic turbine is converted into electrical energy through the generator, and then electricity is obtained, as shown in Figure 3. Scientists use the natural conditions of the water level drop to effectively utilize mechanical energy conversion devices and carefully combine them to achieve the highest power generation, providing people with cheap and pollution-free electricity. At the same time, low-level water circulates and distributes throughout the Earth by absorbing sunlight, thereby returning to high-level water sources. Despite the numerous irreplaceable advantages

of hydropower, its impact on the ecological environment is enormous. It requires the submergence of dams in a wide range of upstream areas, which can damage productive lowlands, forests, wetlands, and grasslands along river valleys, greatly affecting biodiversity. Reservoirs built for hydropower can also cause habitat fragmentation in surrounding areas and lead to soil erosion deterioration [39-40].

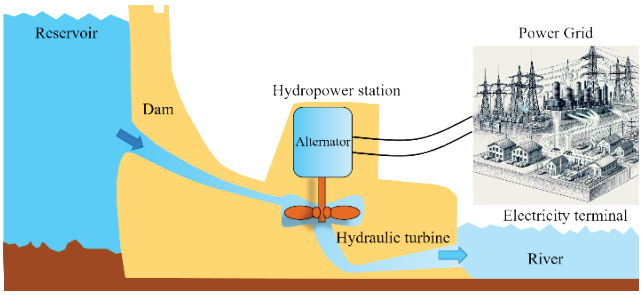

Fig. 3 Schematic diagram of hydroelectric power generation

The main principle of photovoltaic power generation is the photoelectric effect of semiconductors. Silicon atoms have four outer electrons. If an atom with five outer electrons, such as phosphorus, is doped into pure silicon, it becomes an N-type semiconductor. If atoms with three outer electrons, such as boron atoms, are doped into pure silicon, a P-type semiconductor is formed. When P-type semiconductors and N-type semiconductors are combined, the contact surface will form a potential difference, becoming a solar cell. When sunlight shines on the P-N junction, the energy absorbed by electrons is large enough to overcome the internal attraction of the atomic nucleus and do work, and escape to become photoelectrons. Electrons move from the N pole region to the P pole region, while holes move from the P pole region to the N pole region, forming an electric current. Based on this principle, the device that completes the photovoltaic conversion in the photovoltaic power generation system is called the Solar Module Array. Considering that the voltage of the solar cell module is affected by unstable radiation, it is necessary to connect a battery pack to store the energy emitted by the solar cell array when exposed to light and provide power to the load at any time. In addition, the number of cycles of charging and discharging and the depth of discharging are important factors that determine the service life of the battery. In order to prevent overcharging and discharging of the battery, a charging and discharging controller that controls overcharging or discharging of the battery pack is also an essential equipment. The schematic diagram of photovoltaic power generation is shown in Figure 4.

Solar energy, as an inexhaustible source of energy, is the most ideal new energy in the field of power generation. However, the cost of equipment used for power generation is high, the utilization rate of solar energy is low, and it is largely affected by the short service life of photovoltaics.

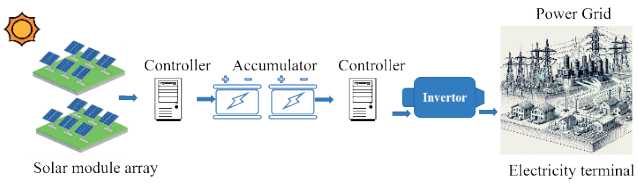

Fig. 4 Schematic diagram photovoltaic power generation

2.1.3 Industrial H_2 production technology

Hydrogen energy is the most promising new energy source in the 21st century, and its prospects have attracted great attention worldwide [41]. China has already laid out a relatively complete hydrogen energy industry chain. At present, China's H_2 production technology is relatively mature and has a certain industrialization foundation. China has become the world's largest producer of H_2, with a total H_2 production capacity exceeding 20 million tons per year [42].

China is a country with extensive coal resources, but lacks oil and natural gas. From the perspective of energy consumption structure, China still relies mainly on coal consumption. According to data from the National Bureau of Statistics, coal consumption in China accounted for 57.7% of the total energy consumption in 2019. By 2050, coal consumption will still account for about 50% of China's energy consumption [43]. The main H_2 production industry relies on two methods to produce H_2 by utilizing coal: coal coking and coal gasification. As to the coal coking H_2 production technology, it is produced by reacting coal with water, air, or oxygen under high temperature and pressure to produce syngas, which is mainly composed of CO and H_2. Subsequently, CO in the synthesis gas further reacts with steam to generate H_2 and CO_2. Finally, CO_2 and other impurities in the H_2 containing flow are removed by a pressure swing adsorption device, resulting in high-purity H_2 gas [44]. However, natural gas is also a good raw material for H_2 production [45]. There are five main H_2 production technologies using natural gas as raw material: methane steam reforming, methane catalytic partial oxidation, methane self-thermal reforming, methane dry reforming, and methane pyrolysis [46]. For petroleum, the H_2 produced by the petroleum industry comes from by-products such as naphtha, heavy oil, petroleum coke, and refinery dry gas. The technology of producing H_2 from naphtha is similar to methane steam reforming technology. In recent years, due to the tight international supply of naphtha, which results the price rising sharply and increasing the cost of H_2 production from naphtha [47]. Therefore, China does not use naphtha to produce H_2 in industrial production. The H_2 production technology from petroleum coke is similar to the H_2 production technology from coal gasification. In recent years, the production of high sulfur petroleum coke in China has been continuously increasing, facing the problems of low utilization rate and excess production [48]. Producing H_2 from petroleum coke has become an ideal way to utilize petroleum coke. It can not only achieve effective utilization of high sulfur petroleum coke, but also reduce the

cost of H_2 production. This technology has good development prospects in China [49-50].

Electrolysis of water for H_2 production is also a commonly used method. According to different electrolytes, water electrolysis can be divided into three categories: alkaline (ALK) water electrolysis, proton exchange membrane (PEM) water electrolysis, and solid oxide water electrolysis (SOEC) [51]. In addition to traditional water electrolysis for H_2 production, renewable energy can also be used for power generation, and then H_2 can be produced through water electrolysis. This process can convert the remaining electricity generated by renewable energy into hydrogen energy, achieving efficient utilization of renewable energy [52-53].

In addition to power generation, renewable energy can also directly produce H_2. Biomass is not only widely distributed, but also has a very large total amount. It is one of the main energy sources that replace fossil fuels such as coal, natural gas, and oil. Biomass H_2 production technology is mainly divided into thermochemical method and microbial method. There are three main types of biomass thermochemical H_2 production technologies: biomass gasification H_2 production, biomass pyrolysis H_2 production, and biomass supercritical conversion H_2 production [54]. Biomass gasification for H_2 production uses air, oxygen, or steam as gasification agents to gasify biomass into H_2 rich gas under high temperature conditions. Biomass pyrolysis for H_2 production involves drying heated biomass under air isolation, converting it into H_2 rich gas, bio-char, and bio-tar. Biomass supercritical conversion for H_2 production involves a series of reactions such as pyrolysis, hydrolysis, condensation, and dehydrogenation between biomass and water under supercritical conditions, resulting in H_2 rich gas and residual carbon.

2.2 Issues in the current main power generation/ H_2 production technologies, industries, and supply systems

2.2.1 Power generation technology and industrial issues

For coal-fired power generation, an important feature of building a new power system is the cleanliness of electricity. Further promoting the cleanliness of coal-fired power has become a trend. Coal power enterprises in various regions have completed a round of ultra-low emission and energy-saving technology transformation, but they still face many difficulties in further investing in deep cleaning transformation. At present, there are still many technological bottlenecks in the clean utilization of coal-fired power. Coal fired power generation technology is at the international advanced level in many indicators such as coal-fired power efficiency, emission level, and power generation performance. However, breakthroughs are still needed in technologies such as supercritical CO_2 power generation, carbon capture, utilization, and storage, coal gasification fuel cell power generation, and coal-fired coupled biomass power generation. At present, the difficulty and cost of technology research and development are high, and it is difficult for coal-fired power enterprises alone to achieve greater breakthroughs. Many coal-fired power companies have reported that the relevant support policies for promoting clean utilization are not yet perfect, and the transformation motivation and enthusiasm of power generation enterprises are insufficient. Coal power enterprises are constantly undergoing technological transformation to adapt to new development requirements, but the increase in power generation costs puts a heavy burden on the enterprise. Relevant departments have problems in promoting clean utilization of coal power, lacking top-level design and collaborative cooperation, making it difficult to implement supporting policies, and sometimes not timely and discounted. Due to various factors, coal-fired power enterprises are currently facing widespread difficulties, and their willingness to undergo clean transformation is not high. Affected by multiple factors such as coal supply shortage, high coal prices, and inverted coal electricity prices, coal-fired power enterprises have been losing money for years and generally face certain operational difficulties. The clean utilization of coal-fired power requires a large amount of technology and capital investment, which puts great pressure on enterprises [55-57].

For renewable energy generation, China has made significant achievements in the development of renewable energy, and the policy system to encourage and support the development of renewable energy is becoming increasingly rich. However, energy planning and policies have not been fully sorted and adjusted according to the logic of energy transformation. Many policies following the Beaten Track still continue or strengthen in the name of promoting low-carbon energy transformation and renewable energy development. In the name of promoting the development of renewable energy, some policies that are not conducive to improving the operational efficiency of the power system still prevail. While the central and eastern regions vigorously promote the construction of photovoltaic power generation and offshore wind power, the western region still continues to invest in the construction of large-scale wind and photovoltaic power generation bases, as well as supporting policies for ultra-high voltage long-distance power transmission. However, optimizing regional power interconnection, distribution networks, and improving load side response technology capabilities are conducive to improving the flexibility of the power system, which is conducive to improving the volatility of power consumption capacity. Investment has not been prioritized; The policy of shutting down coal-fired power units below 300000 kilowatts to improve energy efficiency and reduce emissions, as well as the policy of requiring flexible retrofitting of units of 600000 kilowatts and above, did not take into account the significant decrease in operating hours of thermal power units and further increase in peak valley load differences as the share of volatile renewable energy electricity increases. This means that although energy transformation and energy revolution have become widely accepted concepts, many policies have not truly conducted systematic research and formulation from the logic of energy transformation, and still only formulate and implement renewable energy development policies from the technical level or a single indicator [58-59].

2.2.2 H_2 production technology and industrial issues

According to data provided by Maggio et al and Moliner et al [60-61]. It can be seen that the main technologies for H_2 production abroad are natural gas H_2 production and petroleum H_2 production, accounting for approximately 78% of the total. However, due to the resource characteristics of "coal rich, oil poor, and gas scarce" in China, the main raw material for H_2 production is still coal, accounting for about 62% of the total. In the short term, there are still many technological bottlenecks in the electrolysis of water for H_2 production technology. For renewable energy H_2 production technology, taking photovoltaic H_2 production as an example, the power generation efficiency of commercial photovoltaic panels is between 15% and 25%, and the commercial electrolysis water H_2 production efficiency is between 60% and 90%. Therefore, the theoretical efficiency of photovoltaic electrolysis water H_2 production is 9% to 22.5%. In actual solar power generation, the loss of substation grid connection and grid power downloading to the electrolysis tank device will further reduce the efficiency by about ten percentage points. Therefore, the actual efficiency of solar H_2 is often about 6% to 8%, which is too low [62-63]. Furthermore, the average energy consumption of current commercial electrolysis water H_2 production technology is higher than 4 kWh / standard cubic feet, and besides equipment costs, the operating energy consumption cost is also very expensive. Calculated at an average electricity price of 0.1 USD / kWh, the cost is 0.4 USD / standard square feet; Even if the current costs of solar power generation, wind power, and hydropower are 0.04 USD / kWh, 0.0756 USD / kWh, and 0.046 USD / kWh, respectively, the H_2 production costs are as high as 0.157 USD, 0.3 USD, and 0.184 USD per standard cubic feet, making it difficult to afford [64]. Therefore, the effective utilization efficiency of renewable energy needs to be further developed.

In the next 5-10 years, China's H_2 production raw materials will still be mainly fossil fuels. In addition, through the comparison of various fossil fuel H_2 production technologies, traditional H_2 production processes using coal, natural gas, and oil as raw materials have the following problems: (1) Traditional H_2 production technologies have high carbon emissions and poor environmental benefits. (2) Traditional H_2 production technology not only has high raw material costs, but also requires complex post-processing, resulting in poor economic benefits. (3) Traditional H_2 production technology requires high reaction temperature. It has a high energy consumption and resources have not been fully utilized. The development of low-carbon and green H_2 production technology has become the key to the development of hydrogen energy in China. Therefore, China should further develop low-cost carbon capture, storage, and utilization technologies based on its own resource characteristics, in order to reduce production costs. Finally, achieving green and efficient development of fossil fuel H_2 production technology.

At present, coal-based H_2 production technology holds an important position in China. It has the advantages of large H_2 production capacity and low cost. However, it has drawbacks such as high carbon emissions and incomplete pollutant removal. The H_2 produced by electrolysis water H_2 production technology has high purity, but it also has drawbacks such as high energy consumption and high cost, and the proportion of this technology adopted globally is very low. Although solar energy and biomass are pollution-free and renewable, their application in the field of H_2 production still has drawbacks such as low H_2 production efficiency and high cost. Currently, they are still in the laboratory research stage. If renewable energy, especially wind energy, solar energy, and hydraulic energy, can be reasonably and effectively utilized, the production cost of electrolytic water for H_2 production will be greatly reduced. According to the data provided by [65], it can be found that the electricity potential of "wind, solar, and water" in China can reach 51.5 billion kWh. If China can make more rational use of renewable energy, it will greatly promote the development of hydrogen production through electrolysis of water.

2.2.3 Energy supply system issues

Power energy and hydrogen energy are both secondary energy sources, both of which are artificially produced from primary energy sources. But power energy is a process energy that is hard to store while hydrogen energy belongs to the category of energy carriers and can conveniently store and transport. The main technology of the current global energy supply system is to convert all primary energy (including fossil fuels and renewable energy) into power energy, and then rely on the transmission and distribution of power energy to meet the needs of user terminals. When humans rely on fossil fuels as the main source of primary energy source, we rely on the easy storage and transportation characteristics of fossil fuels as energy carriers. We adopt manual allocation at the source of primary energy to overcome the mismatch between user terminals and energy supply systems in time, space, and geography in social production and life. However, the current power generation is mainly based on fuel combustion and thermal power cycle, emitting huge amounts of harmful substances and greenhouse gases, causing environmental pollution and ecological damage. When the supply structure of energy is transitioned into using process energy such as solar, wind energy and hydraulic energy as the main source of primary energy, it is no longer possible to adopt manual allocation at the source of traditional primary energy. The process endowment of power energy makes it hard to achieve low-cost, sufficient, and long-term storage. This is the fundamental flaw in traditional energy conversion and utilization technologies, industries, and their supply systems. At present, the amount of abandoned power energy produced by renewable energy such as wind and solar power that has been over 100 billion kilowatt hours per year [66]. The fundamental reason for large-scale power energy abandonment is that the existing energy supply system only has a sole power generation unit, and the produced power energy is still process energy, which is difficult to store even when not in use.

3. The new renewable and fossil energy conversion technologies

Based on the current shortcomings of H_2 production from renewable and fossil energy sources, the State Key Laboratory of Multiphase Flow in Power Engineering (SKLMFPE) has developed clean and efficient H_2 production and power generation technologies based on solar energy and coal, respectively, after years of research. This section will focus on introducing the principles, advantages, and applications of the above-mentioned technologies, including new forms of renewable energy conversion and utilization, as well as green, low-carbon, efficient, and pollution-free fossil energy conversion and utilization methods.

3.1 Poly-generation from full-spectrum solar energy

3.1.1 Principles of poly-generation from full-spectrum solar energy

Photocatalytic H_2 production is a process that utilizes photocatalysts to absorb light energy and produce H_2 through the water photolysis. It is a renewable and environmentally friendly method for preparing H_2 as an energy resource [67]. Photocatalytic materials utilize photons from the sun, such as visible or ultraviolet light, to excite electrons in the valence band of the material. This causes the electrons to jump into the conduction band, creating a band gap. The excess electrons in the valence band are referred to as excited state electrons. The excited state electrons subsequently move through the semiconductor and undergo a reduction reaction with water present in solution on the semiconductor surface [68], producing H_2. In solar energy, UV and some visible light with wavelengths between 250 nm and 600 nm can ionize and excite water when absorbed.

Light with a wavelength ranging from 600 nm to 1100 nm is commonly used in photoelectric conversion due to its low energy. This energy is insufficient to directly stimulate the photolytic reaction of water, but it can be absorbed by solar cells. The photoelectric conversion devices are typically made of semiconductor materials that contain energy bands and Fermi energy levels. When light strikes the semiconductor material, it excites the free electrons in the semiconductor band, causing them to move into the conduction band and leaving behind holes. The movement of electrons and holes creates structures such as heterojunctions and PN junctions within the semiconductor material, generating an electric field in the semiconductor. The photocurrent is then driven through the electric field, producing electrical power that is output through an external circuit. Light with wavelengths ranging from 1100 nm to 2500 nm, commonly known as near-infrared light, has low energy levels that are insufficient to directly excite most substances into high-energy states. However, near-infrared-responsive photocatalysts materials can absorb this energy to produce a photothermal effect [68]. This effect relies on both photocatalytic and thermocatalytic processes to increase the rate of H_2 production.

The system of poly-generation from full-spectrum solar energy combines photocatalytic H_2 production, photothermal catalysis, and photoelectric conversion (**Fig. 5.**) to provide stable electricity and heat, and to produce high-quality H_2 as a clean energy reserve. The integration of solar photoelectric technology with poly-generation represents a new form of renewable energy, which can complement local power generation units and H_2 production, and enable flexible and intelligent coupling and decoupling with the power grid. By utilizing this technology, we can transform existing energy systems and build new, stable energy supply systems with renewable energy as the primary source.

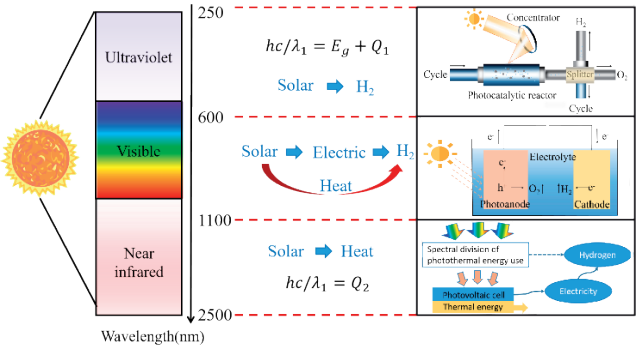

Fig. 5 Ways of utilizing light energy at different wavelengths.

3.1.2 Novel photocatalyst

Catalysts play a crucial role in photo-hydrogen conversion. However, catalysts used for photocatalytic H_2 production often lack high photocatalytic performance due to their composition of a single material. Therefore, optimization of catalysts through modification, hydrothermal treatment, and other methods is necessary to enhance their light absorption, photogenerated carrier separation, and surface reactive sites.

Common catalysts can be divided into sulfide catalysts, oxide catalysts, and organic polymer graphite phase carbon nitride (**Fig. 6.**). Sulfide catalysts, such as CdS [69, 70] and ZnS [71, 72], are mainly composed of metal sulfides with high catalytic activity and stability. Composite catalysts formed by multiple sulfides [73, 74] have higher H_2 production efficiency. Oxide catalysts are mainly based on TiO_2 [75, 76, 77, 78] due to their high efficiency, non-polluting nature, and renewability. It can be compounded with other oxides or metal sulfides to form highly efficient composite catalysts [79, 80]. The composite catalysts can enhance photocatalytic H_2 production through the photothermal effect by absorbing both UV and near-infrared light. Catalysts for H_2 production based on graphitic-phase carbon nitride (g-C_3N_4) are often doped or modified to enhance their catalytic activity. ZnCr layered double hydroxide (ZnCr LDH) [81], α-FeOOH [82] and MoO_3 [83, 84] have been found to be excellent modifiers of g-C_3N_4. The majority of the modified composite catalysts have the morphology and electronic structure of a Z-type heterojunction, which further contributes to promote the

rate of the H_2 production. Moreover, it can be modified with Cu-Ni bimetallic nanoparticles to broaden the range of absorbable spectral for photothermal-assisted photocatalysis [85]. Additionally, the H_2 production efficiency of the catalyst can be enhanced by attaching quantum dots (QDs) such as Co_3O_4 [86], Ti_3C_2 [87], or Zn-In-Se colloids [88] to g-C_3N_4.

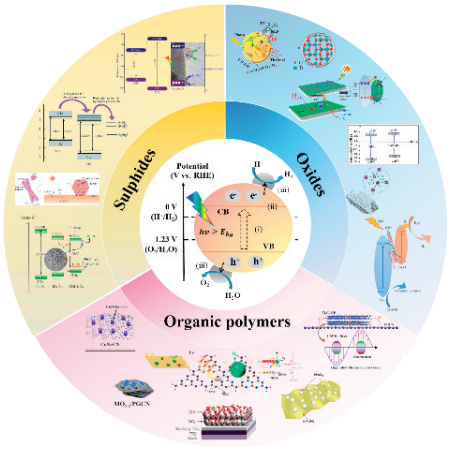

Fig. 6 photocatalysts for H_2 production from full-spectrum solar energy

3.1.3 Reactor design

With the further enhancement of reactor functions, the traditional photocatalytic H_2 production reactor cannot meet the demand of poly-generation anymore. The new reactor is designed with a multi-functional suspended fluid collector, which is able to play three roles simultaneously as liquid lens, crossover filter and photothermal reactor device, significantly increasing irradiation uniformity and improving the power output of the solar photovoltaic module. Under typical daytime solar irradiance and ambient temperature, the system's average electrical, thermal and total energy efficiencies are increased to 11.39%, 64.72% and 76.11%, respectively [89]. The liquid spherical lenses (**Fig. 7.**) act as secondary optics that concentrate and filter infrared light, simultaneously intensifying solar panel heat dissipation and increasing the operating temperature of the electrolyser. The reactor has achieved solar power and H_2 production efficiencies of 31.7% and 22.1% [90], respectively. The study presents the theory of efficient synergistic regulation of field flow. It demonstrates a non-linear acceleration of the rate of H_2 production with increasing light intensity concentration. Additionally, it explains the influence of photoexcitation and thermal excitation on the photo-thermal coupling effect. The photocatalytic and thermocatalytic reactions are accelerated by thermal acceleration and photo-regulation, which effectively reduce energy barriers. Zeng et al. [91] have developed a poly-generation system for full-spectrum solar energy utilization. The system's performance and the ratio of H_2 and electricity production can be regulated by adjusting the parameters of the spectral beam splitter (LSBS) and the photocatalytic loading.

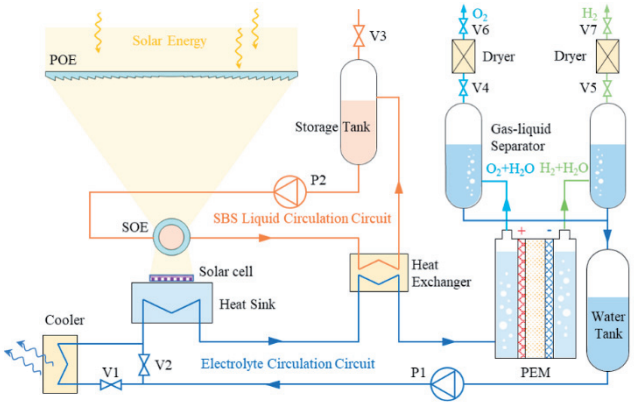

Fig. 7 Flow schematic of poly-generation from full-spectrum solar energy [90]

3.2 Poly-generation based on supercritical water gasification of coal

3.2.1 Principles and advantages on supercritical water gasification of coal

Supercritical water (SCW) is liquid water that forms under high temperature and pressure, after undergoing processes such as compression or heating. It is often considered an ideal medium for the reaction of non-polar organics due to its high density, high solubility, high chemical activity and low viscosity. The process of SCWG of coal consists of two main steps: pyrolysis reaction and gasification reaction. The SCW is used as a reaction medium at high temperature and pressure to convert coal into H_2 (Eq. (1)). It also oxidizes a portion of hazardous substances, such as CO_2 and H_2S, into harmless gases. The gas produced is dissolved in the SCW and exits the gasification reactor as a homogeneous supercritical mixed fluid (**Fig. 8.**) [92, 93].

$$Coal + H_2O \xrightarrow{P\geq 22.1MPa,\ T\geq 374^{\circ}C} H_2 + CO_2 + Ash_{pure} \quad (1)$$

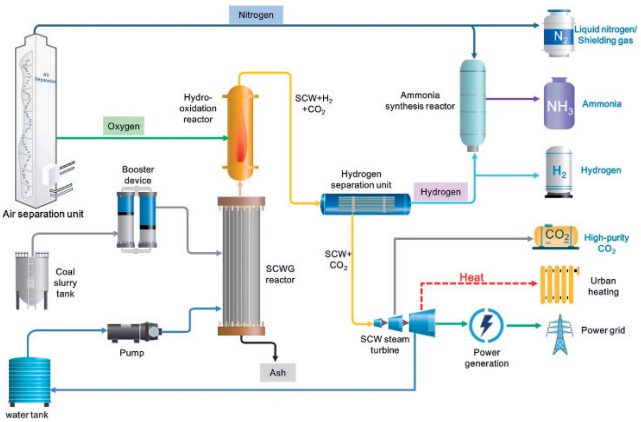

Fig. 8 Flow schematic of the Poly-generation based on supercritical water gasification of coal [94]

Compared to traditional coal-fired power generation, this technology has the following advantages [94]: (1) The power generation process does not emit harmful gases such as SO_x, NO_x, waste liquids, dust particles, or other pollutants. Additionally, it naturally enriches CO_2, achieving carbon-neutral emissions without any additional increase in energy consumption. (2) The efficiency of power generation from coal is greater than 50%. H_2 and CO_2 as well as high-value carbon-containing chemicals can be co-produced during the generation of electricity and heat. (3) The coal consumption is less than 250 g/kWh, and there is no water consumption during power generation. The water consumption of H_2 production is limited to the theoretical water consumption of water electrolysis for H_2 production.

3.2.2 Catalysts for the SCWG of coal

The efficiency of SCWG is always influenced by the catalyst. Alkaline catalysts, such as K_2CO_3 and KOH [95, 96, 97, 98], increase the rate of the H_2 production from SCWG of coal by breaking up the coal matrix and forming formate [99]. Increasing the loading of these catalysts further promotes the rate of carbon gasification and H_2 production. Sun et al [96] compared the catalytic effect of K_2CO_3 in SCWG experiments of Zhundong coal in a batch reactor. The results indicated that K_2CO_3 significantly enhances the decomposition of aromatic structures during supercritical coal gasification. It greatly accelerates the process of hydrolysis, steam reforming, and water-gas shift reactions, greatly improving the efficiency of carbon gasification and the rate of H_2 production. Furthermore, alkali metals, including Na, K, and Mg, can enhance the SCWG reaction process by inhibiting the growth of graphite-like structures and promoting the strong chemisorption of H_2O on carbon structures [98]. Alkaline waste black liquor from pulping, an industrial waste liquid, can be used as an efficient and inexpensive additive for the SCWG of coal due to its alkali and lignin content [100].

3.2.3 Solar-powered CO_2 reduction

CO_2 reduction reaction (CO_2RR) powered by renewable energy can use catalytic technologies such as photo-catalysis to convert CO_2 and renewable energy into energy carriers, where the energy is easy to transport and storage (**Fig. 9.**). Several technologies, including photo-catalysis and photo-electrochemistry, have been developed to achieve solar-driven CO_2 reduction for the production of hydrocarbon fuels so as to achieve the reuse and sustainability of energy. In the whole process, CO_2 emission reduction and chemical production can be seamlessly connected, forming an efficient energy cycle system.

Photocatalysis drives electron leaps within the catalyst by absorbing solar energy. The electron-hole pairs resulting from this process will participate in the CO_2RR. Photoelectrochemistry generates electron-hole pairs in a photoelectrode to form an electric current in a closed circuit, while oxygen evolution reaction (OER) [101] and CO_2RR respectively occurs on the (photo) anode and (photo) cathode surfaces. Photovoltaic electrochemistry (PV-EC) is a technique that combines solar photovoltaic power generation and electrochemistry. The PV convert solar energy into electrical energy, which is then used to convert CO_2 into organic compounds in a reaction cell under specific potential and electrolyte conditions. Nowadays, the techniques mentioned above has been successfully used by scholars to reduce CO_2 and prepare various products, such as HCOOH [102], CH_4, CH_3OH, and CH_3COOH.

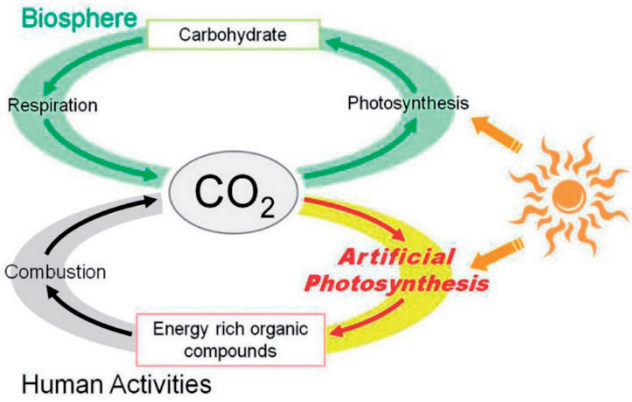

Fig. 9 CO_2RR powered by renewable energy in the production of chemicals [103].

4. Conclusion

Currently, the traditional ways of energy conversion and utilization are mainly by converting primary energy into power, which is a process energy that is difficult to store. Hydrogen energy is also a secondary energy source, but it is also an energy carrier. It can solve the problem of intermittency and consumption of renewable energy as well as the problem of energy storage. Increasing the proportion of primary energy converted to H_2 contributes to the increased renewable energy utilization. However, the current H_2 generation technologies based on renewable and fossil energy sources have many limitations, and there is an urgent need to develop new technologies that can generate H_2 on a large-scale and at low-cost.

After years of research, the SKLMFPE in Power Engineering has researched and developed H_2 and power poly-generation technology based on full-spectrum solar energy and poly-generation based on SCWG of coal:

(1) The technology for poly-generation based on full-spectrum solar energy utilizes different wavelengths of light in frequency division. By combining photothermal, photoelectric, and photocatalytic technologies, the efficiency of power generation and H_2 production can reach up to 31.7% and 22.1%, respectively.

(2) The poly-generation based on SCWG of coal enables the green, clean, efficient, and low-carbon use of fossil energy. These two technologies can form the basis for developing high-efficiency, low-cost, and large-scale poly-generation methods, constructing new types of renewable and fossil energy units, and transforming existing generating units.

5. Perspective

In the future, efforts should be paid to build a new energy system that integrates multiple energy sources. Multi-energy source complementarity and integration, as an advanced method of energy conversion and utilization, organically combines fossil energy and renewable energy through "energy complementarity and energy grade coupling", achieving complementary and efficient integration of different grades of energy. It will effectively overcome the bottleneck of the current rigid chain development model of large-scale renewable energy, tap into the active regulation potential of multi-energy complementarity systems, effectively alleviate regional and temporal supply-demand contradictions, ensure the continuous stability of energy production, and achieve energy matching and coordination between supply and demand sides. Multi-energy complementarity and integration will also form a low-carbon conversion method based on a system concept through the joint complementarity of various types of technology routes such as renewable energy conversion and utilization, fossil energy conversion and utilization, energy storage, and carbon capture，utilization and storage, breaking through the bottleneck of traditional inefficient utilization methods of the combustion on fossil energy and helping to achieve efficient and low-carbon energy conversion.

6. Reference

[1] Seneviratne S, Donat M, Pitman A, et al. Allowable CO_2 emissions based on regional and impact-related climate targets[J]. Nature, 2016, 529(7587): 477-483.

[2] Liu Z, Deng Z, Davis S, et al. Monitoring global carbon emissions in 2021[J]. Nature Reviews Earth & Environment, 2022, 3(4): 217-219.

[3] Liu Z, Deng Z, Davis S, et al. Monitoring global carbon emissions in 2022[J]. Nature Reviews Earth & Environment, 2023, 4(4): 205-206.

[4] Tackett B, Gomez E, Chen J. Net reduction of CO_2 via its thermocatalytic and electrocatalytic transformation reactions in standard and hybrid processes[J]. Nature Catalysis, 2019, 2(5): 381-386.

[5] Zhou Y, Shan Y, Liu G, et al. Emissions and low-carbon development in Guangdong-Hong Kong-Macao Greater Bay Area cities and their surroundings[J]. Applied Energy, 2018, 228: 1683-1692.

[6] Jiang K, Liao G, E J, et al. Thermal management technology of power lithium-ion batteries based on the phase transition of materials: a review[J]. Journal of Energy Storage, 2020, 32: 101816.

[7] Liao G, Jiang K, Zhang F, et al. Thermal performance of battery thermal management system coupled with phase change material and thermoelectric elements[J]. Journal of Energy Storage, 2021, 43: 103217.

[8] Zickfeld K, MacIsaac A, Canadell J, et al. Net-zero approaches must consider Earth system impacts to achieve climate goals[J]. Nature Climate Change, 2023, 13(12): 1298-1305.

[9] Dale S. BP statistical review of world energy[J]. BP Plc: London, UK, 2021: 14-16..

[10] Liang L, Gong P. Urban and air pollution: a multi-city study of long-term effects of urban landscape patterns on air quality trends[J]. Scientific reports, 2020, 10(1): 18618.

[11] Zhu Y, Frey H. Integrated gasification combined cycle (IGCC) systems[M]//Combined Cycle Systems for Near-Zero Emission Power Generation. Woodhead Publishing, 2012: 129-161.

[12] Ladenburg J, Kim J, Zuch M, et al. Taking the carbon capture and storage, wind power, PV or other renewable technology path to fight climate change? Exploring the acceptance of climate change mitigation technologies–A Danish national representative study[J]. Renewable Energy, 2024, 220: 119582.

[13] Bai Y, Wang Y, Xiu H, et al. Experimental study on integrated desulfurization and denitrification of low-temperature flue gas by oxidation method[J]. Scientific Reports, 2024, 14(1): 3527.

[14] Ren S, Feng X, Wang Y. Emergy evaluation of the integrated gasification combined cycle power generation systems with a carbon capture system[J]. Renewable and Sustainable Energy Reviews, 2021, 147: 111208.

[15] Parraga J, Khalilpour K, Vassallo A. Polygeneration with biomass-integrated gasification combined cycle process: Review and prospective[J]. Renewable and Sustainable Energy Reviews, 2018, 92: 219-234.

[16] Bhiogade D. Ultra-supercritical thermal power plant material advancements: a review[J]. Journal of Alloys and Metallurgical Systems, 2023: 100024.

[17] Pryor S, Barthelmie R, Bukovsky M, et al. Climate change impacts on wind power generation[J]. Nature Reviews Earth & Environment, 2020, 1(12): 627-643.

[18] Zhang Y, Ma H, Zhao S. Assessment of hydropower sustainability: Review and modeling[J]. Journal of Cleaner Production, 2021, 321: 128898.

[19] Kuriqi A, Pinheiro A, Sordo-Ward A, et al. Ecological impacts of run-of-river hydropower plants—Current status and future prospects on the brink of energy transition[J]. Renewable and Sustainable Energy Reviews, 2021, 142: 110833.

[20] Li Y, Huang X, Sheriff J, et al. Semitransparent organic photovoltaics for building-integrated photovoltaic applications[J]. Nature Reviews Materials, 2023, 8(3): 186-201.

[21] Aghaei M, Fairbrother A, Gok A, et al. Review of degradation and failure phenomena in photovoltaic modules[J]. Renewable and Sustainable Energy Reviews, 2022, 159: 112160.

[22] Azzolina N, Hamling J, Peck W, et al. A life cycle analysis of incremental oil produced via CO_2 EOR[J]. Energy Procedia, 2017, 114: 6588-6596.

[23] Berdechowski K. Emission of "greenhouse gases" generated during biofuels hydroconversion by co-processing[J]. Przemysl Chemiczny, 2014, 93(2): 199-202.

[24] Li Y, Alharthi M, Ahmad I, et al. Nexus between renewable energy, natural resources and carbon emissions under the shadow of transboundary trade relationship from South East Asian economies[J]. Energy Strategy Reviews, 2022, 41: 100855.

[25] Shirazi M, Mahani H, Tamsilian Y, et al. Full life cycle review of water-based CEOR methods from pre-injection to post-production[J]. Fuel, 2024, 356: 129574.

[26] Sharma A, Jakhete A, Sharma A, et al. Lowering greenhouse gas (GHG) emissions: techno-economic analysis of biomass conversion to biofuels and value-added chemicals[J]. Greenhouse Gases: Science and Technology, 2019, 9(3): 454-473.

[27] Cui Q, He L, Han G, et al. Review on climate and water resource implications of reducing renewable power curtailment in China: A nexus perspective[J]. Applied energy, 2020, 267: 115114.

[28] George A, Shen B, Kang D, et al. Emission control strategies of hazardous trace elements from coal-fired power plants in China[J]. Journal of Environmental Sciences, 2020, 93: 66-90.

[29] Dai S, Finkelman R. Coal geology in China: an overview[J]. Coal Geology of China, 2020: 1-4.

[30] Dale S. BP statistical review of world energy[J]. BP Plc: London, UK, 2021: 14-16.

[31] He B, Liang L, Jiang G. Distributions of arsenic and selenium in selected Chinese coal mines[J]. Science of the Total Environment, 2002, 296(1-3): 19-26.

[32] Liu G, Zhang Y, Qi C, et al. Comparative on causes and accumulation of selenium in the tree-rings ambient high-selenium coal combustion area from Yutangba, Hubei, China[J]. Environmental monitoring and assessment, 2007, 133: 99-103.

[33] Zhang H, Zhang X, Yuan J. Coal power in China: A multi-level perspective review[J]. Wiley Interdisciplinary Reviews: Energy and Environment, 2020, 9(6): e386.

[34] URL: http://www.nea.gov.vn/2023-07/31/c_1310734825.htm (31.7.2023.)

[35] China National Energy Administration. The National Energy Administration releases statistical data on the national power industry from January to June[J]. Electric Power Survey & Design, 2023,(07):65.

[36] China National Energy Administration. The National Energy Administration releases statistical data on the national power industry for 2023[J]. Electric Power Survey & Design, 2024,40(01):95.

[37] Hassan Q, Algburi S, Sameen A Z, et al. A review of hybrid renewable energy systems: Solar and wind-powered solutions: Challenges, opportunities, and policy implications[J]. Results in Engineering, 2023: 101621.

[38] Wachs E, Engel B. Land use for United States power generation: A critical review of existing metrics with suggestions for going forward[J]. Renewable and Sustainable Energy Reviews, 2021, 143: 110911.

[39] Li X, Chen Z, Fan X, et al. Hydropower development situation and prospects in China[J]. Renewable and Sustainable Energy Reviews, 2018, 82: 232-239.

[40] Kougias I, Aggidis G, Avellan F, et al. Analysis of emerging technologies in the hydropower sector[J]. Renewable and Sustainable Energy Reviews, 2019, 113: 109257.

[41] Ehret O, Bonhoff K. Hydrogen as a fuel and energy storage: Success factors for the German Energiewende[J]. International Journal of Hydrogen Energy, 2015, 40(15): 5526-5533.

[42] Maggio G, Nicita A, Squadrito G. How the hydrogen production from RES could change energy and fuel markets: A review of recent literature[J]. International Journal of Hydrogen Energy, 2019, 44(23): 11371-11384.

[43] Wang J, Jiang H, Zhou Q, et al. China's natural gas production and consumption analysis based on the multicycle Hubbert model and rolling Grey model[J]. Renewable and Sustainable Energy Reviews, 2016, 53: 1149-1167.

[44] Liszka M, Malik T, Manfrida G. Energy and exergy analysis of hydrogen-oriented coal gasification with CO_2 capture[J]. Energy, 2012, 45(1): 142-150.

[45] Khalilpour K, Pace R, Karimi F. Retrospective and prospective of the hydrogen supply chain: A longitudinal techno-historical analysis[J]. International Journal of Hydrogen Energy, 2020, 45(59): 34294-34315.

[46] Sengodan S, Lan R, Humphreys J, et al. Advances in reforming and partial oxidation of hydrocarbons for hydrogen production and fuel cell applications[J]. Renewable and Sustainable Energy Reviews, 2018, 82: 761-780.

[47] Stijepovic V, Linke P, Alnouri S, et al. Toward enhanced hydrogen production in a catalytic naphtha reforming process[J]. International Journal of Hydrogen Energy, 2012, 37(16): 11772-11784.

[48] Shan Y, Guan D, Meng J, et al. Rapid growth of petroleum coke consumption and its related emissions in China[J]. Applied Energy, 2018, 226: 494-502.

[49] Ba Z, Zhao J, Li C, et al. Developing efficient gasification technology for high-sulfur petroleum coke to hydrogen-rich syngas production[J]. Fuel, 2020, 267: 117170.

[50] Wang M, Wan Y, Guo Q, et al. Brief review on petroleum coke and biomass/coal co-gasification: Syngas production, reactivity characteristics, and synergy behavior[J]. Fuel, 2021, 304: 121517.

[51] Schmidt O, Gambhir A, Staffell I, et al. Future cost and performance of water electrolysis: An expert elicitation study[J]. International Journal of Hydrogen Energy, 2017, 42(52): 30470-30492.

[52] de Fátima Palhares D, Vieira L, Damasceno J. Hydrogen production by a low-cost electrolyzer developed through the combination of alkaline water electrolysis and solar energy use[J]. International Journal of Hydrogen Energy, 2018, 43(9): 4265-4275.

[53] Baykara S. Hydrogen: A brief overview on its sources, production and environmental impact[J]. International Journal of Hydrogen Energy, 2018, 43(23): 10605-10614.

[54] Meng X, Chen M, Gu A, et al. China's hydrogen development strategy in the context of double carbon targets[J]. Natural Gas Industry B, 2022, 9(6): 521-547.

[55] URL: https://www.nea.gov.cn/2022-01/07/c_1310413767.htm (7.1.2022)

[56] Zhang W, Yan Q, He G, et al. The pathway and strategy of China's power system low-carbon transition under the constraints of climate change[J]. Climate Change Research, 2021,17(01):18-26.

[57] Shu Y, Chen G, He J, et al. Building a New Electric Power System Based on New Energy Sources[J]. Strategic Study of CAE, 2021,23(06):61-69.

[58] Zhu T. The Development Stage and Challenges of Renewable Energy in China[J]. China National Conditions and Strength, 2019,(07):8-12.

[59] Zhuo Z, Zhang N, Xie X, et al. Key Technologies and Developing Challenges of Power System with High Proportion of Renewable Energy[J]. Automation of Electric Power Systems, 2021,45(09):171-191.

[60] Maggio G, Nicita A, Squadrito G. How the hydrogen production from RES could change energy and fuel markets: A review of recent literature[J]. International Journal of Hydrogen Energy, 2019, 44(23): 11371-11384.

[61] Moliner R, Lázaro M, Suelves I. Analysis of the strategies for bridging the gap towards the Hydrogen Economy[J]. International Journal of Hydrogen Energy, 2016, 41(43): 19500-19508.

[62] Lai Y, Zuo M, Mao F, et al. Analysis of hydrogen production methods and photovoltaic hydrogen production systems[J]. Lamps & Lighting, 2023,(11):138-140.

[63] Fen L, Lu J, Xu H, et al. Simulation Study on Hydrogen Production and Storage Systems for Solar Photovoltaic Water Electrolysis in Different Regions[J]. Acta Energiae Solaris Sinica, 2023,44(12):481-486.

[64] IRENA (2023), Renewable power generation costs in 2022, International Renewable Energy Agency, Abu Dhabi.

[65] Chai S, Zhang G, Li G, et al. Industrial hydrogen production technology and development status in China: a review[J]. Clean Technologies and Environmental Policy, 2021, 23(7): 1931-1946.

[66] URL: https://www.gov.cn/xinwen/2019-07/04/content_5405844.htm (4.7.2019)

[67] Jing D, Guo L, Zhao L, et al. Efficient solar hydrogen production by photocatalytic water splitting: from fundamental study to pilot demonstration[J]. International Journal of Hydrogen Energy, 2010, 35(13): 7087-7097.

[68] Nair V, Muñoz-Batista M, Fernández-García M, et al. Thermo-photocatalysis: environmental and energy applications[J]. ChemSusChem, 2019, 12(10): 2098-2116.

[69] Ma L, Liu M, Jing D, et al. Photocatalytic hydrogen production over CdS: effects of reaction atmosphere studied by in situ Raman spectroscopy[J]. Journal of Materials Chemistry A, 2015, 3(10): 5701-5707.

[70] Zhang S, Chen Q, Jing D, et al. Visible photoactivity and antiphotocorrosion performance of PdS–CdS photocatalysts modified by polyaniline[J]. International journal of hydrogen energy, 2012, 37(1): 791-796.

[71] Zhang K, Jing D, Chen Q, et al. Influence of Sr-doping on the photocatalytic activities of CdS–ZnS solid solution photocatalysts[J]. International journal of hydrogen energy, 2010, 35(5): 2048-2057.

[72] Li N, Zhou B, Guo P, et al. Fabrication of noble-metal-free $Cd_{0.5}Zn_{0.5}S$/NiS hybrid photocatalyst for efficient solar hydrogen evolution[J]. International journal of hydrogen energy, 2013, 38(26): 11268-11277.

[73] Luo B, Li J, Wang W, et al. Boosting photocatalytic hydrogen production via interfacial engineering over a Z-scheme core/shell heterojunction[J]. Nano Research, 2023, 16(1): 352-359.

[74] Jing D, Liu M, Guo L. Enhanced hydrogen production from water over Ni doped $ZnIn_2S_4$ microsphere photocatalysts[J]. Catalysis letters, 2010, 140: 167-171.

[75] Li J, Hatami M, Huang Y, et al. Efficient photothermal catalytic hydrogen production via plasma-induced photothermal effect of Cu/TiO_2 nanoparticles[J]. International Journal of Hydrogen Energy, 2023, 48(16): 6336-6345.

[76] Ma X, Ai C, Cao J, et al. Heterojunction formed by TiO_2 supported on lamellar La_2NiO_4 perovskite for enhanced visible-light-driven photocatalytic hydrogen production[J]. Journal of Photonics for Energy, 2021, 11(3): 034001-034001.

[77] Song R, Luo B, Geng J, et al. Photo-thermocatalytic hydrogen evolution over Ni_2P/TiO_2 for full-spectrum solar energy conversion[J]. Industrial & Engineering Chemistry Research, 2018, 57(23): 7846-7854.

[78] Cao J, Zhang J, Guo W, et al. A Type-I Heterojunction by Anchoring Ultrafine Cu_2O on Defective TiO_2 Framework for Efficient Photocatalytic H_2 Production[J]. Industrial & Engineering Chemistry Research, 2023, 62(3): 1310-1321.

[79] Hu S, Shi J, Luo B, et al. Significantly enhanced photothermal catalytic hydrogen evolution over Cu_2O-rGO/TiO_2 composite with full spectrum solar light[J]. Journal of Colloid and Interface Science, 2022, 608: 2058-2065.

[80] Hu S, Geng J, Jing D. Photothermal effect promoting photocatalytic process in hydrogen evolution over graphene-based nanocomposite[J]. Topics in Catalysis, 2021: 1-10.

[81] Luo B, Song R, Jing D. ZnCr LDH nanosheets modified graphitic carbon nitride for enhanced photocatalytic hydrogen production[J]. International Journal of Hydrogen Energy, 2017, 42(37): 23427-23436.

[82] Luo B, Song R, Geng J, et al. Strengthened spatial charge separation over Z-scheme heterojunction photocatalyst for efficient photocatalytic H_2 evolution[J]. Applied Surface Science, 2019, 475: 453-461.

[83] Shi J, Zheng B, Mao L, et al. MoO_3/g-C_3N_4 Z-scheme (S-scheme) system derived from MoS_2/melamine dual precursors for enhanced photocatalytic H_2 evolution driven by visible light[J]. international journal of hydrogen energy, 2021, 46(3): 2927-2935.

[84] Li J, Ma L, Huang Y, et al. In situ construction of oxygen deficient MoO_3-x nanosheets/porous graphitic carbon nitride for enhanced photothermal-photocatalytic hydrogen evolution[J]. International Journal of Hydrogen Energy, 2023, 48(35): 13170-13180.

[85] Li J, Huang Y, Luo B, et al. Efficient photothermal-assisted photocatalytic hydrogen production over a plasmonic CuNi bimetal cocatalyst[J]. Journal of Colloid and Interface Science, 2022, 626: 975-984.

[86] Luo B, Song R, Geng J, et al. Towards the prominent co-catalytic effect of ultra-small CoP particles anchored on g-C_3N_4 nanosheets for visible light driven photocatalytic H_2 production[J]. Applied Catalysis B: Environmental, 2019, 256: 117819.

[87] Li J, Peng H, Luo B, et al. The enhanced photocatalytic and photothermal effects of Ti_3C_2 Mxene quantum dot/macroscopic porous graphitic carbon nitride heterojunction for Hydrogen Production[J]. Journal of Colloid and Interface Science, 2023, 641: 309-318.

[88] Luo B, Liu J, Guo H, et al. High efficiency photoelectrochemical hydrogen generation using eco-friendly Cu doped Zn-In-Se colloidal quantum dots[J]. Nano Energy, 2021, 88: 106220.

[89] Zhu Y, Ma B, Zeng Z, et al. Solar collector tube as secondary concentrator for significantly enhanced optical performance of LCPV/T system[J]. Renewable Energy, 2022, 193: 418-433.

[90] Zhu Y, Ma B, He B, et al. Liquid spherical lens as an effective auxiliary optical unit for CPV/T system with remarkable hydrogen production efficiency[J]. Applied Energy, 2023, 334: 120733.

[91] Zeng Z, Geng J, Ai C, et al. Experimental investigation on parameter optimization of liquid spectral beam splitter for continuous photocatalytic hydrogen production accompanied with photovoltaic power generation under solar full spectrum[J]. International Journal of Hydrogen Energy, 2024, 56: 1202-1215.

[92] Guo L, Jin H. Boiling coal in water: Hydrogen production and power generation system with zero net CO_2 emission based on coal and supercritical water gasification[J]. International Journal of Hydrogen Energy, 2013, 38(29): 12953-12967.

[93] Guo L J, Jin H, Ge Z W, et al. Industrialization prospects for hydrogen production by coal gasification in supercritical water and novel thermodynamic cycle power generation system with no pollution emission[J]. Science China Technological Sciences, 2015, 58: 1989-2002.

[94] Guo L, Ou Z, Liu Y, et al. Technological innovations on direct carbon mitigation by ordered energy conversion and full resource utilization[J]. Carbon Neutrality, 2022, 1(1): 4.

[95] Ge Z, Jin H, Guo L. Hydrogen production by catalytic gasification of coal in supercritical water with alkaline catalysts: Explore the way to complete gasification of coal[J]. International Journal of Hydrogen Energy, 2014, 39(34): 19583-19592.

[96] Sun J, Feng H, Xu J, et al. Investigation of the conversion mechanism for hydrogen production by coal gasification in supercritical water[J]. International Journal of Hydrogen Energy, 2021, 46(17): 10205-10215.

[97] Liu S, Jin H, Wei W, et al. Gasification of indole in supercritical water: nitrogen transformation mechanisms and kinetics[J]. International Journal of Hydrogen Energy, 2016, 41(36): 15985-15997.

[98] Wang R, Lu L, Zhang D, et al. Effects of alkaline metals on the reactivity of the carbon structure after partial supercritical water gasification of coal[J]. Energy & Fuels, 2020, 34(11): 13916-13923.

[99] Ge Z, Guo L, Jin H. Catalytic supercritical water gasification mechanism of coal[J]. International Journal of Hydrogen Energy, 2020, 45(16): 9504-9511.

[100] Cao C, Guo L, Yin J, et al. Supercritical water gasification of coal with waste black liquor as inexpensive additives[J]. Energy & Fuels, 2015, 29(1): 384-391.

[101] He L, Hong X, Wang Y, et al. Achieving 12.0% Solar-to-Hydrogen Efficiency with a Trimetallic-Layer-Protected and Catalyzed Silicon Photoanode Coupled with an Inexpensive Silicon Solar Cell[J]. Engineering, 2023, 25: 128-137.

[102] Shi Y, Wang Y, Yu J, et al. Superscalar phase boundaries derived multiple active sites in $SnO_2/Cu_6Sn_5/CuO$ for tandem electroreduction of CO_2 to formic acid[J]. Advanced Energy Materials, 2023, 13(13): 2203506.

[103] Sahara G, Ishitani O. Efficient photocatalysts for CO_2 reduction[J]. Inorganic chemistry, 2015, 54(11): 5096-5104.

Beyzanur Yavuz[1,2], Müslüm Arıcı[1], Sandro Nižetić[3]

A systematic review on battery thermal management systems for electric vehicles

[1]Mechanical Engineering Department, Engineering Faculty, Kocaeli University, 41001, Kocaeli, Turkey
[2]Mechanical Engineering Department, Engineering Faculty, Düzce University, 81620 Düzce, Turkey
[3]University of Split, FESB, Rudjera Boskovica 32, 21000, Split, Croatia

Abstract

The new technology of electric vehicles (EVs) is a promising alternative to deal with energy crisis, environmental pollution, global warming and climate change problems, as they are more environmentally friendly and efficient than internal combustion engine vehicles. Lithium-ion batteries, considered to be the heart of EVs, require specific operating conditions in terms of temperature. The most efficient operating temperature range for lithium-ion battery technology is between 25°C and 40°C, and the peak temperature difference between cells should be less than 5°C. The performance of battery decreases at values outside of the efficient operating temperature range. Therefore, an effective battery thermal management system (BTMS) is essential to improve the performance of the vehicle in safe and economic conditions. In this review, the methods of effectively dissipating the heat produced in the battery due to fast charging/discharging processes, controlling the undesired temperature rise in the battery, the BTMS and working principles necessary for ensuring EV safety and performance are addressed. In this regard, air-based cooling, phase change material based cooling, heat pipe based cooling, liquid-based cooling, and hybrid cooling methods have been thoroughly investigated. The advantages, drawbacks, application strategies and superior features of each method compared to the other are discussed and recommendations are given for future works.

***Keywords**: Battery thermal management system, Cooling, Electric vehicle, Charging/Discharging.*

1. Introduction

Diesel and gasoline vehicles release large amounts of CO, CO_2, SO_2, NO_x, HC, and particulate matter into the atmosphere [1,2]. Exhaust gases and particulate matter emitted from internal combustion engine vehicles bring with them problems that threaten the whole world, such as environmental pollution, global warming and climate change. 191 countries signed the Paris Climate Agreement to alleviate these problems, which are getting worse on a global scale [3]. With the depletion of fossil resources and the increasing importance of renewable energy sources, scientists have developed electric vehicles (EVs) and hybrid electric vehicles (HEVs) that are more efficient and less harmful to the environment than internal combustion engine vehicles. In addition to promising zero emissions, to create a cleaner environment and a greener future, EVs have also become an attractive vehicle that requires less energy cost per km than gasoline and diesel vehicles [4]. The energy for EVs is supplied by batteries which are one of the most vital components of the electric vehicle. The chemical properties of the battery and the type of battery determine the life of the battery, operating temperature, self-discharge rate, energy density, power capacity, and charge/discharge rate [5]. Although many types of batteries such as nickel-cadmium, lead-acid, solid-state, hybrid-nickel metal and lithium-ion have been used in electric vehicles from past to present, lithium-ion batteries stand out with their high energy density, high output voltage, being more environmentally friendly, no memory effect, less affected by temperature compared to other batteries, and low self-discharge rate [6,7]. However, lithium-ion batteries are very demanding on operating temperatures. The most suitable operating temperature for lithium-ion batteries is between 25°C and 40°C, and the temperature inequality between the battery cells should not exceed 5°C [8]. As the temperature inhomogeneity increases, the battery life decreases [9]. At higher temperatures above these conditions, battery capacity, performance characteristics, life, and chemical structure are adversely affected [10]. At extreme temperatures of 80°C and above, safety dangers such as thermal runaway, electrolytic explosion, and the release of hazardous gases may occur in the battery [11]. Thermal runaway is an undesirable situation that leads to the battery cells to heat up too much, thus shortening the service life of the battery [12]. Since the lithium-ion battery cell is limited to 2.4 - 4.2 V values, battery packs are created by connecting the cells in series and parallel to provide the desired voltage values and required performance [13]. Due to space and weight constraints, battery cells in contact positioned so closely affect each other thermally and may trigger an explosion [14]. In addition, the efforts to charge the EV in a shorter time and the applications to increase the power density to get a more effective performance from the battery also increase the heat generated in the battery, consequently, leading to a rise in the temperature of the battery pack. Considering all these, the battery thermal management system (BTMS) is necessary to ensure the safety of the vehicle, improve driving conditions and increase its performance. BTMSs perform heating and cooling as needed to keep the battery cells operating within the optimum operating temperature [15]. Considering the fact that the vehicle is constantly in motion and the ambient temperature changes depending on the climatic conditions, determining the appropriate BTMS strategy and developing and optimizing the BTMS design is an important research topic. At this point, the cooling load required by the battery, the battery type (cylindrical, prismatic and pouch type), the vehicle type and the ambient temperature are critical in managing the thermal problems of the battery [16].

2. Review Methodology

Currently, there are numerous studies on BTMS. This review paper was compiled based on the studies between 2018 and 2023, especially including recent articles. During these years, the demand for EVs has boosted due to the support of the country's administrations and various environmental concerns. In view of this situation, efforts in this field have accelerated in order to cope with the challenges. Numerous reports and research articles on BTMS in the past and present have attempted to find solutions to the challenges of heat management in electric vehicles. This article primarily focuses on the classification of BTMS, the advantages and disadvantages of each method, and the developments in battery cooling strategies in recent years. Therefore, articles published in distinguished journals by leading scientists working on BTMS were specifically investigated and included in the current study. Research and review articles fallen within the scope of this study were analyzed in detail. In addition, internationally recognized journals and studies written only in English were included in the review and discussion process. In order to determine the most relevant paper for the study, some keywords such as BTMS, BTMS types, air-cooled BTMS, PCM-based BTMS, liquid-cooled BTMS, HP-based BTMS, and Hybrid BTMS were searched. The research, which specifically focused on issues related to thermal management strategies, constraints and applicability of EV batteries, resulted in 94 articles deemed suitable for inclusion in the study. BTMS types are addressed respectively, and their advantages, disadvantages, cooling efficiency, and cost analysis are discussed. Finally, research gaps of BTMSs, possible scenarios, and future studies are presented.

3. Types of BTMS

The BTMS of an electric vehicle must ensure that the battery remains within the effective temperature range by performing heating and cooling in the battery when necessary, so that the vehicle performs within safe limits [17]. Ambient temperature is one of the important parameters affecting the performance of electric vehicles. When the ambient temperature drops below 0°C, the performance of the battery declines significantly, due to fact that, at these low temperatures, a lithium coating can suddenly form in the battery pack [18]. Therefore, BTMS performs heating to maintain the performance and chemistry of the battery. It also performs cooling at temperatures exceeding the limits of battery health and vehicle safety. In addi-

tion to the battery pack, software and hardware equipment are used in BTMS to provide thermal safety [15]. Electric vehicle developers are optimizing the use of high energy density battery packs to increase vehicle range. However, this requires BTMS to work more effectively. Techniques used for BTMS can be divided into 5 groups; liquid-based cooling, air-based cooling, heat pipe (HP) based cooling, phase change material (PCM) based cooling, and combination of at least two aforementioned methods, i.e. hybrid cooling [19]. The advantages, disadvantages, and system component of these systems are presented in Table 1. Literature survey regarding each BTMS technique mentioned above is discussed in separate subsections. The key findings in literature for each technique are summarized in the form of table.

Although the equipment, materials and design parameters used in each of these systems are different, their intended use and cooling performance also differ. Apart from this, BTMSs are also classified according to the amount of energy consumption, active and passive method [20]. The classification of these methods into subtitles is summarized in Figure 1. Passive methods do not require external cooling or heating equipment. The use of fins, HP, and PCM is among the most common passive methods. In the active method, unlike the passive method, an extra energy source such as a pump or fan is needed. Although this improves cooling performance, it is also considered a costly approach [21].

3.1. Air based BTMS

Air-based BTMS is one of the considerable methods that can be used to keep the battery at effective operating temperature [22]. Air-based BTMS continues to be preferred in light-duty EVs thanks to its uncomplicated structure, no risk of leakage, lightness, long life, and low cost [25-25]. However, as liquid-based BTMSs are developed and provide higher cooling performance, air-based BTMSs are falling into the background. Air-based BTMS has disadvantages compared to liquid-based BTMS, such as lower cooling performance, noise problems caused by the fan, and higher energy consumption [26]. The specific heat capacity of air is considerably lower compared to liquids, requiring higher airflow rate to reach the desired results [27]. Additionally, compared to other cooling methods, air cooling can cause high temperature differences between cells. Thus, the battery may not achieve the expected performance, which adversely affects the chemistry and service life of the battery. To prevent these problems, more air flow can be directed to the battery pack within acceptable pressure loss and cost limits or different channel geometries can be considered. However, in conditions where cooling is insufficient, it should be combined with liquid cooling or hybrid cooling methods [28].

In air-based BTMSs, the air flow rate entering the system, the ventilation channel and its structure, the battery pack, and the geometry of the battery used are of great importance [29]. In air-based BTMSs, it is possible to change the battery cell arrangement, adjust the air flow, use different geometry batteries, and change the inlet and outlet geometry to enhance the cooling performance [30].

Table 1. Features of BTMS used in EVs to date.

BTMS	Advantages	Disadvantages	System Components
Air based BTMS	Uncomplicated structure, long life, low cost, electrical safety, no risk of leakage as in liquid-based and PCM-based BTMS	Low cooling performance, high energy consumption	Fans, ventilation channel
Liquid based BTMS	High cooling efficiency, more uniform cell temperature distribution	High energy consumption, risk of leakage and complex structure	Cold plate, heat pipe, jacket, pump
Heat pipe based BTMS	Flexible geometry, less noise compared to air cooling and high cooling	Not sufficient when reaching high discharge rates, risk of leakage and high cost	Heat pipe
PCM based BTMS	More uniform temperature distribution, fast thermal response, no need for extra energy, effective cooling performance when integrated with other systems	Risk of leakage, lower thermal conductivity compared to liquid-based BTMS	Phase Change Material

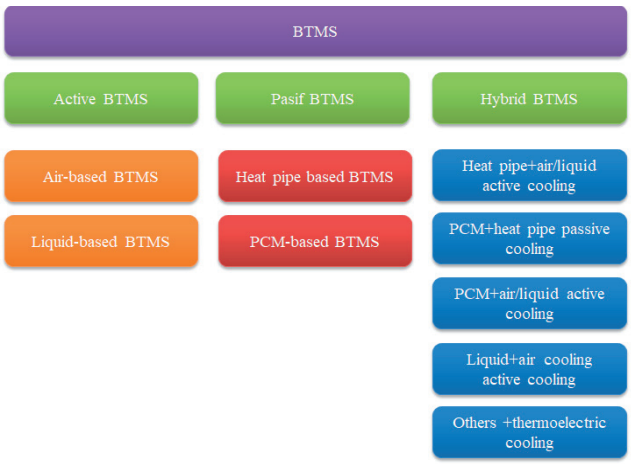

Fig. 1. BTMS classification [21].

Singh et al. [31] suggested air-based BTMS to protect the battery from temperature exposure, ensuring its durability and sustained performance. They utilized 15 cylindrical battery cells, included a straight wall and a wall with different undulation numbers, and compared the results quite comprehensively. It is clear that increasing the air inlet velocity considerably enhances the cooling performance, and the use of undulating walls compared to straight walls leads to a non-negligible temperature drop in the battery temperature. They also discussed the cooling efficiency by altering the number of battery cells. Yang et al. [32] developed a new study to improve temperature uniformity using air-based BTMS. The effect of valve opening and air flow parameters in the valve on temperature changes in the battery was investigated. It was concluded that the valve opening parameter improved the temperature uniformity in the battery and that the valve opening and pressure difference were inversely proportional.

Air-based BTMSs are basically divided into active and passive systems according to the way they use the air. While air intake to passive systems is provided from the atmosphere, auxiliary equipment such as fans are used in active systems [33]. Akbarzadeh et al. [34] compared a 48V battery pack built with 12 prismatic battery cells, air-based and liquid-based BTMS using computational fluid dynamics. Coolant flow rate, coolant temperature, power consumption were the parameters changed. In both systems, it was found that increasing the coolant throughput led to a decrease in the maximum cell temperature. In addition, the increase in coolant throughput had a greater impact compared to the liquid-based BTMS. Table 2 lists studies on air-based cooling methods and highlights the key details of the study.

3.2. PCM based BTMS

Compared to air-based and liquid-based BTMS, PCM are promising materials that allow large amounts of heat to be stored and released during phase change and have become the focus of attention by researchers [35]. The classification of PCM is presented in Figure 2. PCMs have fast thermal responses [36]. PCM provides more uniform temperature distributions in the battery compared to air-based and liquid-based BTMS, but may not be as effective as liquid cooling at high discharge rates [37,38]. In addition, PCMs have good cooling performance without the need for extra energy consumption [39]. But, PCMs are easily and frequently integrated with PCM-liquid cooled or PCM-air cooled BTMSs to rapidly dissipate heat stored in the battery, forming a crucial component of hybrid cooling [10, 40]. However, besides these features, PCM has low thermal conductivity and leaks problem [41]. PCM's low thermal conductivity makes it harder for heat to build up in the battery and to conduct heat out of the battery pack. Therefore, combining PCM and other cooling methods becomes inevitable to improve cooling performance and efficiency. PCM-based BTMSs are more vulnerable to ambient temperatures than air-based and liquid-based BTMSs, therefore their adoption is constrained [16]. Considering all these features, PCMs are not yet widely used in commercial EVs [42]. Numerous studies have been conducted on the temperature behavior, cooling performance and cost effectiveness of using PCM in BTMS. Studies on this topic, which has moved to the centre of scientific attention, continue unabated. Patel and Rathod [43] added fins to improve the multiple cycle cooling performance of PCM-based BTMS. And when the rest time is taken into account in the analysis, it was seen that the fins and 20 minutes rest time for multiple cycles were close to the expected results. Deng et al. [44] used composite phase change material (CPCM) to improve the leakage and poor thermal conductivity problem of PCM. As a result, it was concluded that the optimization of the use of CPCM in EVs and HEVs would yield broadly effective and beneficial results. Bais et al. [45] surrounded a 1.2 Ah, 3.7V single battery cell with 4 mm PCM layer. They performed discharge experiments in the presence and absence of PCM. As a result of the study, they measured temperature behavior and electrical changes separately for 1200 seconds in both cases. It was revealed that when PCM was integrated into the system, the battery cell thermal behavior was provided more perfectly and was more durable compared to the one without PCM in the same experimental environment. Li et al. [46] proposed a BTMS design using PCM. The aim of the research was to reduce the weight of the PCM by keeping it within reliable working temperature under favorable operating conditions. The study with a variable number of battery cells was compared and discussed experimentally and numerically. It is clearly seen that as the PCM radius and the heat generation rate of the battery grow, the peak temperature difference and the battery temperature increase, respectively. Zhang et al. [47] presented BTMS with various fin configurations depending on the PCM to reinforce heat transfer, which is a major phenomenon. The number of fins, thickness, angle, length, area and variable heat transfer coefficient were the parameters investigated. The computational fluid dynamics analysis results were validated by experimental studies. Finally, the novel fins designed possessed outstanding performance characteristics compared to the traditional flat fins. Huo et al. [48] introduced a PCM-based BTMS method to study temperature uniformity, which is a crucial point in the research and improvement of battery technologies. Table 3 presents recent studies on PCM-based cooling methods, discusses the working method and purpose of the study, and classifies the conditions under which the study is conducted.

Table 2. Summary of studies on air-based BTMS.

Author	Method	Battery		Tmax	Remarks
		Type	Number		
Wang et al. [26]	Sim.	Cylindrical	24	304.27K	Channel distance and air inlet velocity optimization
Yu et al. [52]	Sim.	Cylindrical	16	NA	Investigation of the effects of air inlet and outlet cross section on the temperature of the battery pack
Li et al. [53]	Sim.	Cylindrical 2230 mAh	32	41.07 °C	Economic optimization of BTMS, investigation of the relationship between battery temperature and cycle life, determining the relationship between BTMS thermal efficiency increase and cycle cost
Mao-Sung Wu [54]	Sim.	Prismatic	12	NA	Effect of air cooling type on battery thermal performance and energy efficiency, optimization study

Table 3. Summary of studies on PCM-based BTMS.

Author	Method	Battery			Tmax	Remarks
		Type	Number	Load		
El Idi et al. [55]	Exp. +Sim.	Cylindrical 2500 mAh	1	NA	NA	Investigation of cell temperature during charge/discharge cycles
Wu et al. [56]	Exp.	Prismatic	5	1C 3C 5C	53.47 ◦C at 3C	Design criteria of shape memory composite phase change material and testing its applicability on BTMS, investigation of performance characteristics, temperature distribution and heat dissipation capacity of BTMS at different charge/discharge rates
Verma et al. [57]	Sim.	Pouch	1	2C	305 K at the end of 1200 s at 3 mm thickness	Comparison of the effects of capric acid and commonly used paraffin on BTMS at different thicknesses and different ambient temperatures, observing the effect of PCM on BTMS at high discharge rate
Kadam and Kongi [58]	Exp.+ Sim.	Cylindrical	12	1C 2C 3C	NA	Discussing the effect of PCM thickness on battery temperature distribution, cooling performance and weight at different charge/discharge rates.

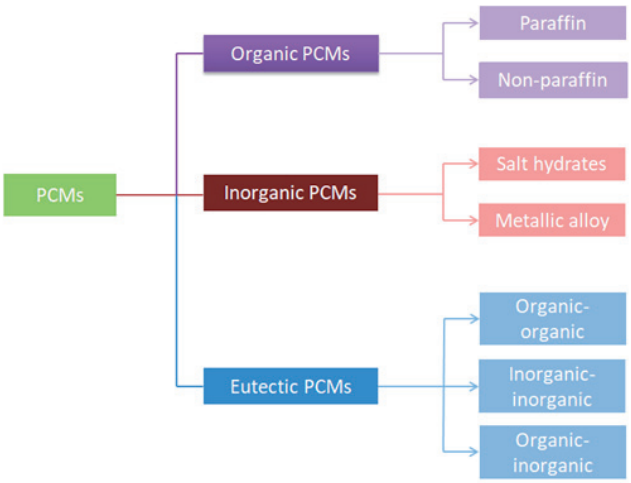

Fig. 2. Classification of PCM [49].

3.3. Liquid-based BTMS

Liquid-based BTMS is one of the most frequently used methods to secure the safe operation of batteries in EVs. Although it requires a more complex structure and more energy consumption compared to air-based BTMS, it provides a very effective cooling performance thanks to the high specific heat capacity of the liquid [50]. However, liquid-based cooling is costly and increases the mass of the battery system considerably [51]. This technique is commonly utilized in leading EVs such as the BMW i3 and Tesla due to its superior cooling ability [38]. Water and glycol are frequently used in these systems. A mixture of water and glycol can also be used according to cost analysis and ambient conditions [59]. Vikram et al. [60] used a mixture of water and different concentrations of Ethylene Glycol and Propylene Glycol as coolant in

BTMS. Temperature change, energy need, and ambient temperature were the analyzed parameters. The battery pack is set to operate at a constant temperature of 25°C. Considering the conditions of India, where the study was conducted, the ambient temperature was started from 30°C and increased by 5°C, up to 50°C. The load on BTMS, cumulative energy consumption value, and temperature profile results were evaluated together. It has been revealed that it takes more time and requires more cumulative energy to reduce the fluid entering the system to 25°C at high ambient temperatures. When water and other fluid concentrations were examined, it was observed that adding 25% propylene glycol and 50% ethylene glycol to the coolant provided effective results.

Liquid-based BTMS is divided into two groups: indirect contact and direct contact. In direct contact cooling, the battery pack has a more effective cooling performance than the indirect cooling because it is in direct contact with the dielectric liquid surrounding its surface [61]. In this way, more heat is removed from the battery pack, but since the dielectric liquid used has a high viscosity, more energy is required to circulate the liquid in the system [61, 62].

In indirect liquid-cooled systems, a cold plate, jacket, and heat pipes are used to remove the heat from the battery pack and keep the vehicle running in safe conditions [62]. Although it provides a more uniform temperature distribution and significantly reduces the temperature difference, the direct contact cooling method is not preferred except for fast charging [63]. While the indirect liquid cooling method is utilized in vehicles such as the Mercedes EQS, Tesla Model Y, Porsche Taycan, the direct liquid cooling method continues to be applied in the McLaren Speedtail model [64]. In Table 4, current studies on liquid-based cooling methods are presented, the key points of the study are highlighted, and the conditions under which the study was conducted are reported.

3.4. Heat pipe based BTMS

The heat pipe is one of the effective methods used to remove the heat generated in the battery. It can significantly reduce the thermal imbalance between battery cells [65]. Heat pipes with a compact structure, flexible geometry, and high cooling performance working with the phase change principle have been developed and studied by scholars recently [66, 67]. Heat pipes possess low thermal resistance, and act as heat exchangers that transmit heat from high temperature to low temperature by using phase changes [68]. They are outstanding components capable of transferring heat despite relatively low temperature differences [69]. Guo et al. [70] developed BTMS with heat pipe and micro heat pipe to enable efficient and high performance operation of batteries. In this way, they compared battery aging, the electrochemical structure of the battery, its service life, and the heat production in the battery. As a result, although a few cycles gave effective results, they could not obtain a satisfactory thermal management result after 1250 cycles owing to the formation of solid electrolyte interphase in the battery. In addition, micro heat pipes offered better results than heat pipes in the management of the peak temperature in the battery pack and the peak temperature difference in the battery cells. Jouhara et al. [71] experimentally studied the effects of a heat mat, which can be easily incorporated into the system, on the peak temperature and temperature uniformity of the battery on prismatic battery cells, using heat pipe-based BTMS. The results were very impressive and at the same time a useful approach model. The heat mat provided a very high performance in absorbing and removing the heat produced in the battery cells, thus reducing the energy requirement from the pump. Ren et al. [72] experimentally studied a BTMS with a preheated U-shaped micro heat pipe to prevent the battery from being affected by low ambient temperature. Variable energy input to the system, the presence or absence of heat pipes surrounded by an insulating material were the parameters tested. The results indicate that heat pipes surrounded by insulating material subjected to preheating undergo a remarkable temperature increase and enable a satisfactory preheating process. It is also concluded that cooling and heating processes can be carried out together. In addition to these studies, research on HP-based cooling methods is presented in Table 5.

3.5. Hybrid cooling

Although researchers are constantly developing battery systems, the proposed systems may be inadequate if used alone. When a single method is insufficient for cooling in battery systems and efficient and desired results cannot be achieved, more than one method is used together, and higher cooling performances are achieved by emphasizing the superior features of these methods. Thus, hybrid BTMSs have been proposed and have become the focus of researchers. Hybrid BTMSs are used for different purposes depending on the application area and expectations [73].

Active systems require excessive energy and cause temperature inequalities and require the support of passive systems. By using these two cooling strategies together, energy consumption decreases and battery temperature is distributed more evenly [74]. Ahmad et al. [75] enhanced a hybrid BTMS design with PCM and air cooling. They added fins to their system to improve heat transfer and comprehensively analyzed its contribution to cooling performance with and without PCM. It was observed that the wings added to the developed hybrid BTMS facilitated the air flow and yielded excellent results compared to the other analysis conditions tested. While the highest temperature value was obtained for Fin-Air BTMS, PCM-Fin-Air BTMS remained at a more controllable and reasonable level. There was a temperature improvement of 18.6% between PCM-Fin-Air BTMS and Fin-Air BTMS. The study offered a fresh outlook, particularly in the context of high charge and discharge environments, and was highly encouraging for the future of green energy initiatives. Mousavi et al. [85] designed a cooling system that combined PCM and liquid-based BTMS using prismatic battery cells to improve cooling performance.

Table 4. Summary of studies on liquid-based BTMS.

Author	Method	Type	Battery Number	Load	Tmax	ΔT	Remarks
Li et al. [76]	Exp. +Sim.	Prismatic 64 Ah	12	1C 1.5C 2C 2.5C 3C	313 K	5 K at <3C	Analysis of the effects of operating conditions and battery pack design on the pressure drop, temperature and cooling performance of the BTMS, effect of coolant flow direction on temperature gradient
Wang et al. [77]	Sim.	Pouch battery 50 Ah	9	0.8C	311.2592 K	13.1092 K	Investigation of cooling performance of coolant flow rate and direction on BTMS
Wang et al. [78]	Exp. +Sim	Cylindrical	20	3C	53.48 °C	18.72°C (flow rate is 40 ml/min, serial cooling mode)	Improving pressure drop, energy consumption and temperature uniformity discussing the effects of coolant flow rate and serial or parallel design of the cooling system on BTMS.
Tousi et al. [79]	Sim.	Cylindrical	12	3C 5C 7C	305.59 K	1.07 K	Analyzing the effects of the inlet speed and amount of nanofluid-added liquid cooling at different discharge rates on BTMS performance and efficiency.
Chen et al. [80]	Exp.	Prismatic	8	0.5C 1C 1.5C 2C 2.5C	33.35°C	NA	Development of the regression model of the most effective and efficient BTMS in the fast charge-discharge

Table 5. Summary of studies on HP-based BTMS.

Author	Method	Type	Battery Number	Load	Tmax	Remarks
Zhang and Wei [81]	Exp.+ Sim.	Prismatic	5	4C 6C 8C	54.3 °C	Discussion of experimental and analysis results of flat heat pipe design and temperature distribution, cost and performance at different discharge rates.
Behi et al. [82]	Exp.+ Sim.	Prismatic	15	8C	43.8 °C at 0.2 m/s	Experimental and numerical discussion of different types of cooling, Investigation of battery pack temperature change by changing input speed
Liang et al. [83]	Exp.	Prismatic	2	NA	NA	Experimental discussion of the effects of coolant flow rate, coolant temperature, ambient temperature, heat generation per cell and BTMS start-up time on battery health and thermal performance.
Wang et al. [84]	Exp.+ Sim.	Cylindrical	12	3C 5C	31.55 °C	Comparing and discussing the analysis and experimental results of the effects of the design parameters of the conductive structural element in contact with the battery on the temperature distribution.

Table 6. Summary of studies on hybrid BTMS.

Author	Method	BTMS Type	Battery Type	Battery Number	Load	Remarks	Tmax	ΔT
Wang et al. [87]	Exp.+ Sim.	PCM+Liquid cooling	Cylindrical	12	1C 2C	coolant flow and inlet temperature optimization, control of energy consumption	57.6 °C, 44.8 °C	4.1 °C, <2 °C
Liu et al. [88]	Exp.+ Sim.	PCM+Liquid cooling	Cylindrical	16	1C 2C 3C 4C 5C	ambient temperature, coolant inlet temperature, flow direction optimization	46.2 °C	4.2 °C
Peng et al. [89]	Exp.+ Sim.	PCM+Heat pipe	Cylindrical	40	0.5 C 1C 2C	investigation of the effect of PCMs with different properties on the thermal performance of the battery	47.7 °C at 2C	NA
Chen et al. [90]	Sim.	Air cooling+ PCM	Cylindrical	16	1C 2C 4C 8C	investigation of ambient temperature, inlet velocity and melting and solidification temperature of PCM	NA	NA
Li et al. [91]	Exp.+ Sim.	Air cooling + Liquid cooling	Pouch battery 16 Ah	1 and 5	1C 3C 5C	effects of air velocity, air inlet location, different number of fans, cold plate thickness on BTMS	64.3 °C at 5C	NA
Yuan et al. [92]	Exp.	Heat pipe + Liquid cooling	Prismatic 50Ah	1	0.5–2C	coolant flow rate, evaporation section and condensing section length of HP-CP, ambient and inlet coolant temperature, battery discharge rate	34.1 °C	1 °C
Wang et al. [93]	Exp.	Heat pipe + PCM	Cylindrical	40	2C	effect of PCM tube and HP hybrid system on BTMS	47.7 °C	2.5 °C
Jang et al. [94]	Exp. + Sim.	Heat pipe + Liquid cooling	Prismatic 40Ah	10	0.5–2C	determination of the effects of discharge rate, liquid mass flow rate, liquid temperature and ambient temperature on BTMS		

They carried out the analysis with the help of ANSYS FLUENT at 1C, 2C, and 3C variable discharge rates. They concluded that the PCM plates integrated into the battery system provide a more significant cooling effect as the discharge rate increases. They discussed the cooling performance when 1 and 3 PCM plates were added to the system without using PCM by changing the speed of the refrigerant entering the mini-channel cooling plates at 3C discharge rate. When the refrigerant velocity was 0.01 m/s and a 100% increase in flow rate was made, a significant temperature drop of 9 K and 15 K occurred in the battery. Faizan et al. [86] developed a new cooling design by combining PCM and cooling plate with 3 mm diameter in different channel structures.

Isfahani et al. [88] proposed a new approach by combining PCM and microchannels to alleviate the extreme temperature and temperature inequality that pose a major threat to the battery. As a result, PCM/metal foam shows the highest temperature, although it is more excellent in terms of temperature uniformity and temperature standard deviation. In contrast, microchannels exhibit the opposite behavior. Therefore, the utilization of these two techniques together ensures that the battery operates within the desired operating temperatures. Additionally, an analysis of the response characteristics of battery cells and packs has been conducted, highlighting that the effect of surrounding battery cells is substantial and should not be underestimated. Zhao et al. [89] created a hybrid system

by integrating air-based BTMS with liquid-based BTMS to improve the cooling effect. Coolant flow rate, number of pipes used in the system, fan position, and distance between coolant and battery were studied on COMSOL software and results were discussed. As a result of the analysis, it was seen that the change in the number of pipes did not have much effect on the maximum temperature in the battery. Additionally, it was concluded that there was an improvement in the temperature uniformity of the battery pack when the liquid flow rate entering the system was increased. In terms of cooling performance and energy efficiency, it is recommended that the air entering the system must not exceed 0.4 m/s. Zhou et al. [90] created a novel approach by combining an air jet and a helical flow coil into the battery system. The results revealed that this innovative hybrid system achieved a lower peak temperature difference than the liquid-based one when air cooling is applied at the positive and negative ends of the battery cell. Air inlet velocity and temperature were the parameters investigated and it was observed that varying them did not cause a major improvement in cooling performance. Wang et al. [91] proposed a novel BTMS with different flow orientations by combining PCM and liquid cooling with wavy microchannel structure. Increasing the number of liquid microchannels utilized in the improved hybrid system and different oriented flow enhanced the cooling efficiency. In addition, by switching from a microchannel cooling plate system to a hybrid system, there has been a substantial decrease in weight, which is also very advantageous in terms of cost and energy savings. Zhao et al. [92] conducted an experimental and numerical study on ANSYS FLUENT by combining composite phase change material and liquid cooling using 20 cylindrical type batteries. The study was carried out separately with pure PCM and hybrid cooling method under different experimental conditions. They inferred that with the liquid cooling included in the system in addition to PCM, the heat produced in the battery is transferred more effectively, but as a result, the temperature difference and the required energy increase. In the study conducted under 0.5C, 1C, and 2C discharge rates and variable discharge depth, when the discharge rate was 2C, the change in Reynolds number from 0 to 112 caused a 6 K decrease in the peak temperature, 59W power requirement and temperature differences. Table 6 presents a summary of the comprehensive report, organized and ranked based on recent research findings.

4. Conclusions

In this review, BTMSs of electric vehicles developed to cope with the increasing energy crisis, environmental pollution and global warming and to alleviate these problems are discussed and systematically addressed. Electric vehicles are designed to be more efficient than those powered by internal combustion engines, and they do not contribute to greenhouse gas emissions in the environment. To ensure that these vehicles operate within safe limits and with high performance, the battery must be kept in efficient operating conditions. Batteries are very sensitive to temperature, so they can be kept within safe temperature limits one of air-based cooling, liquid-based cooling, heat pipe-based cooling, PCM-based cooling or hybrid cooling methods. This also maintains battery health and chemistry and increases cycle life. The following conclusions have been formulated based on a thorough examination of the relevant literature:

- Air-based cooling is one of the most preferred basic methods with its uncomplicated structure, no risk of leakage, lightness and low cost. However, since the specific heat capacity of air is lower than that of liquid, the cooling performance is lower than liquid cooling. Additionally, due to the application strategy of this method and the thermophysical properties of air, significant temperature differences can occur between the cells in the battery pack. This can degrade the performance and lifespan of batteries. To enhance the cooling efficiency of air-based cooling, the air flow rate, ventilation channel and structure, battery type and arrangement can be improved. Yet, when all these adjustments are insufficient, air-based cooling should be applied with other types of cooling techniques to maintain the battery within the range.
- Liquid-based cooling is one of the methods widely used in electric vehicles today to keep the battery in the optimum temperature range and provides high cooling performance. However, since liquid-based cooling has a complex system structure, energy consumption and cost can be relatively high. Today, many automotive manufacturers such as Mercedes, Tesla, Porsche, and McLaren have applied liquid-based BTMS instead of air-based BTMS due to its effective thermal management performance.
- PCM-based cooling is one of the BTMSs that is increasingly becoming the focus of researchers' attention and is constantly being developed. PCMs can absorb and dissipate large amounts of energy without needing extra energy. They have fast response times and a structure that can be easily integrated with other systems. However, PCMs have low thermal conductivity and leakage problems. Although various research studies have been conducted on the cooling performance, system compatibility and cost optimization of PCM, it has not yet been fully utilized commercially in EVs.
- Heat pipe-based cooling is one of the methods studied with great interest by researchers. Heat pipes with a compact structure and flexible geometry can remove the heat produced in the battery without needing extra energy. These systems, which work on the phase transformation principle, are sensitive to even low temperature differences and can operate efficiently.
- When a solely battery management system alone is insufficient for securing efficient run of batteries, more than one method can be employed simultaneously. In this way, systems that provide superior cooling performance can be created with hybrid cooling. Excess energy demanded by active systems can be compensated by the inclusion of passive systems. Furthermore, the control of the maximum temperature of the battery pack and the distribution of the cell temperature can be substantially improved.

5. Recommendation and future work

The numerical analysis of the battery is a complicated and extensive process in itself, and it is very essential that the results are consistent with the actual driving cycle. Deviation levels must be within acceptable limits and can be further improved. Although a variety of studies have been carried out regarding BTMS, several critical aspects still need to be examined. The majority of the weight of existing EVs consists of battery systems. This also leads to higher transportation costs. A key aspect of ongoing studies involves the replacement of the existing battery with a higher energy density variant to minimize weight. However, this creates certain problems, such as, under fast charge/discharge cycles, the higher energy density battery generates more heat. To dissipate this heat generated in the battery pack, a BTMS is necessary to maintain effective and safe conditions for continuous cycling. For variable battery types, cost analysis, weight, volume, and energy consumption values should be evaluated all together to reach optimum operating temperature range conditions. Although several parameters such as battery geometry and arrangement, ambient temperature, fluid inlet velocity, channel structures, number of channels, fluid type, and additives have been investigated for different BTMS types, it has been observed that there is a gap in cost effectiveness and energy efficiency studies. Therefore, it is thought to be beneficial for future studies to shift to this area, which is a key factor for BTMS. In addition, when the methods used in BTMSs are discussed separately, the following approaches may be valuable for potential research and can be focused on these issues.

- BTMSs for safe driving conditions: Advanced technology EV batteries have a higher energy density compressed into the battery and operate under continuous fast charge/discharge cycles. Without an appropriate control mechanism, this situation may adversely affect the battery, resulting in considerable destruction. In case of crash or collision, it may cause the release of poisonous gas, fire, explosion or even loss of life. BTMS is required to eliminate all these negativities and ensure the operation of the battery within a controlled temperature range. However, it is necessary to study in depth for different battery technologies to prevent the risk of thermal runaway, fire and explosion. Additionally, it is essential to consider the entire battery system, rather than just individual battery cells, when developing effective cooling strategies and thermal management solutions.

- During fast charge/discharge cycles, the cooling capacity required by the battery and the recommended cooling system must match each other. In order to choose the most appropriate cooling method, battery type and geometry, energy density of the battery, and discharge/charge conditions must be determined correctly. This approach is essential for preventing the battery from overheating.

- Air-based BTMSs: Air-based BTMS has significant restrictions that can lead to some problems. This method, in terms of its structure and applicability, may cause unequal temperature distribution between the cells in the battery pack, and it may produce undesirable levels of noise when operated at high levels. In terms of cooling efficiency, it is more suitable for use in light commercial vehicles. In order to enhance the cooling performance of air-based BTMS under safe and economic conditions, it is recommended to integrate air-based BTMS with other cooling strategies and to conduct deeper studies in this field in future studies. In addition, the distance between battery cells can be regulated within the allowed dimensions in order to control the battery temperature and ensure safe driving conditions. Moreover, this method can be further improved with the help of differently directed air flow and air duct with different geometry.

- PCM-based BTMSs: PCM-based cooling, which promises great potential, has not yet been fully commercialized. More research and development work are needed on these materials, to be utilized in EVs. System feasibility and material characteristics can be further enhanced by incorporating composite PCMs into BTMS. It is expected that the improvement of the flammability issue of PCMs, optimization of system size, and advancement of weight and thermal performance values will facilitate the inclusion of PCM in the EV market. The problem of decreasing PCM latent heat in continuous cycle should be addressed, and studies should be carried out to prevent the risk of leakage. In addition, by integrating PCM and liquid-based BTMS under appropriate operating conditions to meet the requirements of the system, more effective thermal control can be achieved than using these methods alone.

- Liquid-based BTMSs: Liquid-based BTMS is capable of effectively managing battery temperature in systems where high cooling performance is demanded. However, if not designed properly, it can result in a high temperature difference between cells. When this situation repeats in a continuous cycle, the service life of the battery is shortened and battery chemistry may deteriorate. In liquid-based BTMS, the selection of the coolant that corresponds to the cooling capacity required by the battery and its compatibility with the system is crucial. Especially in liquid-based BTMSs, additives utilized to improve cooling performance and conductivity coefficients cause heterogeneity problems in the closed loop. In the long term, efforts to ensure the flow of liquid cooling in homogeneous and appropriate conditions should continue. Additionally, studies should be developed to increase heat transfer by increasing the contact area of the battery component and the cooling interface. A major drawback for liquid-based BTMS is the leakage problems and the risks associated with it. This challenge can be mitigated by the development of a design that works in harmony with the requirements of the system and the inclusion of suitable sealing components. When all these complicated constraints and challenges are fully investigated and addressed with innovative solutions, liquid-based BTMS can be transformed into a safe and secure system.

- HP-based BTMSs: For thermal management, enhancing the heat transfer properties of the HP is the primary focus, considering that the battery is in constant operation. It is preferable to start research by developing heat pipe design, battery-heat pipe layout and material properties. Aluminum HPs are expected to be preferred to provide an advantage when weight is taken into account.
- Hybrid cooling: Hybrid cooling systems are created by integrating these methods together when air-based BTMS, PCM-based BTMS, liquid-based BTMS, and HP-based BTMS are insufficient alone. Hybrid method, which includes advanced and new technologies, requires more space, and increases weight as it involves different cooling methods. Additionally, the real-time thermal performance of this method on lithium-ion batteries needs to be improved. Especially by combining HP and PCM, various thermal management combinations can be designed that provide superior cooling compared to other approaches. However, studies should be carried out to determine the most optimal strategy considering different aspects such as cost, volume, weight, and time management. In addition, when the current researches in the literature are investigated, it is noticed that initially the cooling performance of the battery is aimed to be improved. However, there are very limited efforts on the response and sustainability of all these management technologies in the long term. This is a huge gap in the literature and the focus of future studies should be concentrated on this field. The hybrid cooling method is considered a very promising approach for the EV market and future studies that transition to high-performance and fast charging conditions. However, since it incorporates versatile cooling strategies, design configurations and cooling equipment must be selected harmoniously.

6. References

[1] Kim, I., Kim, Y., Kwon, J., Lee, C., & So, J. J. Beyond concept: The viability of exclusive lanes for zero emission vehicles on expressways. Transportation Research Part D: Transport and Environment 121 (2023) 103803.

[2] Kothare, C. B., Kongre, S., Malwe, P., Sharma, K., Qasem, N. A., Ağbulut, Ü., ... & Panchal, H. Performance improvement and CO and HC emission reduction of variable compression ratio spark-ignition engine using n-pentanol as a fuel additive. Alexandria Engineering Journal 74 (2023) 107-119.

[3] Shrinet, E.S., A. Mukherjee, and L. Kumar, A novel thermal management system design based on variable contact area to maintain uniform temperature in Li-ion battery module. Journal of Energy Storage 72 (2023) 108332.

[4] Wankhede, S. and L.V. Kamble, A novel battery cooling system using nanofluids on MATLAB Simulink. Energy Storage 5.3 (2023) e418.

[5] Gong, H. and T. Hansen, The rise of China's new energy vehicle lithium-ion battery industry: The coevolution of battery technological innovation systems and policies. Environmental Innovation and Societal Transitions 46 (2023) 100689.

[6] Wang, C., Xu, J., Wang, M., & Xi, H. Experimental investigation on reciprocating air-cooling strategy of battery thermal management system. Journal of Energy Storage 58 (2023) 106406.

[7] Aswin Karthik, C., Kalita, P., Cui, X., & Peng, X. Thermal management for prevention of failures of lithium ion battery packs in electric vehicles: A review and critical future aspects. Energy Storage 2.3 (2020) e137.

[8] Son, Y.W., D. Kang, and J. Kim, Passive battery thermal management system for an unmanned aerial vehicle using a tetrahedral lattice porous plate. Applied Thermal Engineering 225 (2023) 120186.

[9] Rao, Z., Y. Wen, and J. Zhao, Thermal performance of battery thermal management system using composite matrix coupled with mini-channel. Energy Storage 1.3 (2019) e59.

[10] Ebbs-Picken, T., C.M. Da Silva, and C.H. Amon, Design optimization methodologies applied to battery thermal management systems: A review. Journal of Energy Storage 67 (2023) 107460.

[11] Bhutto, Y. A., Pandey, A. K., Saidur, R., Sharma, K., & Tyagi, V. V. Critical Insights and Recent Updates on Passive Battery Thermal Management System Integrated with Nano-enhanced Phase Change Materials. Materials Today Sustainability 23 (2023) 100443.

[12] Chavan, S., Venkateswarlu, B., Prabakaran, R., Salman, M., Joo, S. W., Choi, G. S., & Kim, S. C. Thermal runaway and mitigation strategies for electric vehicle lithium-ion batteries using battery cooling approach: A review of the current status and challenges. Journal of Energy Storage 72 (2023) 108569.

[13] Ghaeminezhad, N., Z.S. Wang, and Q. Ouyang, A Review on lithium-ion battery thermal management system techniques: A control-oriented analysis. Applied Thermal Engineering 219 (2023) 119497.

[14] Murugan, M., Saravanan, A., Elumalai, P. V., Murali, G., Dhineshbabu, N. R., Kumar, P., & Afzal, A. Thermal management system of lithium-ion battery packs for electric vehicles: An insight based on bibliometric study. Journal of Energy Storage 52 (2022) 104723.

[15] Thakur, A. K., Sathyamurthy, R., Velraj, R., Saidur, R., Pandey, A. K., Ma, Z. & Ali, H. M. A state-of-the art review on advancing battery thermal management systems for fast-charging. Applied Thermal Engineering 226 (2023) 120303.

[16] Vikram, S., Vashisht, S., Rakshit, D., & Wan, M. P. Recent advancements and performance implications of hybrid battery thermal management systems for Electric Vehicles. Journal of Energy Storage 90 (2024) 111814.

[17] Kalaf, O., Solyali, D., Asmael, M., Zeeshan, Q., Safaei, B., & Askir, A. Experimental and simulation study of liquid coolant battery thermal management system for electric vehicles: A review. International journal of energy research 45.5 (2021) 6495-6517.

[18] Xiao, J., Zhang, X., Bénard, P., Yang, T., Zeng, J., & Long, X. Fin structure and liquid cooling to enhance heat transfer of composite phase change materials in battery thermal management system. Energy Storage 5.6 (2023) e453.

[19] Ranjbaran, Y.S., M.H. Shojaeefard, and G.R. Molaeimanesh, Thermal performance enhancement of a passive battery thermal management system based on phase change material using cold air passageways for lithium batteries. Journal of Energy Storage 68 (2023) 107744.

[20] Khaboshan, H. N., Jaliliantabar, F., Abdullah, A. A., & Panchal, S. Improving the cooling performance of cylindrical lithium-ion battery using three passive methods in a battery thermal management system. Applied Thermal Engineering 227 (2023) 120320.

[21] Luo, J., Zou, D., Wang, Y., Wang, S., & Huang, L. Battery thermal management systems (BTMs) based on phase change material (PCM): A comprehensive review. Chemical Engineering Journal 430 (2022) 132741.

[22] Sikarwar, S., Kumar, R., Yadav, A., & Gwalwanshi, M. Battery thermal management system for the cooling of Li-Ion batteries, used in electric vehicles. Materials Today: Proceedings 2023.

[23] Moosavi, A., A.-L. Ljung, and T.S. Lundström, A study on the effect of cell spacing in large-scale air-cooled battery thermal management systems using a novel modeling approach. Journal of Energy Storage 72 (2023) 108418.

[24] Wu, T., Wang, C., Hu, Y., Fan, X., & Fan, C. Research on spray cooling performance based on battery thermal management. International Journal of Energy Research 46.7 (2022) 8977-8988.

[25] Liu, L., X. Zhang, and X. Lin, Recent Developments of Thermal Management Strategies for Lithium-Ion Batteries: A State-of-The-Art Review 10.6 (2022) 2101135.

[26] Wang, Y., Liu, B., Han, P., Hao, C., Li, S., You, Z., & Wang, M. Optimization of an air-based thermal management system for lithium-ion battery packs. Journal of Energy Storage 44 (2021) 103314.

[27] Hua, Y., Zhou, S., Cui, H., Liu, X., Zhang, C., Xu, X., & Yang, S. A comprehensive review on inconsistency and equalization technology of lithium-ion battery for electric vehicles. International Journal of Energy Research 44.14 (2020) 11059-11087.

[28] Chen, K., Zhang, Z., Wu, B., Song, M., & Wu, X. An air-cooled system with a control strategy for efficient battery thermal management. Applied Thermal Engineering 236 (2024) 121578.

[29] Zhang, F., Zhang, L., Lin, A., Wang, P., & Liu, P. Multi-method collaborative optimization for parallel air cooling lithium-ion battery pack. International Journal of Energy Research, 46.10 (2022) 14318-14333.

[30] Li, C., Ding, Y., Zhou, Z., Jin, Y., Ren, X., Cao, C., & Hu, H. Parameter optimization and sensitivity analysis of a Lithium-ion battery thermal management system integrated with composite phase change material. Applied Thermal Engineering 228 (2023) 120530.

[31] Singh, L.K., R. Kumar, and A.K. Gupta, A novel strategy of enhanced thermal performance in air cooled lithium-ion battery by wavy walls. Thermal Science and Engineering Progress 43 (2023) 101964.

[32] Yang, R.Y., M.W. Wang, and H. Xi, Thermal investigation and forced air-cooling strategy of battery thermal management system considering temperature non-uniformity of battery pack. Applied Thermal Engineering 219 (2023) 119566.

[33] Ren, R., Zhao, Y., Diao, Y., Liang, L., & Jing, H. Active air cooling thermal management system based on U-shaped micro heat pipe array for lithium-ion battery. Journal of Power Sources 507 (2021) 230314.

[34] Akbarzadeh, M., Kalogiannis, T., Jaguemont, J., Jin, L., Behi, H., Karimi, D. & Berecibar, M. A comparative study between air cooling and liquid cooling thermal management systems for a high-energy lithium-ion battery module. Applied Thermal Engineering 198 (2021) 117503.

[35] Ismail, K. A., Lino, F. A., Machado, P. L. O., Teggar, M., Arıcı, M., Alves, T. A., & Teles, M. P. New potential applications of phase change materials: A review. Journal of Energy Storage 53 (2022) 105202.

[36] Wu, X., Wang, K., Chang, Z., Chen, Y., Cao, S., Lv, C. & Wang, Y. Experimental and numerical study on hybrid battery thermal management system combining liquid cooling with phase change materials. International Communications in Heat and Mass Transfer 139 (2022) 106480.

[37] Ni, R., Zhang, D., Wang, R., Xie, Z., & Wang, Y. Prevention and suppression effects of phase change material on thermal runaway in batteries. Case Studies in Thermal Engineering 48 (2023) 103160.

[38] Wang, R., Liang, Z., Souri, M., Esfahani, M. N., & Jabbari, M. Numerical analysis of lithium-ion battery thermal management system using phase change material assisted by liquid cooling method. International Journal of Heat and Mass Transfer 183 (2022) 122095.

[39] Lin, X.W. and X.L. Zhang, Research Progress of Phase Change Storage Material on Power Battery Thermal Management. Energy Technology 9.4 (2021) 2000940.

[40] Youssef, R., Kalogiannis, T., Behi, H., Pirooz, A., Van Mierlo, J., & Berecibar, M. A comprehensive review of novel cooling techniques and heat transfer coolant mediums investigated for battery thermal management systems in electric vehicles. Energy Reports 10 (2023) 1041-1068.

[41] Lee, S., U. Han, and H. Lee, Development of a hybrid battery thermal management system coupled with phase change material under fast charging conditions. Energy Conversion and Management 268 (2022) 116015.

[42] Bernagozzi, M., Georgoulas, A., Miché, N., Rouaud, C., & Marengo, M. Novel battery thermal management system for electric vehicles with a loop heat pipe and graphite sheet inserts. Applied Thermal Engineering 194 (2021) 117061.

[43] Patel, J.R. and M.K. Rathod, Novel approach for the performance augmentation of phase change material integrated battery thermal management system for number of charging/discharging cycles. Energy Storage, 5.6 (2023) e456.

[44] Deng, J., Li, X., Li, C., Wang, T., Liang, R., Li, S. & Zhang, G. Multifunctional flexible composite phase change material with high anti-leakage and thermal conductivity performances for battery thermal management. Journal of Energy Storage 72 (2023) 108313.

[45] Bais, A., D. Subhedar, and S. Panchal, Experimental investigation of longevity and temperature of a lithium-ion battery cell using phase change material based battery thermal management system. Materials Today: Proceedings 2023.

[46] Li, Y., Du, Y., Xu, T., Wu, H., Zhou, X., Ling, Z., & Zhang, Z. Optimization of thermal management system for Li-ion batteries using phase change material. Applied Thermal Engineering 131 (2018) 766-778.

[47] Z hang, F., Lu, F., Liang, B., Zhu, Y., Gou, H., Xiao, K., & He, Y. Thermal performance analysis of a new type of branch-fin enhanced battery thermal management PCM module. Renewable Energy 206 (2023) 1049-1063.

[48] Huo, Y., X. Pang, and Z. Rao, Investigation on the effects of temperature equilibrium strategy in battery thermal management using phase change material. 2020. 44.9 (2020) 7660-7673.

[49] Gu, H., Chen, Y., Yao, X., Huang, L., & Zou, D. Review on heat pump (HP) coupled with phase change material (PCM) for thermal energy storage. Chemical Engineering Journal 455 (2023) 140701.

[50] Rabiei, M., A. Gharehghani, and A.M. Andwari, Enhancement of battery thermal management system using a novel structure of hybrid liquid cold plate. Applied Thermal Engineering 232 (2023) 121051.

[51] Shen, X., Cai, T., He, C., Yang, Y., & Chen, M. Thermal analysis of modified Z-shaped air-cooled battery thermal management system for electric vehicles. Journal of Energy Storage 58 (2023) 106356.

[52] Yu, Q., Abidi, A., Mahmoud, M. Z., Malekshah, E. H., & Aybar, H. Ş. Numerical evaluation of the effect of air inlet and outlet cross-sections of a lithium-ion battery pack in an air-cooled thermal management system. Journal of Power Sources 549 (2022) 232067.

[53] Li, W., Wang, N., Garg, A., & Gao, L. Multi-objective optimization of an air cooling battery thermal management system considering battery degradation and parasitic power loss. Journal of Energy Storage 58 (2023) 106382.

[54] Wu, M.-S., Multi-objective optimization of U-type air-cooled thermal management system for enhanced cooling behavior of lithium-ion battery pack. Journal of Energy Storage 56 (2022) 106004.

[55] El Idi, M.M., M. Karkri, and M. Abdou Tankari, A passive thermal management system of Li-ion batteries using PCM composites: Experimental and numerical investigations. International Journal of Heat and Mass Transfer 169 (2021) 120894.

[56] Wu, T., Wang, C., Hu, Y., Zhou, L., & He, K. Research on novel battery thermal management system coupling with shape memory PCM and molecular dynamics analysis. Applied Thermal Engineering 210 (2022) 118373.

[57] Verma, A., S. Shashidhara, and D. Rakshit, A comparative study on battery thermal management using phase change material (PCM). Thermal Science and Engineering Progress 11 (2019) 74-83.

[58] Kadam, G. and P. Kongi, Battery thermal management system based on PCM with addition of nanoparticles. Materials Today: Proceedings 72 (2023) 1543-1549.

[59] Altuntop, E. S., Erdemir, D., Kaplan, Y., & Özceyhan, V. A comprehensive review on battery thermal management system for better guidance and operation. Energy Storage 5.8 (2023) e501.

[60] Vikram, S., S. Vashisht, and D. Rakshit, Performance analysis of liquid-based battery thermal management system for Electric Vehicles during discharge under drive cycles. Journal of Energy Storage 55 (2022) 105737.

[61] He, L., Jing, H., Zhang, Y., Li, P., & Gu, Z Review of thermal management system for battery electric vehicle. Journal of Energy Storage 59 (2023) 106443.

[62] Alnaqi, A.A., Numerical analysis of pressure drop and heat transfer of a Non-Newtonian nanofluids in a Li-ion battery thermal management system (BTMS) using bionic geometries. Journal of Energy Storage 45 (2022) 103670.

[63] Zuo, S.G., S.P. Chen, and B. Yin, Performance analysis and improvement of lithium-ion battery thermal management system using mini-channel cold plate under vibration environment. International Journal of Heat and Mass Transfer 193 (2022) 122956

[64] Maiorino, A., Cilenti, C., Petruzziello, F., & Aprea, C. A review on thermal management of battery packs for electric vehicles. Applied Thermal Engineering (2023) 122035.

[65] Wang, J., Lu, S., Wang, Y., Ni, Y., & Zhang, S. Novel investigation strategy for mini-channel liquid-cooled battery thermal management system 44.3 (2020) 1971-1985.

[66] Wang, Y., Mu, X., Xie, Y., Li, W., Dan, D., Qian, Y., & Zhang, Y. A coupled model and thermo-electrical performance analysis for flat heat pipe-based battery thermal management system. Applied Thermal Engineering 223 (2023) 121116.

[67] Han, U., Lee, S., Jun, Y. J., & Lee, H.Experimental investigation on thermal performance of battery thermal management system with heat pipe assisted hybrid fin structure under fast charging conditions. Applied Thermal Engineering 230 (2023) 120840.

[68] Shailesh, K., Y. Naresh, and J. Banerjee, Heat transfer performance of a novel PCM based heat sink coupled with heat pipe: An experimental study. Applied Thermal Engineering 229 (2023) 120552.

[69] Weragoda, D. M., Tian, G., Burkitbayev, A., Lo, K. H., & Zhang, T. A comprehensive review on heat pipe based battery thermal management systems. Applied Thermal Engineering 224 (2023) 120070.

[70] Guo, Z., Xu, Q., Wang, Y., Zhao, T., & Ni, M. Battery thermal management system with heat pipe considering battery aging effect. Energy 263 (2023) 126116.

[71] Jouhara, H., Serey, N., Khordehgah, N., Bennett, R., Almahmoud, S., & Lester, S. P. Investigation, development and experimental analyses of a heat pipe based battery thermal management system. International Journal of Thermofluids 1 (2020) 100004.

[72] Ren, R., Zhao, Y., Diao, Y., & Liang, L. Experimental study on preheating thermal management system for lithium-ion battery based on U-shaped micro heat pipe array. Energy 253 (2022) 124178.

[73] Zhao, C., Zhang, B., Zheng, Y., Huang, S., Yan, T., & Liu, X. Hybrid Battery Thermal Management System in Electrical Vehicles: A Review. Energies 13 (2020) 6257.

[74] Liu, L., X.L. Zhang, and X.W. Lin, Recent Developments of Thermal Management Strategies for Lithium-Ion Batteries: A State-of-The-Art Review. Energy Technology 10.6 (2022) 2101135.

[75] Ahmad, S., Liu, Y., Khan, S. A., Hao, M., & Huang, X. Hybrid battery thermal management by coupling fin intensified phase change material with air cooling. Journal of Energy Storage 64 (2023) 107167.

[76] Li, M., Ma, S., Jin, H., Wang, R., & Jiang, Y. Performance analysis of liquid cooling battery thermal management system in different cooling cases. Journal of Energy Storage 72 (2023) 108651.

[77] Wang, N., Li, C., Li, W., Chen, X., Li, Y., & Qi, D. Heat dissipation optimization for a serpentine liquid cooling battery thermal management system: An application of surrogate assisted approach. Journal of Energy Storage 40 (2021) 102771.

[78] Wang, H., Tao, T., Xu, J., Mei, X., Liu, X., & Gou, P. Cooling capacity of a novel modular liquid-cooled battery thermal management system for cylindrical lithium ion batteries. Applied Thermal Engineering 178 (2020) 115591.

[79] Tousi, M., Sarchami, A., Kiani, M., Najafi, M., & Houshfar, E. Numerical study of novel liquid-cooled thermal management system for cylindrical Li-ion battery packs under high discharge rate based on AgO nanofluid and copper sheath. Journal of Energy Storage 41 (2021) 102910.

[80] Chen, S., Bao, N., Garg, A., Peng, X., & Gao, L. A Fast Charging–Cooling Coupled Scheduling Method for a Liquid Cooling-Based Thermal Management System for Lithium-Ion Batteries. Engineering 7.8 (2021) 1165-1176.

[81] Zhang, Z. and K. Wei, Experimental and numerical study of a passive thermal management system using flat heat pipes for lithium-ion batteries. Applied Thermal Engineering 166 (2020) 114660.

[82] Behi, H., Karimi, D., Behi, M., Jaguemont, J., Ghanbarpour, M., Behnia, M. & Van Mierlo, J. Thermal management analysis using heat pipe in the high current discharging of lithium-ion battery in electric vehicles. Journal of Energy Storage 32 (2020) 101893.

[83] Liang, J., Y. Gan, and Y. Li, Investigation on the thermal performance of a battery thermal management system using heat pipe under different ambient temperatures. Energy Conversion and Management 155 (2018) 1-9.

[84] Wang, J., Gan, Y., Liang, J., Tan, M., & Li, Y. Sensitivity analysis of factors influencing a heat pipe-based thermal management system for a battery module with cylindrical cells. Applied Thermal Engineering 151 (2019) 475-485.

[85] Mousavi, S., Zadehkabir, A., Siavashi, M., & Yang, X. An improved hybrid thermal management system for prismatic Li-ion batteries integrated with mini-channel and phase change materials. Applied Energy 334 (2023) 120643.

[86] Faizan, M., S. Pati, and P. Randive, Effect of channel configurations on the thermal management of fast discharging Li-ion battery module with hybrid cooling. Energy 267 (2023) 126358.

[87] Wang, J., Mei, W., Mao, B., & Wang, Q. Investigation on the temperature control performance and optimization strategy of a battery thermal management system combining phase change and liquid cooling. Applied Thermal Engineering 232 (2023) 121080.

[88] Liu, Z., Wang, B., Tan, Y., & Li, P. Thermal management of lithium-ion battery pack under demanding conditions and long operating cycles using fin-enhanced PCMs/water hybrid cooling system. Applied Thermal Engineering 233 (2023) 121214.

[89] Peng, P., Y. Wang, and F. Jiang, Numerical study of PCM thermal behavior of a novel PCM-heat pipe combined system for Li-ion battery thermal management. Applied Thermal Engineering 209 (2022) 118293.

[90] Chen, F., Huang, R., Wang, C., Yu, X., Liu, H., Wu, Q. & Bhagat, R. Air and PCM cooling for battery thermal management considering battery cycle life. Applied Thermal Engineering 173 (2020) 115154.

[91] Li, X., He, F., Zhang, G., Huang, Q., & Zhou, D. Experiment and simulation for pouch battery with silica cooling plates and copper mesh based air cooling thermal management system. Applied Thermal Engineering 146 (2019) 866-880.

[92] Yuan, X., Tang, A., Shan, C., Liu, Z., & Li, J. Experimental investigation on thermal performance of a battery liquid cooling structure coupled with heat pipe. Journal of Energy Storage 32 (2020) 101984.

[93] Wang, Y., Peng, P., Cao, W., Dong, T., Zheng, Y., Lei, B., ... & Experimental study on a novel compact cooling system for cylindrical lithium-ion battery module. Applied Thermal Engineering 180 (2020) 115772.

[94] Jang, D. S., Yun, S., Hong, S. H., Cho, W., & Kim, Y. Performance characteristics of a novel heat pipe-assisted liquid cooling system for the thermal management of lithium-ion batteries. Energy Conversion and Management 251 (2022) 115001.

G. A. Acosta-Fernandez[1,2], N. M. Castrejon-Esparza[1,2], S. Morales-Inzunza[1,2], K.E. Martinez-Torres[1,2], L.A. Vargas-Robles[3], M.E. Gonzalez-Trevizo[1,2]*

Utilizing Satellite Remote Sensing and Geographic Information Systems for Assessing Urban Heat Island Effects as Urban Planning Tools for Emerging Economies

[1]Universidad Autónoma de Baja California, Facultad de Ingeniería Arquitectura y Diseño, C. Transpeninsular Ensenada - Tijuana 3917, 22860, Ensenada, México.
[2]PRISMA Research Group, C. Transpeninsular Ensenada - Tijuana 3917, 22860, Ensenada, México.
[3]Universidad Iberoamericana León, Departamento de Arquitectura y Diseño, Blvd. Jorge Vértiz Campero 1640, 37238, León, México.

Abstract

This research investigates the use of remote sensing methods to assess the Surface Urban Heat Island (SUHI) phenomenon in an emerging economy city with a Mediterranean climate by using a case study of Ensenada, Mexico, specifically analyzing data from the years 2019 and 2023. With the increase in urban populations, especially in developing countries, the effects of urbanization on climate, energy, and health become more crucial. The research utilizes Landsat 8 satellite spectral images to evaluate variations in Land Surface Temperature (LST) and urban heat island intensity. Employing the Normalized Difference Vegetation Index (NDVI), the research uncovers substantial temperature elevations, with an average increase of 1.5 °C affecting 42.37% of the city. The northeastern region experienced significant temperature fluctuations, driven by the growth of urban areas and the decrease in green infrastructure. The research emphasizes the need to include green infrastructure, such as parks and green roofs, in urban planning to alleviate urban overheating impacts. Furthermore, it emphasizes the need for ongoing surveillance via Geographic Information Systems (GIS) and remote sensing to direct sustainable city growth. These results provide practical insights for urban planners, government authorities, and private sector stakeholders to create policies that seek to reduce heat-related vulnerabilities.

***Keywords**: Surface Urban Heat Island, Land Surface Temperature, Urban planning, Heat vulnerability, Remote sensing*

1. Introduction

In 2022, the worldwide urban population was roughly anticipated to be about 4.5 billion, accounting for 56.9% of the overall population. Urban regions record continuous growth, and by 2050, more than 70% of the global is anticipated to be located in urban centers, mostly driven by Less Developed Regions (LDR) or emerging economies [1], where five out of six people live in social and economic inequities and lack of regulation. In this context, Latin America is projected to have substantial urban expansion, which might result in an additional 53 million people living in metropolitan areas by 2035 [2].

The majority of urban land development is expected to take place in low-income nations. If not properly planned, urban sprawl might become a pressing worldwide concern. Small cities and towns with a population of 250,000 people play a crucial role in creating sustainable urban futures in low-income nations. Therefore, it is necessary to improve planning capacity, particularly for emerging cities facing challenges such as high population density, lack of access to energy, and inequality. These issues are urgent global aspects that need immediate attention. According to the UN World City report, "*A multidimensional approach is key to an inclusive urban future*" [3].

Urbanization affects attempts to mitigate climate change by contributing to land cover degradation via extensive deforestation. At the same time, urban atmospheric air quality is affected by the modification of land through construction materials. This modification alters the normal thermal storage, radiative, and turbulent heat transfer, as well as the sensible heat flux [4]. These changes result from the thermal and optical properties of the materials used and from the lower evaporative cooling of infrastructures with low emissivity [5]. These factors contribute to increased human exposure to the negative effects of global warming at the local scale [6]. The higher albedo and Land Surface Temperature (LST) of urban areas compared to their natural surroundings, along with the impact of urban geometry, anthropogenic heat, and the region's geographical and microclimatic conditions, influence the thermal balance of the urban environment. The multivariable phenomenon is the main cause of the exacerbation of the Urban Heat Island Intensity (UHII) [7], [8].

In the climate change context, science-based urban planning is undeniably advantageous for reducing urban overheating and its effects on human vulnerability caused by global warming [9], thus the spatiotemporal evolution in urban microclimate has a serious effect on environmental heterogeneity, and urban policies to address this urgent topic must be developed [10]. Satellite remote sensing is a valuable method for sustainable urban planning, particularly in addressing the Urban Heat Island (UHI) phenomenon through the analysis of multiple indices, and socio-demographic, and environmental approaches such as Local Climate Zones (LCZ), which allow associating the characteristics of the urban environment with Land

Surface Temperature and identifying patterns during the day, enabling urban planners to classify metropolitan areas by examining building geometry and land cover using satellite data from numerous sources [11]. Multiple studies have shown the existence of temperature changes during the day, which may be accurately observed by analyzing data from Landsat and ASTER satellites. Moreover, the configuration and composition of Land Use and Land Cover (LULC), and cover materials have a significant impact on LST, such as the findings found by Ejiagha [12] where it was identified that residential and industrial areas were the largest contributors to LST during 2015 and 2018, increasing LST by up to 6.95 °C. In addition, the combination of remote sensing and spatial network analysis can provide useful insights into the impact of various urban areas such as the findings presented by Mohamed [13]. Governments around are implementing green city strategies to transform obstacles into possibilities. Saudi Vision 2030 advocates for intelligent development to enhance the economy while safeguarding natural resources. The urban heat island (UHI) - who performed a comparison of LST between two districts in Saudi Arabia, finding that the Al-Shrashef district whose main spatial characteristic is the compact urban fabric presents a lower LST up to 1 °C compared to the Al Eskan district which presents large tracts of open space. On the other hand, Jato-Espino [14] developed ArcUHI, a Geographic Information System (GIS) attributes the increase in UHI to building height and albedo, so they developed ArcUHI, a tool that combine GIS and machine learning algorithms, to model Surface UHI and predict LST with high accuracy, to adopt mitigation strategies that can be used to guide strategic actions, such as the adoption of green roofs and walls, reflecting coatings, or cool pavements/roofs, to reduce the heat absorption capacity of built surfaces as reviewed by others [15]. By incorporating these elements, planners can create cities that are both environmentally sustainable and favorable to human-well-being, while also considering socio-demographic factors.

In Mexico, the National Projects for Research and Incidence (PRONAII) managed by the National Council of Humanities, Sciences, and Technologies (abbreviated CONAHCyT) integrates scientific-technical expertise to facilitate cooperation between academic and private or public entities [16]. This research initiative include metropolitan institutes of research and planning, enhancing the use of official data resources to tackle urban climate change and reach the UN Sustainable Development Goals for sustainable cities and communities, and fostering National Development Plans, addressing social, environmental, and demographic issues by suggesting multicriteria studies to mitigate the Urban Heat Island effects.

The present work addresses the constraints of climatic information provided by traditional meteorological stations in the national meteorological system of Mexican cities. The climatological data mentioned above are often standardized to examine heat exposure in urban areas. However, unlike remote sensing instruments, they lack the ability to offer a comparative geospatial resolution for conducting temporal analysis to assess the intensity of urban heat islands and the changes in land surface temperature within urban areas. The primary objective of this study derived from PRONAII was to use spectral images from the Landsat 8 satellite to compare and assess the urban land cover and Surface Urban Heat Island effects of the City of Ensenada, Baja California. Specifically, the study focused on comparing average typical summer days in 2019 and 2023.

2. Method

This research was conducted in the sparsely populated city of Ensenada, Mexico. The coastal city is located at latitude 32° 12’ 10” N and longitude 116° 53’ 03” W, bordering the Pacific Ocean. It covers an area of 71.446 km^2, has 119,796 inhabited dwellings, and an average occupancy rate of 3.16 inhabitants per urban dwelling. The average population density is 9 residents per square kilometer (residents/sq.km) [17] that can reach 58.46 residents/sq.km in the northeast sector of the city [18]. The population is projected to grow by 66,226 more people by 2030 compared to 2020, with an annual growth rate of 0.98% according to the State Development Planning Committee (COPLADE) [19]. The maximum housing land use intensity allowed in the 2034 urban strategic plan is 182 inhabitants per hectare (people/ha) for single-family dwellings and 500 people/ha for multi-family dwellings [20]. The lack of an adequate regulation plan will result in significant social and environmental impacts, including the degradation and disappearance of green infrastructure. Additionally, the disorderly growth of the city in peripheral areas will lead to an increase in informal housing [21]. The climate in Ensenada is classified as BSk (cold semi-arid climate) according to the Köppen-Geiger climate classification system. This classification refers to a cold semi-arid climate, which is characterized by wet, rainy, and cold winters, as well as hot and dry summers [22].

For the land cover analysis, three primary climatic indicators were chosen: NDVI, LST, and SUHI. NDVI is a numerical indicator that represents the amount of vegetation on the surface; it is measured on a scale from -1 to 1, where negative values imply high reflectivity and positive values indicate the presence of vegetation [23-24]. On the other hand, the LST is influenced by factors such as time, day, ground cover, and meteorological conditions, causing its readings to fluctuate, high LST readings suggest the presence of warm surfaces, whereas low values are typically linked with vegetated areas, water bodies or cool spots in the city [25]. The SUHI phenomenon pertains to the variation in LST caused by the absorption and emission of heat by urban surfaces [26]. It is employed through different methodologies to extract and refine leveraged satellite data in order to assess the heat island intensity [27].

Remote sensing techniques were utilized to estimate the intensity of NDVI, LST, and SUHI. This estimation was carried out through a 6-stage process, as seen in Figure 1. The first stage of the research aimed to identify the typical extreme summer day for 2019 and 2023. This was done

by analyzing ambient temperature oscillation and mean temperature, which involved calculating the monthly total of the absolute differences between the daily average dry bulb temperature (DBTd-avg) and the daily average oscillation (OSCd-avg). The Landsat 8 satellite spectral imagery from the United States Geological Survey (USGS) earth explorer database [28] of September 05, 2019, and August 22, 2023, were selected based on the usual harsh weather conditions, cloud cover, and precipitation. The Operational Land Imager (OLI) and relevant Band 4 (Red): 0.64 – 0.67 micrometers (μm) and Band 5 (Near-Infrared, NIR): 0.85 – 0.88 micrometers (μm), were utilized to capture multispectral imagery in different wavelength bands and estimate NDVI. At the same time, Band 10: 10.60 – 11.19 micrometers (μm) employ the Thermal Infrared Sensor (TIRS) to capture earth´s surface infrared radiation.

In order to conduct the SUHI evaluation (See Eq.7), it was previously necessary to calculate the $L\lambda$: spectral radiance (See Eq. 1), and LST (See Eq. 6), which was derived from the spectral indices of emissivity (ε) (See Eq.5) and brightness temperature (T_B) (See Eq.2). The value of ε was determined by using Equation 5, which is dependent on the NDVI. Equation 4 was used to calculate the NDVI by measuring the reflectance of the RED and NIR bands. The estimation of T_B was performed using spectral radiance, as shown in Eq. 2. The approach mentioned above was computed using the GIS software ArcGIS v10.8.2 by analyzing the spectral imagery, ArcGIS is considered as a decision support tool, widely used for its spatial data integration and multi-criteria decision-making enhancement [29] the process of determining these national responsibilities and conservation priorities is time intensive when considering many species across geographic scales.

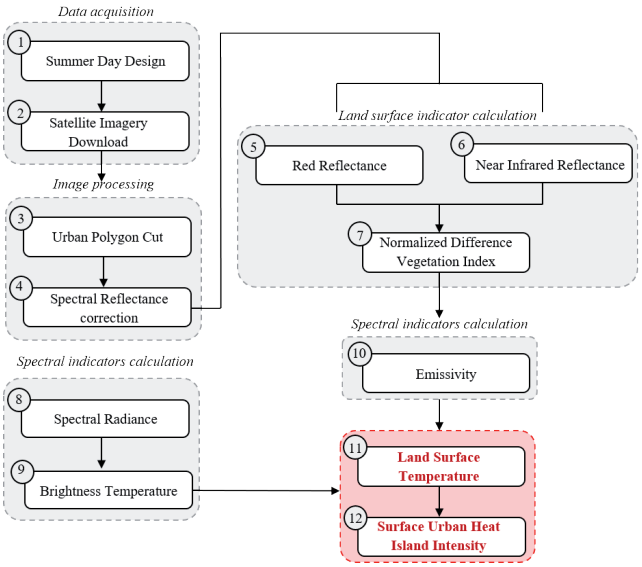

Fig. 1. Methodological workflow for calculating LST and SUHI.

Table 1. Different spectral indices used for calculation.

Index	Equation		Ref
L_λ	$M_L \times DN_{band} + A_L$	(1)	[30]
T_B	$\frac{K_2}{ln\left(\frac{K_1}{L_\lambda}+1\right)}$	(2)	[31]
ρ_λ*	$\frac{\rho}{sin(\theta\pi\ /\ 180)}$	(3)	[30]
NDVI	$\frac{(\rho_{NIR}-\rho_{red})}{(\rho_{NIR}+\rho_{red})}$	(4)	[32]
ε_λ	$\{\varepsilon_s\ \ \varepsilon_s\ \ \varepsilon_s\} = \{\varepsilon_s,\ \ \varepsilon_{(m,)}\ \ \varepsilon_v\}$	(5)	[33]
LST	$\left(\frac{T_B}{1+\left(\frac{\lambda T_B}{\alpha}\right) ln\ \varepsilon}\right) - 273.15$	(6)	[34]
SUHI	$\frac{LST_i - LST_{min}}{LST_{max} + LST_{min}}$	(7)	[35]

Note: Where: M_L: radiance multiplicative scaling factor, A_L: radiance additive scaling factor, DN_{band}: raw band digital numbers, α: surfaces radiation constant adjustment, ε_s: emissivity bare soil (NDVI<0.2), ε_v: emissivity vegetation (NDVI>0.5), ε_m: emissivity mixed areas (NDVI>0.2 & NDVI<0.5), *Spectral range dependent index (adapted), being Red Reflectance: ρ_{red} and NIR Reflectance: ρ_{NIR}.

After normalizing the skewed SUHI data, the current approach utilized Jenks' natural breaks data classification technique to assess the intensity of the phenomena. This optimization method allows for the grouping of data into clusters and optimizes the distinction between groups minimizing the variance between them to facilitate normalization across multiple dimensions. In order to achieve this objective and provide natural data groupings, a 5-class scale was employed, utilizing the categories suggested by Zhang [36].

3. Results and discussion

In order to analyze the distribution pattern of the Surface Urban Heat Island in Ensenada, we obtained a series of maps showing the LST and SUHI on a typical extreme summer day in 2019 and 2023. These maps were generated using data from the Landsat 8 satellite, technical assumptions regarding the urban overheating in relation to typical physical properties, such as emissivity (ε) variations across the urban surface -comprising different building materials (0.85 – 0.95), asphalt pavements (0.90 – 0.95), and vegetation (0.7 – 0.95)- were appropriately calculated to ensure stability and reliability. Atmospheric conditions, including clear-sky conditions with normal atmospheric transmissivity, and Aerosol Optical Depth (AOD) values were also accounted for to maintain consistency and accuracy in processing the city's heterogene-

ity [37]. In terms of satellite thermal bands, the radiance multiplicative scaling factor for Band 10 (0.000342) and the radiance additive scaling factor (0.1) were considered. Additionally, the reflectance multiplicative scaling factor (0.00002) and the reflectance additive scaling factor (0.1) for Bands 4 and 5 were also taken into account. There are notable disparities in the spatial arrangement of LST in the designated region between the years 2019 and 2023. According to the data presented in Figure 2a, the LST trend in 2019 exhibits a greater accumulation of high temperatures in the northern and northeastern regions of the city. These temperatures can reach values as high as 38.65 °C. The eastern urban edge of the city is undergoing rapid and uncontrolled expansion, leading to the formation of densely populated areas with limited water bodies and vegetation. In contrast, the western section of the city exhibits LST values of 23.64 °C as a result of its close proximity to the water.

Conversely, the year 2023 had a rise in the distribution of maximum temperatures, primarily centered in the central and northeastern areas of the city, reaching a peak of 40.23 °C. Similarly, it was noted that in 2023, the regions with the lowest LST are situated in the northwest. These areas have a minimum LST value of 22.89 °C, which can be attributed to their closeness to bodies of water and the cooling effect of wind as a convective mechanism (Fig. 2b).

The classification of SUHI intensity grade was defined by correlating these pixel values with land surface temperatures, to classify SUHI intensity based on the distribution and concentration of temperature anomalies across the urban landscape from 2019 and 2023, taking into account the distribution of temperature data for each year observed. This resulted in a five-category scale, as shown in Table 2.

Table 2. Classification of the degree of intensity of SUHI

SUHI 2019	SUHI 2023	SUHI Intensity
<0.40	<0.37	I. Cool Island
0.41-0.55	0.38-0.50	II. Weak SUHI
0.56-0.66	0.51-0.60	III. Moderate SUHI
0.67-0.75	0.61-0.70	IV. Strong SUHI
>0.75	>0.71	V. Extreme SUHI

The SUHI intensity estimation findings can be seen in Fig. 2c. In 2019, there was an extreme SUHI (V) in the northeast and southeast regions of the city, with an intensity ranging from 0.70 to 1. In contrast, the southeastern region exhibited a significant SUHI effect, with intensities ranging from 0.56 to 0.66 and 0.67 to 0.75, respectively. On the other hand, this investigation also discovered a Cool island located in the southwest area, characterized by an intensity ranging from 0 to 0.40.

In 2023, the intensity of the urban heat island (V) is highest in the center and northern areas of the city, with values exceeding 0.71. In contrast, the southern zone of the city experiences mostly significant urban heat island effects (IV), with values ranging from 0.61 to 0.70. The primary fluctuations in SUHI intensity are observed in the northeastern and southeastern regions. These changes can be attributed to disruptions on the Earth's surface, resulting in variations in NDVI of up to 0.02 (See Fig. 2d).

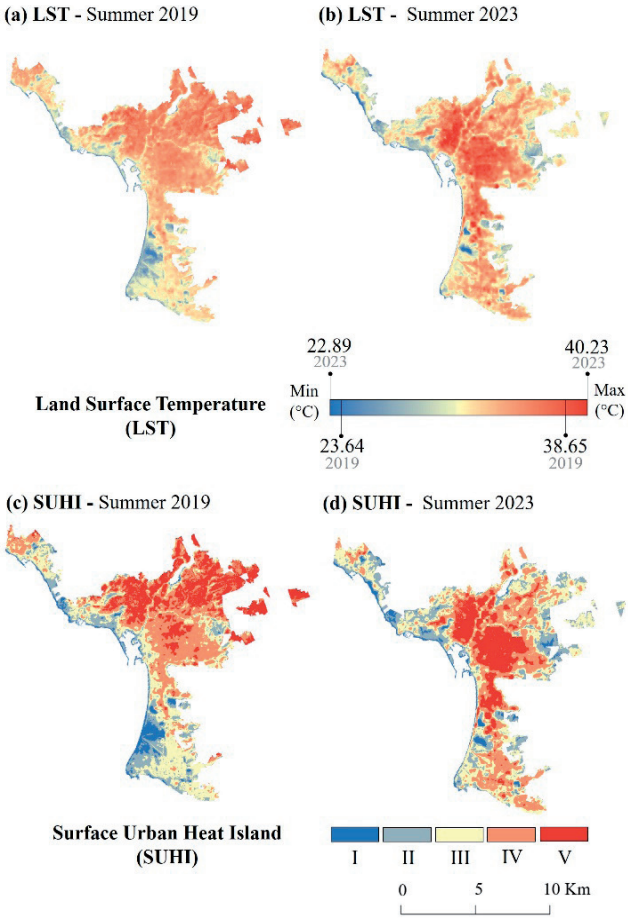

Fig. 2. LST - SUHI 2019-2023 spatial distribution.

Fig. 3a displays the results of the relative differences in the extreme temperatures of LST between the years 2019 and 2023. The National Institute of Statistics and Geography (INEGI) defined the Basic Geostatistical Area (AGEB) as the spatial unit of analysis for the census in Mexico. The urban area of Ensenada encompasses a total of 269 AGEBs.

According to the map, 42.37% of the AGEBs (114 AGEBs) experience a rise in surface temperature. The temperature fluctuates between 0.06 to 4.35 °C in the central and southern parts of the city. In 2023, there is an average increase of 1.5 °C in severe temperatures compared to 2019 in the city. The rise is due to a reduction in the NDVI index by 24.16%, impacting 65 out of the 269 AGEBs that were examined. In contrast, the northeastern region observed a decline in temperature, ranging from 1 to 6 °C.

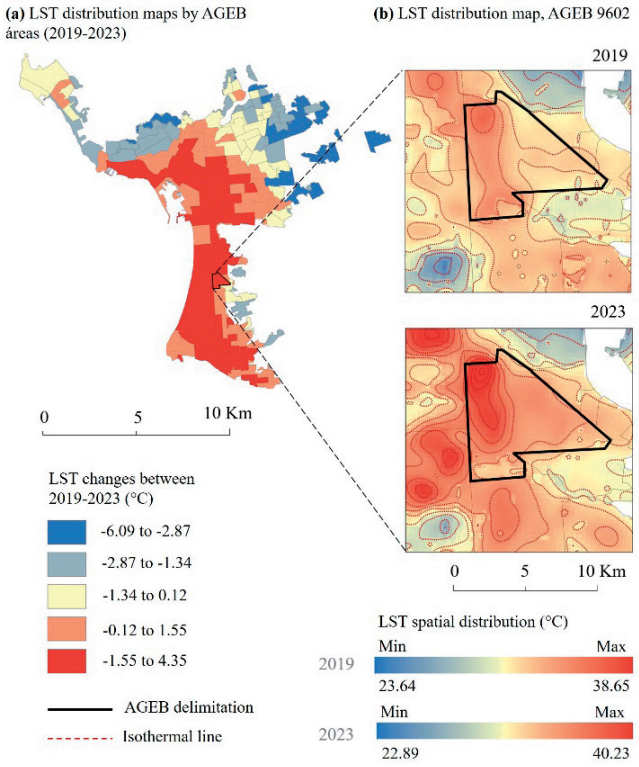

Fig. 3. AGEB LST 2019-2023 comparative analysis.

Similarly, AGEB 9602 characterized by a mixed land use (commercial and services), presents the typical features of an LCZ-3 (compact low rise), in the eastern part of the AGEB, characterized by the presence of residential buildings, and an LCZ-7 (lightweight low rise), in the western part of the AGEB, attributable to the commercial zone. This region also presents a large extension of impervious surfaces, traffic affluence, and lack of green infrastructure, which led to a greater increase in temperature, coinciding with the findings presented by Ejiagha [12], who attributes the LST increase in residential zones to the extensive impervious surfaces, and the high construction density. In 2019, the maximum recorded LST was 38.65 °C, while in 2023, it reached 40.23 °C, indicating a temperature increase of 4.35 °C. The rise in temperature can lead to heat stress episodes, which have varying impacts on health depending on age and pre-existing illnesses. These effects are particularly pronounced in individuals with heart disease, children, and adults over the age of 60, and the female population [38]. The heat-sensitive population in this AGEB is spread among the following age groups: The female population accounts for 52.9% of the total population of 2,857 inhabitants. Among this group, 19.42% are aged 0 to 14 years and 8.64% are adults older than 60 years. Based on the information provided in Figure 3b, AGEB 9602 displays isotherms corresponding to different temperature increments. These isotherms have a mostly west-northwest orientation and cover an area of 0.02 square kilometers. The isotherm exhibits a steady variability, characterized by a gradual rise in temperature from the northwest and a subsequent decrease towards the east of the AGEB. On the other hand, Fig. 3a displays isotherms that are oriented in a northwest-southwest direction, indicating that the isotherm surface expanded by 0.13 km² towards the southwest area.

Based on the information provided in Figure 3b, AGEB 9602 displays isotherms corresponding to different temperature increments. These isotherms have a mostly west-northwest orientation and cover an area of 0.02 square kilometers. The isotherm exhibits a steady variability, characterized by a gradual rise in temperature from the northwest and a subsequent decrease towards the east of the AGEB. On the other hand, Fig. 3a displays isotherms that are oriented in a northwest-southwest direction, indicating that the isotherm surface expanded by 0.13 km² towards the southwest area.

Fig. 4. Street-level view and satellite overview. Google Earth

The aforementioned phenomenon can be linked to the decline in green infrastructure, as indicated by a 0.06 fall in NDVI caused by the expansion of urban areas. As depicted in Figure 4, this AGEB exhibits compact and low-rise structures, which are indicative of LCZ - 3 (Compact low-rise). Similarly, in the hottest temperature zone, there is a significant presence of extensive pavements and materials like steel and concrete, which are characteristic of LCZ - 8 (Large Low-rise). The urban plan in this area follows a north-south orientation for main highways and an east-west orientation for subsidiary and local roads. According to Manni [39], the east-west orientation is regarded as undesirable since it results in a longer exposure to sun radiation and, consequently, a rise in the mean radiant temperature. In addition, the flow of vehicles on roads significantly impacts the increase in LST, influenced by factors such as heat and pollutant emissions, and interactions with paved surfaces. These effects intensify the urban heat island phenomenon, especially in areas with high traffic density. In the case of AGEB 9602, it is observed that the area is bordered by main and secondary roads with vehicular traffic volumes reaching up to 2,600 and

839 vehicles per hour [40], respectively. This exacerbates the urban heat island effect due to the high concentration of vehicles and their influence on heat transfer in the urban environment.

4. Conclusions and Recommendations

This study utilized remote sensing techniques to evaluate the magnitude of the SUHI in Ensenada, Mexico, from 2019 to 2023 as a relevant spatial tool for smart urban planning. The main findings are summarized below:

- Elevated LST: The analysis indicated an increase in LST over a substantial area (42.37%) of Ensenada from 2019 to 2023. The mean temperature rise was 1.5 degrees Celsius.
- Changing the intensity of the SUHI: The study documented a change in the intensity of the SUHI that occurred in different locations. The northeastern region had a decline in temperature, but the central and southern zones of the city observed an increase that must be addressed under a LCZ typological analysis, due to its density aspects.
- AGEB 9602 had the highest temperature rise, with a substantial increase of 4.35 °C. This region exhibits a significant concentration of population groups that are particularly vulnerable to heat (such as children, elderly individuals, and females) and is deficient in terms of green infrastructure, failing to provide adequate evapotranspiration, a higher albedo effect, shaded areas to reduce the overall heat, and the reduction of heat-absorbing surfaces.
- The urban morphology of AGEB 9602 is a contributing factor to the increasing temperatures. The presence of compact low-rise buildings and broad asphalt pavements exacerbates the urban heat island effect by trapping heat due to the high solar exposure during the day, which can reach an annual total solar radiation that exceeds 2,000 kWh/m^2/year in the 25-35° tilt angle for street surfaces in the region [41].
- The decline in NDVI values, which indicates a loss in vegetation, is consistent with regions facing rising temperatures. This emphasizes the vital need for green infrastructure in moderating the urban heat island effect in urban configurations with scarce vegetation.

These findings allow for the following recommendations to be made for urban planners and architects, local and national government authorities, and public health officials, as well as for key participants in the private sector such as real estate developers, Non-Governmental Organizations (NGOs), and academic and research institutions:

- The development and implementation of green infrastructure as territorial reserves in strategic districts with critical microclimatic conditions. A robust integrated urban policy to enhance the presence of environmentally friendly areas within the urban landscape, including the distribution of parks, gardens, and green roofs. This will aid in the regulation of temperatures and deliver a cooling impact known as cooling islands.
- Urban Design Modifications: Consider updating urban design plans to include elements that reduce heat absorption. This may entail integrating additional shade from trees and buildings, using lighter-colored reflective pavements, and advocating for a north-south building orientation.
- Perform a sensitivity assessment to determine places with a high likelihood of experiencing heat stress and identify the populations that are most vulnerable to its impacts. This will enable precise interventions and public health initiatives, including cardioprotective spaces that must be strategically distributed in specific urban districts with high exposure, like in the case of AGEB 9602.
- Surveillance and assessment: Utilize remote sensing techniques to consistently monitor the intensity of LST and SUHI. This will provide an ongoing assessment of the efficacy of adopted strategies.
- Geographical Information System analysis using remote sensing enables the smooth integration of data, predictive analytics, and improved decision-making. In the future, IoT-based ecosystems will provide interoperability with Urban Building Energy Models (UBEM) and digital twins (DTs) to evaluate important aspects of preventing the increasing heat-related mortality rate and energy poverty.
- In future technological applications, the Internet of Things (IoT) can be integrated into the evaluation of the spatio-temporal distribution of urban overheating in real time for multi-criteria decision-making (MCDM) in GIS-based smart urban planning. Remote sensing techniques can be used to estimate the urban centrality of residential areas in relation to tourist clusters, industrial zones, cultural heritage districts, multimodal mobility hubs, traffic hubs, and short-term territorial reserves. This allows for the implementation of strategic actions and local smart grids to promote efficient governance, public safety and security, waste management, water security, epidemiological prevention, and e-services for urban ecosystems.

Finally, it is crucial to include a demographic analysis of AGEB in urban planning schemes that consider the environmental factors of vulnerability and exposure when designing urban areas. This should include the establishment of Enhanced Urban Green places, often known as urban forests, as well as Cooling Centers that provide refuge for vulnerable people during periods of high heat. Moreover, it is important to promote Public Awareness Campaigns and solutions for prevention. Furthermore, it is essential to take into account heat health warning systems, water delivery, accessible healthcare, and transportation services.

5. References

[1] United Nations Department Economic and social affairs, “Population Facts,” Life expectancy at birth increasing in less developed regions.

[2] UNCTAD, "UN Trade and Development Handbook of statistics: Total and urban population," Genova, 2024.

[3] UN-Habitat, "Envisaging the Future of Cities," 2022.

[4] C. R. de Almeida, A. C. Teodoro, and A. Gonçalves, "Study of the urban heat island (Uhi) using remote sensing data/techniques: A systematic review," *Environ. - MDPI*, vol. 8, no. 10, pp. 1–39, 2021, doi: 10.3390/environments8100105.

[5] U.S. Environmental Protection Agency, "Urban Heat Island Basics," Washington, 2008. doi: 10.1109/IICPE.2016.8079546.

[6] IPCC, "IPCC Fourth Assessment Report: Climate Change 2007," Zurich, 2007. [Online]. Available: https://archive.ipcc.ch/publications_and_data/ar4/wg1/en/ch3s3-2-2-2.html

[7] G. Levermore, J. Parkinson, K. Lee, P. Laycock, and S. Lindley, "The increasing trend of the urban heat island intensity," *Urban Clim.*, vol. 24, pp. 360–368, 2018, doi: 10.1016/j.uclim.2017.02.004.

[8] I. D. Stewart and T. R. Oke, "Local climate zones for urban temperature studies," *Bull. Am. Meteorol. Soc.*, vol. 93, no. 12, pp. 1879–1900, 2012, doi: 10.1175/BAMS-D-11-00019.1.

[9] A. Karimi, P. Mohammad, A. García-Martínez, D. Moreno-Rangel, D. Gachkar, and S. Gachkar, *New developments and future challenges in reducing and controlling heat island effect in urban areas*, vol. 25, no. 10. Springer Netherlands, 2023. doi: 10.1007/s10668-022-02530-0.

[10] C. Wu *et al.*, "Spatiotemporal evolution of urbanization and its implications to urban planning of the megacity, Shanghai, China," *Landsc. Ecol.*, vol. 38, no. 4, pp. 1105–1124, 2023, doi: 10.1007/s10980-022-01578-7.

[11] X. Chen, Y. Xu, J. Yang, Z. Wu, and H. Zhu, "Remote sensing of urban thermal environments within local climate zones: A case study of two high-density subtropical Chinese cities," *Urban Clim.*, vol. 31, no. July 2019, p. 100568, 2020, doi: 10.1016/j.uclim.2019.100568.

[12] I. R. Ejiagha, M. R. Ahmed, Q. K. Hassan, A. Dewan, A. Gupta, and E. Rangelova, "Use of remote sensing in comprehending the influence of Urban landscape's composition and configuration on land surface temperature at neighbourhood scale," *Remote Sens.*, vol. 12, no. 15, 2020, doi: 10.3390/RS12152508.

[13] M. Mohamed, A. Othman, A. Z. Abotalib, and A. Majrashi, "Urban heat island effects on megacities in desert environments using spatial network analysis and remote sensing data: A case study from western Saudi Arabia," *Remote Sens.*, vol. 13, no. 10, 2021, doi: 10.3390/rs13101941.

[14] D. Jato-Espino, C. Manchado, A. Roldán-Valcarce, and V. Moscardó, "ArcUHI: A GIS add-in for automated modelling of the Urban Heat Island effect through machine learning," *Urban Clim.*, vol. 44, no. June, 2022, doi: 10.1016/j.uclim.2022.101203.

[15] P. K. Diem *et al.*, "Remote sensing for urban heat island research: Progress, current issues, and perspectives," *Remote Sens. Appl. Soc. Environ.*, vol. 33, no. October 2023, p. 101081, 2024, doi: 10.1016/j.rsase.2023.101081.

[16] CONAHCYT, "PRONACES," National Project for Research and Incidence.

[17] Instituto Metropolitano de Investigación y Planeación de Ensenada, "Anuario estadistico municipal de Ensenada [in spanish]," Ensenada, 2018.

[18] Gobierno Municipal, *Plan estratégico municipal de Ensenada. Vision 2034 [in spanish]*, no. 66. Mexico, 2020.

[19] COPLADE, "Población de los Municipios de Baja California 2013-2030," *Año*, vol. 4, pp. 1–7, 2013.

[20] Instituto Metropolitano de Investigación y Planeación de Ensenada, *Proyecto Programa de desarrollo Urbano del Centro de Población de Ensenada PDUCPE 2024-2036 [in spanish]*. Mexico, 2024.

[21] Instituto Metropolitano de Investigación y Planeación de Ensenada, *Proyecto Programa de desarrollo Urbano del Centro de Población de Ensenada PDUCPE 2020-2030 [in spanish]*. Mexico: IMIPENS, 2022.

[22] M. Kottek, J. Grieser, C. Beck, B. Rudolf, and F. Rubel, "World map of the Köppen-Geiger climate classification updated," *Meteorol. Zeitschrift*, vol. 15, no. 3, pp. 259–263, 2006, doi: 10.1127/0941-2948/2006/0130.

[23] S. Guha and H. Govil, "Land surface temperature and normalized difference vegetation index relationship: a seasonal study on a tropical city," *SN Appl. Sci.*, vol. 2, no. 10, pp. 1–14, 2020, doi: 10.1007/s42452-020-03458-8.

[24] S. Garai *et al.*, "Assessing correlation between Rainfall, normalized difference Vegetation Index (NDVI) and land surface temperature (LST) in Eastern India," *Saf. Extrem. Environ.*, vol. 4, no. 2, pp. 119–127, 2022, doi: 10.1007/s42797-022-00056-2.

[25] P. Rajagopal, R. S. Priya, and R. Senthil, "A review of recent developments in the impact of environmental measures on urban heat island," *Sustain. Cities Soc.*, vol. 88, no. May 2022, p. 104279, 2023, doi: 10.1016/j.scs.2022.104279.

[26] P. Smith Guerra, O. Peralta Trigo, P. Sarricolea Espinosa, F. Thomas Cabrera, and O. Meseguer-Ruiz, "Climate-sensitive planning. Opportunities through the study of LCZs in Chile," *Build. Environ.*, vol. 242, no. February, p. 110444, 2023, doi: 10.1016/j.buildenv.2023.110444.

[27] M. Zargari, A. Mofidi, A. Entezari, and M. Baaghideh, "Climatic comparison of surface urban heat island using satellite remote sensing in Tehran and suburbs," *Sci. Rep.*, vol. 14, no. 1, pp. 1–23, 2024, doi: 10.1038/s41598-023-50757-2.

[28] U.S. Geological Survey, "Science for a changing world." Accessed: Jul. 18, 2024. [Online]. Available: https://earthexplorer.usgs.gov/

[29] Y. P. Lin *et al.*, "A GIS-based policy support tool to determine national responsibilities and priorities for biodiversity conservation," *PLoS One*, vol. 15, no. 12 December, pp. 1–23, 2020, doi: 10.1371/journal.pone.0243135.

[30] A. García-Haro, "Guide for calculate the basic remote sensing indices in ArcGIS and QGIS. Procedure, authors and general notes during calculation," 2019. [Online]. Available: https://upcommons.upc.edu/bitstream/handle/2117/184167/Guia_RemoteSensing_2019.pdf

[31] U.S. Geological Survey, "Using the USGS LandsAt Level-1 Data product," Landsat missions. [Online]. Available: https://www.usgs.gov/landsat-missions/using-usgs-landsat-level-1-data-product

[32] J. Weier and D. & Herring, "Measuring Vegetación (NDVI & EVI)," NASA Earth Observatory. [Online]. Available: https://earthobservatory.nasa.gov/Features/MeasuringVegetation/measuring_veg%0Aetation_1.php%0D

[33] J. A. Sobrino, J. C. Jiménez-Muñoz, and L. Paolini, "Land surface temperature retrieval from LANDSAT TM 5," *Remote Sens. Environ.*, vol. 90, no. 4, pp. 434–440, 2004, doi: 10.1016/j.rse.2004.02.003.

[34] D. A. Artis and W. H. Carnahan, "Survey of emissivity variability in thermography of urban areas," *Remote Sens. Environ.*, vol. 12, no. 4, pp. 313–329, 1982, doi: 10.1016/0034-4257(82)90043-8.

[35] A. Mathew, S. Khandelwal, and N. Kaul, "Investigating spatial and seasonal variations of urban heat island effect over Jaipur city and its relationship with vegetation, urbanization and elevation parameters," *Sustain. Cities Soc.*, vol. 35, no. April, pp. 157–177, 2017, doi: 10.1016/j.scs.2017.07.013.

[36] Y. Zhang *et al.*, "Spatiotemporal characteristics of the surface urban heat island and its driving factors based on local climate zones and population in beijing, china," *Atmosphere (Basel).*, vol. 12, no. 10, 2021, doi: 10.3390/atmos12101271.

[37] Z. L. Li *et al.*, "Satellite-derived land surface temperature: Current status and perspectives," *Remote Sens. Environ.*, vol. 131, pp. 14–37, 2013, doi: 10.1016/j.rse.2012.12.008.

[38] K. L. Ebi *et al.*, "Extreme Weather and Climate Change: Population Health and Health System Implications," *Annu. Rev. Public Health*, vol. 42, pp. 293–315, 2020, doi: 10.1146/annurev-publhealth-012420-105026.

[39] M. Manni *et al.*, "Development and validation of a Monte Carlo-based numerical model for solar analyses in urban canyon configurations," *Build. Environ.*, vol. 170, no. November 2019, p. 106638, 2020, doi: 10.1016/j.buildenv.2019.106638.

[40] IMIPENS, "Estudio de tránsito de tránsito vehicular de la ciudad de Ensenada, B.C.," 2009.

[41] J. F. Armendariz-Lopez, A. Luna-Leon, M. E. Gonzalez-Trevizo, A. P. Arena-Granados, and G. Bojorquez-Morales, "Life cycle cost of photovoltaic technologies in commercial buildings in Baja California, Mexico," *Renew. Energy*, vol. 87, pp. 564–571, 2016.

CAETS 2023 Conference

e^2-mobility
Solutions and Opportunities

Croatian Academy of Engineering was presiding over International Council of Academies of Engineering and Technical Sciences (CAETS), world alliance of 31 academies, during year 2023, and its presidency culminated in organisation of CAETS 2023 conference e2-mobility - Solutions and Opportunities, held in Zagreb, on **October 9-11, 2023.** The conference was attended by 85 registered participants from academies and industry.

Abstract

Decarbonisation of transport will bring significant changes to the way humanity moves people and goods around. While electrification may help with both greenhouse and local emissions, it will also convey huge change to car production and servicing chains. Electrification of transport makes car more of IT product, having battery management software at the core. Such informatisation then brings also changes to interaction between driver and vehicle, slowly removing the driver from the steering wheel. Will that free more time, or result in more mobility? What will happen to car ownership? Will it persist, or transport will move towards being a mobility service? Will the service then be personal, or more like public transport today? In the end, what we need are passenger-km and ton-km, how we will supply them? Will the batteries cover all our needs, or the energy density will be a limitation to heavy transport and hydrogen and/or electrofuels will help? What about e-roads, would they be preferred option to hydrogen? Will new technologies develop in the same regions where old car industry is, or will the cards be shuffled again? Shall we have enough resources? What about recycling batteries? How will e-mobility be integrated to the power grids, will it help to the integration of variable renewables, or will it bust the grids? These and many other questions related to the transition of transport systems will have to be answered and we see CAETS as an excellent forum to debate it.

Programme

Main topics were covered by sessions, introduced by invited speaker, and then discussed by 4-5 panellists.

The first panel „Electrification of transport and integration with energy systems" on the topic of connecting electrified transport and the power system, including issues such as: S curve adoption of EVs, smart charging and smart grids, the role of V2G in balancing, fast charging, potential of e-roads, and more on integration of electric vehicles with power system; was moderated by **prof. Neven Duić** from the Faculty of Mechanical Engineering and Naval Architecture of the University of Zagreb in front of the Croatian Academy of Technical Sciences. The panel consisted of prof. Henrik Lund (in absence), prof. Katherine Woodthorpe (Australian Academy of Technical Sciences and Engineering), prof. Joeri Van Mierlo (Director of the Research Center for Electromobility MOBI, Vrije Universiteit Brussels, Belgium), prof. Hrvoje Pandžić (University of Zagreb Faculty of Electrical Engineering and Computing), and prof. Ulrich Wagner (Technical University of Munich).

The second panel, on the development of electric vehicle batteries, future prospects of lithium-ion batteries, solid state batteries, importance of battery management software, and transition resources and bottlenecks, was moderated by prof. Željko Tomšić from the University of Zagreb Faculty of Electrical Engineering and Computing in front of the Croatian Academy of Technical Sciences. Invited speaker **Wu Kai**, PhD, the leading scientist of the world's largest manufacturer of car batteries, Chinese CATL, presented the current state of development of batteries for electric cars.
The panel consisted of Kai Wu (CATL), Tony Harper (Head of Battery Systems Development, Faraday Battery Challenge UK / Challenge Director for Faraday Battery Challenge at UK Research and Innovation), Prof. Mario Vašak (Laboratory for Renewable Energy Source Systems, University of Zagreb Faculty of Electrical Engineering and Computing) and Prof. Zoran Mandić (University of Zagreb Faculty of Electrochemistry, FKIT).

The third panel was initiated by the invited speaker, **Prof. Frano Barbir** of the University of Split, Faculty of Electrical Engineering, Mechanical Engineering and Naval Architecture, from Croatia, speaking on the topics of hydrogen as a flexible energy carrier, hydrogen production and storage challenges, fuel cell systems, performance and durability of fuel cells, and the role of electrofuels in heavy transport.

The panel was moderated by Prof. Bruno Zelić, University of Zagreb, Faculty of Chemical Engineering and Technology, Croatia. Panel also featured Prof. Tomaž Katrašnik of the University of Ljubljana, Faculty of Mechanical Engineering, Slovenia, prof. Rodolfo Taccani, the Prorector for Technology Transfer at the University of Trieste, Italy, and Prof. Ankica Kovač of the University of Zagreb, Faculty of Mechanical Engineering and Naval Architecture in Croatia, head of Power Engineering Laboratory.

The fourth panel on “Autonomous driving“, was moderated by Prof. Vedran Mornar, University of Zagreb, Faculty of Electrical Engineering and Computing, Croatia, covering the topics of Sensors, artificial intelligence, traffic control and connected autonomous vehicles, legal issues and consequences on ownership models. The panel was initiated with the invited speaker **Mr. Sacha Vrazic**, Rimac Automobili, Croatia, presenting the recent advancements in autonomous driving performed by Rimac Automobili laboratory. The panel featured also Prof. Subhasis Chaudhuri, the Kamalnayan Bajaj Chair Professor in the Department of Electrical Engineering of IIT Bombay, India, Prof. Ivan Petrović, Faculty of Electrical Engineering and Computing, University of Zagreb, Croatia, Prof. Kumares Sinha, Distinguished Professor of Civil Engineering at Purdue University, USA, and Prof. Alexander Katriniok, Eindhoven University of Technology (TU/e), Netherlands.

The last panel on the topic of “Modal shift – roads, railways or planes?”, moderated by Prof. Hrvoje Gold, University of Zagreb, Faculty of Transport and Traffic Sciences, Croatia, covered the topics of Modal integration using Mobility as a Service (MaaS), intelligent modal shift, modal route optimization, last-mile delivery, new e-transport technologies. Discussion was initiated by the invited speaker, **Prof. Borna Abramović**, University of Zagreb, Faculty of Transport and Traffic Sciences, Croatia. The panel also featured Prof. Edna Mrnjavac, Faculty of Tourism and Hospitality Management in Opatija of the University of Rijeka, Croatia, Prof. Elmar Fürst, Institute for Transport and Logistics Management at WU Vienna, Austria, Prof. Ádám Török, Budapest University of Technology and Economics, and Prof. Marko Ševrović, Faculty of Transport and Traffic Sciences, University of Zagreb.

The conference also included **e2-Mobility Working Group** meeting on the first day (9th of October), where the internal draft of the CAETS 2023 e-mobility report on the decarbonization of transport was presented to the working group.

Further on, **CAETS Board Meeting** was held on the same morning, while the first day of the conference was closed with the Communication Prize Award Ceremony.

On the second day of the conference, 10th of October, the **CAETS Council Meeting** took place in the afternoon.

Third day of the conference, 11th of October, was dedicated to **a study visit** of the participants to the **Rimac Automobili laboratories and factory near Zagreb**.

Video materials from all panels can be found on the YouTube channel of the media Croatian Academy of Engineering.

Organizing Committee

Neven Duić, Chair
Vedran Mornar
Nikola Čavlina
Vladimir Mrša
Hrvoje Gold
Igor Kuzle
Bruno Zelić
Željko Tomšić
Vladimir Andročec

International Scientific Committee

Neven Duić, Chair
Vedran Mornar
Nikola Čavlina
Hrvoje Gold
Igor Kuzle
Bruno Zelić
Željko Tomšić
Frano Barbir
Iva Ridjan Skov
Vedran Kirinčić

Programming Committee

Vedran Mornar, Chair
Neven Duić
Gérard Creuzet
Hrvoje Gold
Ruth A. David
Oscar Vignart

Engineering Power – *Bulletin of the Croatian Academy of Engineering* Vol. 18(2-3) 2023 – ISSN 1331-7210 (Print)
ISSN 2718-322X (Online)
Publisher: Croatian Academy of Engineering (HATZ), 28 Kačić Street, P.O. Box 14, HR-10105 Zagreb, Republic of Croatia
Editor-in-Chief: Prof. Vedran Mornar, Ph.D., President of the Academy
University of Zagreb, Faculty of Electrical Engineering and Computing
Editor: Prof. Bruno Zelić, Ph.D., Vice-President of the Academy
University of Zagreb, Faculty of Chemical Engineering and Technology
Guest-Editor: Prof. Sandro Nižetić, Ph.D., Assoc. Prof. Goran Krajačić, Ph.D.
Activities Editor: Tanja Miškić Rogić
Editorial Board: Prof. Vedran Mornar, Ph.D., Prof. Vladimir Andročec, Ph.D., Prof. Bruno Zelić, Ph.D., Assoc. Prof. Mario Bačić, Ph.D., Prof. Neven Duić, Ph.D.
Editorial Board Address: Croatian Academy of Engineering (HATZ), "Engineering Power" – Bulletin of the Croatian Academy of Engineering, Editorial Board, 28 Kačić Street, P.O. Box 14, HR-10105 Zagreb, Republic of Croatia
E-mail: hatz@hatz.hr
Graphical and Technical Editor: Tiskara Zelina, Ltd., Zelina
Proof-reader: Miroslav Horvatić, MA
Press: Tiskara Zelina, Ltd., Zelina
Circulation: 200